

CROSS-SCALE ANALYSIS OF SURFACE-ADJUSTED MEASUREMENTS IN DIGITAL
ELEVATION MODELS

by

MEHRAN GHANDEHARI

B.Sc., University of Isfahan, 2010

M.Sc., University of Tehran, 2012

A thesis submitted to the
Faculty of the Graduate School of the
University of Colorado in partial fulfillment
of the requirement for the degree of
Doctor of Philosophy
Department of Geography
2019

ProQuest Number: 13807161

All rights reserved

INFORMATION TO ALL USERS

The quality of this reproduction is dependent upon the quality of the copy submitted.

In the unlikely event that the author did not send a complete manuscript and there are missing pages, these will be noted. Also, if material had to be removed, a note will indicate the deletion.



ProQuest 13807161

Published by ProQuest LLC (2019). Copyright of the Dissertation is held by the Author.

All rights reserved.

This work is protected against unauthorized copying under Title 17, United States Code
Microform Edition © ProQuest LLC.

ProQuest LLC.
789 East Eisenhower Parkway
P.O. Box 1346
Ann Arbor, MI 48106 – 1346

This dissertation entitled:

Cross-Scale Analysis of Surface-Adjusted Measurements in Digital Elevation Models
written by Mehran Ghandehari
has been approved for the Department of Geography

Professor Barbara P. Buttenfield (Chair)

Professor Stefan Leyk

Date _____

The final copy of this thesis has been examined by the signatories, and we
find that both the content and the form meet acceptable presentation standards
of scholarly work in the above mentioned discipline.

Mehran Ghandehari (Ph.D., Geography)

Cross-Scale Analysis of Surface-Adjusted Measurements in Digital Elevation Models

Dissertation directed by Professor Barbara P. Buttenfield

Terrain is commonly modeled in GIScience on a grid of pixels, assuming that elevation values are constant within any single pixel of a Digital Elevation Model (DEM) (a ‘rigid pixel’ paradigm). This paradigm can generate imprecise measurements because it does not account for the slope and curvature of the terrain within each pixel. The objective of this research is to relax the rigid pixel assumption, allowing detection of possible sub-pixel variations (a ‘surface-adjusted’ paradigm). The surface-adjusted approach incorporates the slope and curvature of the terrain into computations, and fills a critical gap in the literature regarding the impacts of rigid-pixel paradigm in terrain modeling uncertainty.

Demonstration of the surface-adjusted paradigm is proposed along two lines. First, this research employs realistic digital terrain using different interpolation methods and the information from adjacent pixels, searching for a more accurate interpolation of elevation values. Sub-pixel variations in DEMs across different resolutions is investigated to develop a foundation of surface-adjusted computations. Second, surface-adjusted area measurements are investigated. Area is commonly measured in Euclidean space and so the slope and curvature of the terrain is ignored, resulting in under-estimation, especially in higher slope or rough terrain.

This research examines the sensitivity of surface adjustment to different interpolation methods, different contiguity configurations, different terrain type and a progression of spatial

resolutions. There is a general increase in the residuals at coarser resolutions. RMSE values decrease to varying degrees moving from rough and non-uniform terrain to smooth and uniform terrain. It found that bicubic interpolation can increase the accuracy of estimating elevation and area from regular gridded DEMs at coarse resolutions and in rough and/or non-uniform terrain. In fine DEM resolutions, and/or smooth and uniform terrains, linear or bilinear methods provide the highest accuracy. The bicubic method also incur the highest processing time. Therefore, to maintain a balance between the increased computations needed to measure surface-adjusted elevation and area against the improvement in precision or for large volume data sets, linear and bilinear methods seem to be better choices.

To my wife,

Sara

&

To my parents,

Hassan and Jamileh

Acknowledgments

I worked with and learned from my incredible professors, colleagues and friends during my whole PhD journey. I would like to express my sincere gratitude to everyone for their help and support with this dissertation. There are too many names to acknowledge, though I mention a few of them here.

First and foremost, I have the highest gratitude for my advisor Professor Barbara (babs) P. Buttenfield. About four years of continuous and close work with babs was a unique and rewarding experience, and I am so happy that I was one of those few lucky students who get to work with one of the most well-known GIScientists in the word on a regular basis. She directed my research in the right direction, while giving me a great degree of freedom to explore my topics of interest and to fulfil my scientific curiosity. I always enjoyed our discussions about the research, and she enlightened me with valuable advice and inspired me to explore diverse possibilities. She has taught me how to teach, conduct research, and live in a scientific community. I learned a lot of other things about real life as well. I hope I can use them in my life and also teach them to others.

I would like to express the deepest appreciation to my committee members, Professor Stefan Leyk, Professor Carson Farmer, Professor Yi Qiang, and Doctor Roland Viger, whose guidance, encouragement, suggestion, and very constructive criticism have contributed immensely to the evolution of my ideas on this project. Their positive attitude and deep passion for my research has provided deeper interest in my own research.

I gratefully acknowledge the Grand Challenge Initiative “Earth Lab” funded by the University of Colorado (<https://www.colorado.edu/earthlab/>) for funding this PhD project. I also

acknowledge the USGS Center for Excellence in Geospatial Information Science (CEGIS) for data and analytic advice.

I would like to acknowledge the financial support and the scholarships from the Department of Geography at the University of Colorado, which greatly benefited the financial needs for my project and academic obligations. Needless to say, I am grateful to many other faculties that make Geography of CU Boulder such a great place to study and work. I am glad to emphasize the administrative staff for their dedicated work: Jeff Nicholson, Darla Shatto, Karen Weingarten, and Leslie Yakubowski. I experienced a lot of enjoyment in carrying out this work in this department. I gratefully acknowledge for all of the opportunities I was given to conduct my research and further my dissertation.

My appreciation also extends to my laboratory colleagues, Alex Stum, Hamid Zoraghein, Johannes Uhl, and Georgios Charisoulis who have supported and helped me so much throughout this period. Their unwavering enthusiasm for GIScience and their personal generosity made my time at CU Boulder enjoyable.

At the end, I would also like to thank my parents for their wise counsel and sympathetic ears. They are always there for me. I acknowledge my wife, Sara, who is my champion and blesses me with a life of joy. No words can describe my love and thanks to her.

CONTENTS

CHAPTER I

1.1. General Overview	1
1.2. Problem Statement	3
1.3. Research Goals.....	6
1.4. Significance of the Research.....	7
1.5. Clarification of Terms.....	8
1.6. Research Questions	10
1.7. Structure of the Dissertation	12

CHAPTER II

2.1. Introduction.....	14
2.2. Digital Terrain Modeling	15
2.2.1. Morphometric Parameters.....	17
2.2.2. Feature Extraction.....	20
2.2.3. Surface Modeling.....	21
2.2.4. Uncertainty in Surface Models	23
2.2.5. Scale and Resolution.....	27
2.3. Spatial Analysis in Non-Euclidean Space.....	29
2.4. Elevation Estimation from a Regular Gridded DEM.....	35
2.5. Surface Area Estimation from a Regular Gridded DEM	37
2.6. Summary	42

CHAPTER III

3.1. Introduction.....	43
3.2. Justification for the Research Approach	44
3.3. Dataset and Study Areas	45
3.4. Methods.....	50
3.4.1. Interpolation Methods	51
3.4.2. Contiguity Configuration	56
3.4.3. Workflow and Processing.....	57
3.4.4. Accuracy Assessment	58
3.5. Results.....	59
3.5.2. Optimal Configuration for Weighted Average Interpolator	63
3.5.3. Optimal Configuration for Least Squares Fitting	64
3.5.4. Optimal Quadratic Polynomial Method.....	65
3.5.5. Analysis of Surface-Adjusted Elevations Methods	66
3.5.6. Processing Time Comparison	68
3.5.7. Results for Other Study Areas	69
3.6. Discussion and Summary.....	75

CHAPTER IV

4.1. Introduction.....	78
4.2. Surface Area Calculations.....	79
4.3. Interpolation Methods used in the Modified Jenness Method	83

4.4. Workflow and Processing	84
4.5. Results.....	86
4.5.1. Areal Characteristics of the Six Data Sets	86
4.5.3. Analysis of Surface Area Measurements.....	88
4.5.2. Analysis of Surface Area Measurements based on the Modified Jenness Method	90
4.5.3. Processing Time Comparison	92
4.6. Discussion and Summary.....	94

CHAPTER V

5.1. Introduction.....	96
5.2. Conceptual Surface-Adjusted Framework.....	97
5.3. Surface-Adjusted Elevation Framework.....	100
5.4. Surface-Adjusted Area Framework	103
5.5. A Proposed Framework for the Surface-Adjusted Elevation and Surface-Adjusted Area..	106
5.6. Limitations of the Proposed Frameworks	107
5.6. Summary	108

CHAPTER VI

6.1. Surface-Adjusted Terrain Measurement: Why is it Important?.....	110
6.2. Research Objectives and Methodology	111
6.3. Research Questions and Answers	112
6.4. Limitations of the Experiments on Surface Adjustment.....	115
6.5. Conclusions and Future Work	117
BIBLIOGRAPHY.....	121

TABLES

CHAPTER III

Table 3.1. The morphometric characteristics of study areas	46
Table 3.2. Summary statistics of residuals.....	59
Table 3.3. Correlation between residuals and terrain derivatives.....	62
Table 3.4. Correlation between slope and residuals	63
Table 3.5. RMSEs for the weighted average method	63
Table 3.6. RMSEs for the least squares fitting method	65
Table 3.7. RMSEs for the quadratic Polynomials.....	66
Table 3.8. Accuracy assessment parameters for North Carolina	67
Table 3.9. Processing time for different interpolation methods.....	68
Table 3.10. RMSE values the remaining five study areas	70

CHAPTER IV

Table 4.1. RMSEs of surface area measurements.....	89
Table 4.2. Summary statistics of surface area rasters	91
Table 4.3. RMSEs of the modified Jenness methods.....	92
Table 4.4. Processing time compression.....	94

CHAPTER IV

Table 5.1. The morphometric characteristics of study areas	99
Table 5.2. Surface-adjusted elevation RMSE values.....	101
Table 5.3. Surface-adjusted area RMSE values.....	104

FIGURES**CHAPTER I**

Figure 1.1. (a) The surface-adjusted paradigm 3

CHAPTER II

Figure 2.1. Different types of bivariate quadratic polynomials 22

Figure 2.2. Triangle inequality 32

Figure 2.3. Parallel postulate 32

CHAPTER III

Figure 3.1. Study areas 47

Figure 3.2. 20,000 randomly selected points in North Carolina 49

Figure 3.3. Research methodology 51

Figure 3.4. Contiguity configurations 57

Figure 3.5. Distribution of residuals 60

Figure 3.6. Outliers of residuals 61

Figure 3.7. Residuals and terrain derivatives 62

Figure 3.8. RMSE values of the weighted average method 64

Figure 3.9. Estimated elevations for Louisiana 71

Figure 3.10. Estimated elevations for North Carolina 71

Figure 3.11. Frequency distribution of slope values 71

Figure 3.12. RMSE values in different slope categories 73

Figure 3.13. Frequency distribution of roughness values 74

Figure 3.14. RMSE values in different roughness categories 75

CHAPTER IV

Figure 4.1: Surface area calculations using slope.....	80
Figure 4.2. Jenness's original method versus modified Jenness method.....	82
Figure 4.3. Modified Jenness method.....	83
Figure 4.5. Surface area calculations in AWS	86
Figure 4.4: Areal characteristics of the six sata sets	87
Figure 4.5: Difference between surface area and planar area.....	88
Figure 4.6. A subset in North Carolina	93

CHAPTER V

Figure 5.1. The conceptual surface-adjusted framework.....	98
Figure 5.2. Surface-adjusted elevation workflow	103
Figure 5.3. Surface-adjusted area workflow	105

CHAPTER VI

Figure 6.1. Mismatching of 100 m and 1000 m DEMs	116
--	-----

Chapter I

Introduction

1.1. General Overview

Terrain models guide scientists and planners in multiple ways that have fundamental impacts on society, safety, and resource management. For example, digital terrain data is used by natural hazards scientists to model flooding inundation and debris flows (Griffin *et al.* 2015) and by hydrologists to model water flow direction and accumulation (Stanislawski, Falgout, and Buttenfield 2015). Soil scientists investigate the spatial distribution of soil properties using terrain models (Florinsky 2016). Ecologists use terrain models to delineate habitats and nesting territory or to predict the presence of certain species (Czarnecka and Chabudziński 2014). Avalanche risk is measured using solar insolation metrics based on slope and aspect (Jaboyedoff *et al.* 2012). Civil engineers plan construction of road and railroad networks on the basis of elevation and slope in conjunction with other factors (Zhao, Wang, and Wang 2005). Understanding the terrain surface can guide realistic characterization of these processes and applications.

Terrain data is frequently gathered as a set of elevation points. After collecting the terrain information, an interpolation function is employed in order to regularize elevations in a Digital Elevation Model (DEM). Each point in a DEM represents a small area by a horizontal planar surface, which can be described as a zero order polynomial function. Therefore, a DEM provides

a discretized sample of the continuous elevation surface. The regularized grid format is widely used in terrain modeling due to its simplicity and small storage size (Burrough, McDonnell, and Lloyd 2015). Mathematical operations can be easily carried out using Map Algebra (Tomlin 1990). The resolution of a grid DEM is based on the cell size of the grid; the larger the cell size, the coarser the resolution. The data structure for a regular grid DEM can be a cell by cell storage in a matrix, a binary file, or a hierarchical model such as a quad tree (Samet 1984).

Regardless of data structure, the regularized grid approach that is commonly used for implementing local, neighborhood, and global raster functions neglects within pixel variations and discontinuities in the actual surface due to the projection of terrain features into a planar surface. In a regular gridded DEM, each pixel is processed as a rigid horizontal planar surface with a constant elevation (Wood 1998; Schneider 2001). As stated by Longley *et al.* (2005: 327), “The elevation of a grid cell is often the elevation of the cell’s central point”, though “sometimes it is the mean elevation of the cell, and other rules have been used to define the cell’s elevation.”. In this dissertation, this modeling precondition is referred as ‘*rigid pixel*’ paradigm (Figure 1.1). This paradigm does not account for the slope and curvature of terrain within each pixel, generating imprecise measurements, particularly as pixel size increases or in uneven terrain. Historically, this paradigm was adopted for pragmatic reasons, given limits of computation speeds, of data resolution, and lack of understanding about data modeling and uncertainty.

Interpolation methods (e.g., bilinear, bicubic) can be used to reconstruct the surface of a pixel for estimating elevation, and terrain derivatives (e.g., slope and curvature) within a pixel (‘*surface-adjusted*’ paradigm) (Buttenfield *et al.* 2016). This paradigm relaxes the rigid pixel assumption by acknowledging that sub-pixel variations may occur in elevation, slope, and curvature. Therefore, the surface-adjusted paradigm investigates different interpolation methods

to reconstruct the surface of a DEM pixel in order to increase the accuracy of DME-based measurements, such as elevation, distance and area. The improvement in measurements can be relatively small, but additive effects across a study area can become significant particularly at coarser resolutions, and rough or non-uniform terrain. Such errors propagate into modeling applications, distorting applications such as routing or freight cost estimates, least cost path determination, and hydrologic flow accumulation. This dissertation examines the sensitivity of surface adjustment to different interpolation methods, different contiguity configurations, different terrain type and a progression of spatial resolutions.

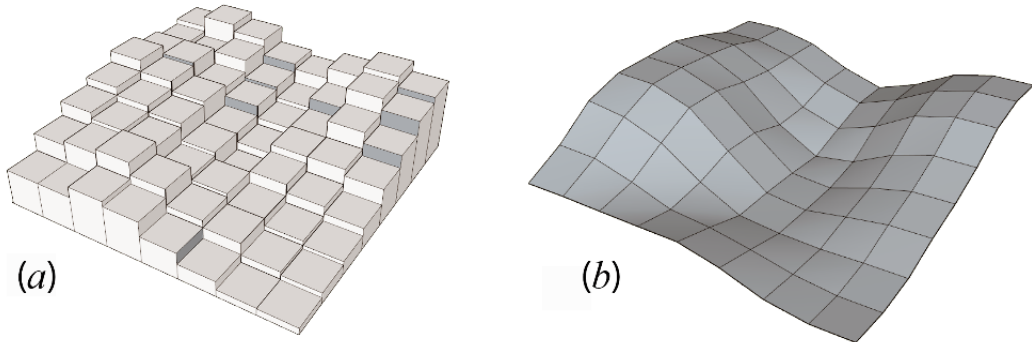


Figure 1.1. (a) The rigid pixel paradigm and (b) the surface-adjusted paradigm.

1.2. Problem Statement

In a regular gridded DEM, the terrain surface is modeled on a grid of pixels, which elevation is constant within each pixel. It is obvious that this model leads to imprecise measurements because it does not account for the slope and curvature of the terrain within each pixel. Advances in processing speed and the availability of lidar data in recent years permits reconsideration of the rigid pixel assumption of invariance, especially given its introduction of imprecise estimates of elevation and derivative metrics that underlie nearly all environmental

models. In the recent decade, Light Detection and Ranging (lidar) has provided new and opportunities for studying Earth surface processes, by providing more precise measurements than previous capture technologies (Tarolli 2014). Lidar data has become more available in recent years, but processing is still a challenge due to issues relating to managing larger data volumes and longer processing times. Lidar data needs to be filtered as a preprocessing step to remove artifacts and to extract bare earth points. The filtering process reduces the accuracy of the original data and might eliminate or distort significant features (Favorskaya and Jain 2017; Passalacqua *et al.* 2015). Furthermore, most GIS projects call for integration of various data layers. Ancillary data in the form of vegetation, precipitation, or soil data, is generally available at resolutions that are coarser than lidar, enforcing the need for filtering to accomplish appropriate data harmonization. Finally and most importantly, the current availability of lidar data is not comprehensive in developed nations, and sparse or non-existent in rural and developing regions of the “global south”, raising compelling reasons to develop guidelines for the propagation of error that can and does occur under the rigid pixel paradigm. Terrain data is used to understand social and natural processes, and finding and validating methods that benefit society in less developed and undeveloped regions are emerging efforts of terrain-based regional and global modeling (Buttenfield *et al.* 2016).

The surface-adjusted approach, which is investigated in this dissertation, incorporates the slope and curvature of the terrain into DEM-based measurements, and fills a critical gap in the literature regarding the impacts of rigid-pixel paradigm in terrain modeling uncertainty. To calculate the surface-adjusted measurements, a continuous surface should be modeled to reconstruct the surface of a pixel. Because the DEM is a discretized representation, interpolation methods are used to reconstruct the continuum. Uncertainty is introduced in both the initial terrain discretization and the subsequent surface reconstruction (Weibel and Heller 1993). Uncertainty of

reconstructed surfaces (i.e., shape uncertainty) is difficult to quantify on a conceptual level as a surface can be reconstructed from a given date points in various ways that cannot be considered as the correct description of a terrain surface (Schneider 2001). Therefore, finding a suitable mathematical representation of a surface and its associated uncertainty is considered a challenge. In this research, various interpolation methods are applied, and the accuracy of outputs are assessed using lidar DEM as a benchmark to find the interpolation method that is most accurate for surface-adjusted measurements.

Sub-pixel variations in DEMs are investigated across different resolutions and different terrain types to develop a foundation of surface-adjusted computations. Different DEM resolutions are tested to investigate the variation of spatial errors in estimation of surface-adjusted measurements across resolutions. It is anticipated that the accuracy of surface-adjusted measurements decreases in courser resolutions. This research aims to investigate the performance of each surface-adjustment method in different DEM resolutions. It should be noted that the cross-scale analysis mentioned in this dissertation refers to the analysis of surface-adjusted measurements across DEM resolutions. Terrain type is another important factor that should be considered in this dissertation. Different terrain types are employed in the experiments conducted in this research to see how terrain roughness and terrain uniformity play a role in surface-adjusted measurements. It is predicted that errors introduced by the rigid-pixel paradigm are more significant in a rough and non-uniform terrain than a smooth and uniform terrain. Also, choosing a proper interpolation method for terrain reconstruction depends to a great degree on terrain roughness and terrain uniformity.

Demonstration of the surface-adjusted paradigm is proposed along two lines. First, this research employs different interpolation methods and the information from adjacent pixels,

searching for a more accurate interpolation of elevation values of off-centroid points from a regular gridded DEM. Second, surface-adjusted area measurements are investigated. In this research, the scale-, algorithm-, and topographic-dependence of surface area calculations are investigated. At the end, this dissertation provides a framework for estimating elevation and surface area from a regular gridded DEM using commonly applied interpolations methods. This framework takes the DEM resolution, and terrain type into account for choosing an appropriate surface-adjusted method.

1.3. Research Goals

Spatial analysis is commonly conducted in Euclidean space and the characteristics of terrain surface are ignored. More realistic terrain measurements can improve the precision and reliability of spatial analyses that rely upon terrain metrics. The overall goal of this work is to develop a set of surface-adjusted measurements (elevation and surface area) that incorporate terrain slope and curvature. This study will (1) investigate sub-pixel variations in DEM elevations at various resolutions and in different terrain types; and (2) develop and compare cross-scale surface-adjusted area estimates. More specifically, the study has the following testable objectives:

- To identify errors introduced by use of rigid-pixel measurements computed from a regular gridded DEM and propose solutions to compensate for these errors.
- To advance understanding of error introduced when the rigid pixel paradigm is assumed to be correct.
- To assess the accuracy of different interpolation methods used for surface-adjusted measurements (here, elevation and surface area).

- To advance understanding of how spatial error varies across resolutions, a cross-scale terrain analytics component that is at present not well understood.
- To examine the balance between the increased computations needed to derive surface-adjusted measurements against the improvements in accuracy.
- To investigate how the results vary with different types of terrain.
- To propose a framework for estimating elevation and surface area from a regular gridded DEM.

1.4. Significance of the Research

This research is important for several reasons. First, distance, area and volume form the basis of most if not all geospatial analyses. For example, kernel densities, variogram analysis, interpolation are founded in Euclidian distance. When the distance, area and volume measurements are based on the rigid-pixel paradigm, discrepancies (error magnitudes) can be expected to vary with size of study area, DEM resolution, and terrain roughness. This error can be negligible for individual pixels, but it can be substantial for measurements that encompass many pixels or when pixel sizes are large, corrupting terrain-based measurements and spatial modeling outcomes.

Second, the results of this research will fill a critical gap in the literature regarding the impacts of the rigid-pixel paradigm in modeling terrain uncertainty, not only for surface area and volume estimates but also for higher level analyses that are based upon surface area and volume, particularly flood inundation. And third, with advances in computer processing speed and increased data availability, the scientific community must address limitations of existing modeling methods (e.g., rigid-pixel paradigm) to provide decision-makers the best possible information about critical environmental issues including biophysical and anthropogenic factors and

interactions. A surface-adjusted approach incorporates the slope and curvature of the terrain into computations to make the terrain-based GIS analysis more realistic. It should be noted that the added computations might not be worth the improvements in accuracy. In this research, therefore, the balance between the increased computations needed to measure surface-adjusted elevation against the improvement in accuracy is considered.

1.5. Clarification of Terms

Different terms are used in this dissertation that is clarified in the following:

Digital Elevation Model (DEM): DEM represents the bare ground surface. A DEM can be represented as a regular grid or as a vector-based triangular irregular network (TIN). In this dissertation, regular gridded DEMs in different resolutions (i.e., pixel size) are used for surface-adjusted analysis. In fact, this dissertation addresses a problem in a regular gridded DEM data structure. Lidar data in a regular grid format is used as a benchmark as well. Lidar data is used as a benchmark because it has the finest DEM resolution and the highest vertical accuracy in comparison to other DEM resolutions used in this research. Therefore, 3 m lidar DEM is used as a benchmark (i.e., truth) to compute an accuracy metric for each surface-adjusted method.

Rigid-pixel paradigm: A DEM pixel contains infinite terrain points, but always the pixel centroid is designated to represent a grid cell (point's region of influence), for computational simplicity. For example, based on this paradigm, the elevation of an off-centroid point is estimated from a regular gridded DEM based on the closest centroid (i.e., elevation of the pixel that the point is located on). In this dissertation, this model is referred to as the rigid-pixel paradigm.

Surface-adjusted paradigm: The surface-adjusted paradigm aims to incorporate the variation of slope, and/or curvature within a DEM pixel into computations (e.g., estimating

elevation, and area from a regular gridded DEM). In fact, the surface of each DEM pixel is reconstructed using an interpolation method to increase the accuracy of DEM-based measurements. In this dissertation, this model is referred to as the surface-adjusted paradigm.

Sub-pixel variation: the variation of elevation within a DEM pixel is called sub-pixel variation. In this research, sub-pixel variation in a regular gridded DEM is modelled using different interpolation methods.

Surface-adjusted elevation: In this research, possible sub-pixel variations are used to interpolate the elevation of arbitrary points from a regular gridded DEM. The estimated elevation of off-centroid points given the sub-pixel variation of elevation in a regular gridded DEM is called surface-adjusted elevation.

Surface-adjusted area: Area is commonly measured in a 2D Euclidean space (i.e., planar area) and so the slope and curvature of the terrain is ignored, resulting in under-estimation, especially in higher slope or rough terrain. In this dissertation, area is calculate from a regular DEM by considering localized variations on the terrain surface. The estimated area is called surface-adjusted area or surface area.

Contiguity configuration: interpolation methods are employed in this research to reconstruct the actual surface of each pixel using contextual information from adjacent pixels. For example, a bilinear polynomial estimates a surface at each data point using the four closest pixel centroids, or a bicubic polynomial estimates a surface at each data point using the sixteen closest pixel centroids. Adjacent pixels can be combined in different ways that is called contiguity configuration. In this research, the first and second order neighboring pixels are used in different interpolation methods.

Cross-scale analysis: Scale is an important concept in terrain modeling that involves pixel size (i.e., resolution) and the spatial extent of the DEM (the size of study area). In this dissertation, cross-scale analysis refers to the analysis of surface-adjusted measurements in different DEM resolutions. That is, cross-scale means multi-resolution in this research.

1.6. Research Questions

This dissertation examines sub-pixel variations in elevation to improve estimation of DEM-derived parameters and measurements (i.e., surface-adjusted measurements). Various interpolation methods, DEM resolutions, and terrain types are examined to investigate the factors influencing the surface-adjusted measurements. Several key questions are central to the proposed research:

Research question 1: How can surface-adjusted elevation and surface-adjusted area be more accurately estimated from a DEM? What is the best mathematical model to reconstruct the surface of a DEM cell to estimate elevation, and surface area?

At present, terrain measurements are most often calculated under the assumption that elevation within DEM pixels are uniform, and that within-pixel variations are ignored to simplify processing and modeling. This research relaxes the rigid pixel assumption, allowing for possible sub-pixel variations. Elevation of randomly generated points within a pixel are estimated using different interpolation methods. The estimated elevations are compared with the corresponding elevation of a fine resolution lidar pixel centroid to investigate sub-pixel variation in elevation, and to assess the relative accuracy of different interpolation methods. Furthermore, Polynomial functions reconstruct the surface of a DEM for surface area calculations. For estimating elevation and area, the accuracy and processing time of different functions are both assessed to find the most balanced choice of surface-adjusted method.

Research question 2: *How does the accuracy of surface-adjusted elevation and surface-adjusted area vary with changing spatial resolution? And does this vary with the method of surface adjustment, and/or terrain roughness?*

In this dissertation, the errors introduced by the rigid pixel assumption in DEMs is discussed. Furthermore, the errors introduced by applying partial and full surface adjustment (i.e., adjusting only for slope, as opposed to adjusting for slope and curvature) is investigated. This dissertation also addresses the propagation of error in surface-adjusted measurements across spatial resolution and in terrains of varying roughness. Uncertainty is assessed statistically using RMSE, residuals analysis and similar accuracy metrics.

To address this question, the dissertation systematically investigates the scale- and topography-dependence of elevation and surface area calculations in DEMs. Four independently compiled DEM resolutions (i.e., 10 m, 30 m, 100 m, and 1,000 m), and six study areas reflecting varied terrain across the conterminous United States for which LiDAR data is available and can serve to validate elevation and area estimations are analyzed. It is expected that the surface-adjusted measurements make a greater difference in courser resolutions and rough terrain.

Research question 3: *What computational cost does the surface-adjusted paradigm add to computations for estimating elevation and surface area? And does the added cost vary with resolution and geographic conditions?*

The assumption of non-rigid pixels carries an additional computational load, as it must incorporate not only elevation and pixel size, but also slope and curvature. The performance of different surface-adjusted methods are compared. This research addresses the balance between the increased computations needed to measure surface-adjusted measurements against the improvement in precision.

1.7. Structure of the Dissertation

Chapter two provides a detailed background on terrain modeling, geomorphometry and the analysis of error. Furthermore, a literature review of the relevant work for this dissertation situates this work in the context of the existing body of knowledge.

Chapter three introduces study areas and various interpolation methods used to reconstruct the surface of DEM pixels. Different contiguity configurations mandated by each interpolation method are also presented. This part of the research examines sub-pixel variations by incorporating slope, and curvature to interpolate the elevation of an arbitrary point within a DEM pixel by several methods, comparing outcomes with respect to pixel size and terrain type.

Chapter four systematically evaluates the scale-, algorithm-, and topography-dependence of surface area computations. Various polynomial methods will be used to model the surface of a pixel and calculate its surface area. Similar to the previous chapters, surface area is calculated for six different study areas, and various DEM resolutions.

Chapter five discusses a surface-adjusted framework for estimating elevation and area from a regular gridded DEM. This framework aims to facilitate the selection of appropriate methods to meet a certain accuracy for estimating elevation and surface area from a regular gridded DEM based on DEM resolution, and terrain type.

Chapter six presents a summary of this research, considers implications for higher level modeling, and gives directions for future work.

Chapter II

Previous Work on Cross-Scale Analysis of Surface-Adjusted Measurements in DEMs

2.1. Introduction

In digital elevation models, the terrain surface is conventionally modeled on a grid of pixels. The assumption is that elevation is constant within each pixel. As discussed in the previous chapter, this model leads to imprecise measurements because it does not account for the slope and curvature of the terrain within each pixel. As pixel size increases, for example in continental or global scale modeling, errors introduced by the rigid pixel paradigm can become dramatic. Several researchers acknowledge sub-pixel variations in elevation using different interpolation methods, with varying success. Reviewing the literature in terrain modeling, and investigating the pros and cons of the widely used methods in terrain modeling lead to a justification about how this dissertation research implements the elements of surface-adjusted paradigm, and provides a foundation for doing the work in the subsequent chapters. A brief background of digital terrain modeling is provided first. Secondly, parameters of slope and curvature are introduced and the widely used methods are investigated. These parameters vary within a DEM pixel, though they are reported for the pixel centroid and do not describe the properties of the entire pixel. Stream extraction from a regular gridded DEM is discussed to see how the rigid-pixel assumption

introduces errors in the extracted streams from DEM. Alternative approaches used for terrain surface modeling are introduced. It will be discussed that the surface-adjusted approach is going to model terrain variation within each pixel and eliminate the problems of the current approaches. Afterward, uncertainties propagated in surface models are discussed, and the metrics used for reporting the accuracy of terrain models. DEM errors are reviewed and the errors introduced by the rigid pixel assumption is discussed as an additional source of uncertainty.

Subsequently, scale and resolution are reviewed to argue that these concepts form one of the most important topics of terrain analysis. DEM resolution has an important role in the surface-adjustment measurements that is further discussed in this section. After discussing scale and resolution, a brief background of spatial analysis in non-Euclidean space is introduced along with use some non-Euclidean surface-adjusted measurements in spatial analysis. Discussion of previous studies on spatial analysis in non-Euclidean space provide a direction for future work of this dissertation.

Finally, estimation of elevation and surface area from a regular gridded DEM as the main focus of this dissertation are discussed to explain that when slope and curvature of the terrain is ignored under-estimation can result, especially in higher slope or rough terrain. Previous studies on estimating elevation and surface area from a regular gridded DEM is reviewed to justify the research methodology and systematic empirical testing presented in this dissertation.

2.2. Digital Terrain Modeling

The science of digital terrain modeling and quantitative terrain surface analysis is called geomorphometry (Wilson 2012). It also has been defined as the science that "... treats the geometry of the landscape" (Chorley, Malm, and Pogorzelski 1957, p.138), or "the measurement

and analysis of those characteristics of landform which are applicable to any continuous rough surface" (Evans 1972, p.18). This science was introduced in 1958 at MIT by photogrammetrists (Pike, Evans, and Hengl 2009). The focus of geomorphometry is on the extraction of terrain surface parameters (e.g., slope, aspect, curvature, roughness, etc.) and features (e.g., streams, ridges and structure lines) from terrain data (Hengl and Reuter 2008). A regular gridded DEM is widely used as a data model in geomorphometry to represent the terrain surface. Terrain is considered as a mathematical surface, and differential geometry is used to calculate the terrain parameters. The surface is estimated in a local moving window (usually a 3 by 3 window), and then the morphometric parameters for the central pixel are based on the estimated surface (Olaya 2009).

The accuracy needed by a use case, size of the geographic footprint, DEM resolution and terrain type are among the most important factors that need to be considered in terrain modeling (Zhou 2017; Florinsky 2016; Li, Zhu, and Gold 2004; Hengl and Reuter 2008). For geometric measurements such as distance or area, the terrain surface might be considered flat in a very small spatial footprint. But, if the study area is large or if a very high precision is required, then a more reliable model of the land surface should be used. Furthermore, DEMs are generated at multiple resolutions, and parameter estimates can differ at each resolution. For example, length increases at finer resolutions (Mandelbrot 1966). The quality of the extracted parameters (e.g., slope and curvature) and features (e.g., streams and ridges) is greatly influenced by the spatial resolution of the DEM as well (e.g., Kienzle 2004; Band and Moore 1995). Currently, various levels of spatial resolution are offered by different datasets, such as lidar data (e.g., 1 and 3 meters), Shuttle Radar Topography Mission (SRTM) data (e.g., 30 and 90 meters), and the National Elevation Dataset (NED) (e.g., 10, 30, and 100 meters). Moreover, terrain type plays a critical role in the accuracy of measurements (Hengl and Reuter 2008). Measurements based on the rigid-pixel paradigm in

rough terrain are thought to lead to less accurate results than the measurements in a flat terrain (Buttenfield *et al.* 2016). So, the required accuracy, size of the geographic footprint, DEM resolution, and terrain type should guide decisions about how the land surface should be modeled (modeling as a flat surface or taking the effects of earth curvature into account). In this research, different DEM resolutions, and terrain types are tested to evaluate error magnitudes in the results.

2.2.1. Morphometric Parameters

The historic development of terrain surface parameters in the last four decades is reviewed by Evans (2013). First and second derivatives of a terrain surface are gradient and curvature. These derivatives represent the rate of change in elevation, and slope, respectively. Also, the third derivative (i.e., rate of change in curvature) has been introduced as a promising terrain parameter that could be used in more applications in the future (Minár *et al.* 2013). Typically, elevation, gradient (slope and aspect), and curvature (profile and plane curvature) are three main attributes used to describe terrain surfaces (Evans 2013). In what follows, the gradient and curvature that are the main components examined in the surface-adjusted paradigm are explained in more detail.

Gradient: The first derivative of terrain surface (i.e., the rate of change in elevation) is considered the most important geomorphometric parameter of terrain (Evans 1972). Together, slope and aspect are referred to as “gradient”, measured as a vector that represents the direction (aspect) and steepness (slope) of the maximum drop in elevation at a pixel centroid, and defined by a tangential plane situated at a pixel centroid at the steepest direction. Gradient is used for calculating surface area, flow speed, and flow direction, soil wetness index, and other metrics. Traditionally, gradient was measured in the field, but different methods have been developed for calculating slope from the DEM. Horn’s (1981) method (a third-order finite difference method) uses the eight surrounding pixels in a way that weights the four nearest pixels (i.e., pixels located

on north, south, east, and west of the central pixel) more than the four corner pixels in a 3 by 3 pixel arrangement. Evans' (1972) method (a quadratic polynomial fitted to nine points in a 3 by 3 pixel arrangement using least squares) has the highest accuracy (Evans 2013; Florinsky 1998; Skidmore 1989) in most landscape conditions. Horn's method is simpler to implement (Skidmore 2006); and Bolstad (2005) claims that it is a better method for rough terrain. He also discusses a simple method that only uses the four nearest points, which is a good choice for smooth terrain, but is more sensitive to DEM vertical accuracy. Based on synthetic mathematical models and a controlled environment, it is reported that the accuracy of derived slope and aspect is higher in steeper terrain (i.e., the RMSE of derived slope and aspect is negatively correlated with terrain slope) (Zhou, Liu, and Sun 2006; Florinsky 1998). In the landscape, a terrain surface is continuous, and discretization into DEM pixels introduces errors in the slope and aspect calculations. In this research, this assumption is investigated to illustrate how the slope varies within a DEM pixel.

Curvature: Curvature is defined as the second derivative of a terrain surface, that is, the rate of change in slope (Wilson and Gallant 2000). Calculating curvature can be complicated, as the rate of change in slope is never constant in reality (Krebs *et al.* 2015). Curvature expresses the concavity and convexity of the terrain, and usually is measured as profile and plan curvature. Plan curvature is measured perpendicular to the slope direction and profile curvature is measured in the direction of steepest descent. Plan curvature indicates convergence and divergence of flow, and profile curvature indicates acceleration and deceleration of flow (Kimerling, Buckley, and Muehrcke 2012).

Additional measures of curvature are used less frequently in GIScience, but are applied in geomorphometry (Hengl and Reuter 2008). For example, tangential curvature that is measured along the line that is perpendicular to the steepest descent, and is dependent on both plan curvature

and the slope. It is suggested that tangential curvature is more appropriate to investigate the convergence and divergence of flow as extreme values for shallow slopes are adjusted (Wilson and Gallant 2000). Another measure is streamline (rotor) curvature that is the rate at which flow direction changes along a river or the divergence of contour lines. To characterize the curvature of any surface in 3 dimensions, Evans (2013) advises the use of streamline curvature, in addition to plan and profile curvature.

Curvature of the land surface within a pixel in a DEM is commonly calculated based on a polynomial surface that is fitted to nine elevation points (i.e., a 3*3 kernel around a cell) (Márkus 1986). It has been shown that quadratic algorithms are more stable than other polynomials for calculating curvature (Schmidt, Evans, and Brinkmann 2003). Two kinds of quadratic polynomials may be utilized. One is called a partial quadratic model with nine coefficients fitted exactly to 9 sample points. The other is called a full quadratic function with only six coefficients that are fitted using a least squares technique. Evans (1990) claims that errors always exist in the data and the full quadratic function is more reliable due to the usage of least squares estimations. Furthermore, the full quadratic function provides an error metric. However, Zevenbergen and Thorne (1987) argue that the partial quadratic model works better for rugged terrain. As it was mentioned for the gradient, curvature also is calculated and reported at the pixel centroid as a cell-wide constant. As a result, the variation of curvature within a pixel is ignored. In this research, the sub-pixel variations of curvature are examined to see how much uncertainty is introduced due to the rigid-pixel paradigm.

Roughness: Terrain roughness affects many parameters and objects extracted from a DEM. Roughness for an area of interest is quantified in many different ways: (1) standard deviation of elevation; (2) local relief (maximum minus minimum elevation); (3) a "ruggedness number"

that is the product of maximum basin relief and drainage density within the drainage basin; (4) the summed length of contour lines in a given area; (5) the ratio of surface area (3D) and planar area (2D); and (6) bump elevation frequency distribution (Hobson 1972). (7) Fractal dimension, which was introduced by Mandelbrot (1983), is a statistical parameter used to describe the complexity (or roughness) of a curve or a surface across spatial resolutions. (8) Semivariance is another parameter that is used to show the autocorrelation of a terrain surface and consequently its roughness. In this research, terrain roughness is measured as the standard deviation of elevation. This measure is used to investigate the correlation between DEM errors introduced by the rigid-pixel paradigm and terrain characteristics.

2.2.2. Feature Extraction

A DEM is extensively used by many authors to extract parameters and features. Parameters are commonly calculated for individual pixels using the immediately surrounding pixels. For extracting features such as streams and watersheds, the entire DEM is often processed. Feature extraction from DEMs has been an important research topic in terrain modeling for some years (Pike 1988). Various features such as peaks, pits, saddles, ridge lines, and course lines can be extracted from DEMs (Clarke and Romero 2017). Stream extraction from DEMs is one of the most widely examined and often cited examples of terrain analysis (Bai *et al.* 2015; Pelletier 2013; Montgomery and Foufoula-Georgiou 1993; O'Callaghan and Mark 1984). Assuming that water flows along the path of steepest descent, DEM-based methods track the simulated flow of water to calculate flow direction and flow accumulation (Tarboton 2005; Tarboton, Bras, and Rodriguez-Iturbe 1991). Slope is calculated for each pixel to find the path of steepest descent and flow direction. For stream network delineation, a threshold for flow accumulation is defined; and all cells in the flow accumulation matrix with a value greater than the threshold define the stream

channels. In general, the accuracy of DEM-derived streams are a function of the DEM spatial resolution (McMaster 2002), the algorithms used to define flow direction and flow accumulation in order to extract streams (Heine, Lant, and Sengupta 2004), and landscape characteristics (Hastings 2014). Stream extraction from a regular gridded DEM is negatively affected by the rigid-pixel paradigm as well; single flow direction algorithms assume that water flows from pixel centroid to pixel centroid without considering the variations within a pixel. Flow accumulation also is conventionally calculated based on the upstream planar area. Therefore, the surface-adjusted measurements can be incorporated in the feature extraction algorithms to have a better estimate of terrain features. That is, upstream surface area can be considered for calculating the flow accumulation matrix. Feature extraction is not the focus of this dissertation and so the impacts of rigid-pixel assumption on DEM-based features are not investigated in this research.

2.2.3. Surface Modeling

The DEM is a discrete model depicting the continuous surface of terrain. It is based on a set of homogenous rectangular cells representing a terrain surface with abrupt changes at cell edges. This model is used in many applications (e.g., cost path analysis, viewshed analysis, etc.). An alternative surface model is based on a linear interpolation that is partially adjusted to the terrain surface (Li, Zhu, and Gold 2004). A linear surface is constructed based upon 3 points; or a bilinear surface requires 4 points. First order changes (slope and aspect) can be estimated from a linear or a bilinear surface. Higher order derivatives (e.g., plan and profile curvature) cannot be extracted from a linear surface as it has a constant slope and so its curvature is always zero. Evans (1972) uses a biquadratic function to approximate the surface at the central point of each local pixel. The coefficients in this model are solved using least square equations and so the surface might not pass through the central point. Lam (1983) solved this limitation by forcing the surface

to pass through the central point. A biquadratic polynomial can take one of three different shapes: elliptic, parabolic, or hyperbolic (Figure 2.1). These forms can be used to identify features on a DEM. Pits and peaks have an elliptic shape, rivers and ridges have a parabolic shape, and passes have a hyperbolic shape (Wood 1996). Planar surfaces need fewer points, but are not suitable to model a rugged terrain. On the other hand, polynomials of order 3 or higher require at least 10 points, which requires a local window of more than 3 by 3 cells. As a result of the larger focal window, the interpolated surface is smoother; but the accuracy might decrease due to unpredictable undulations that may occur in the terrain.

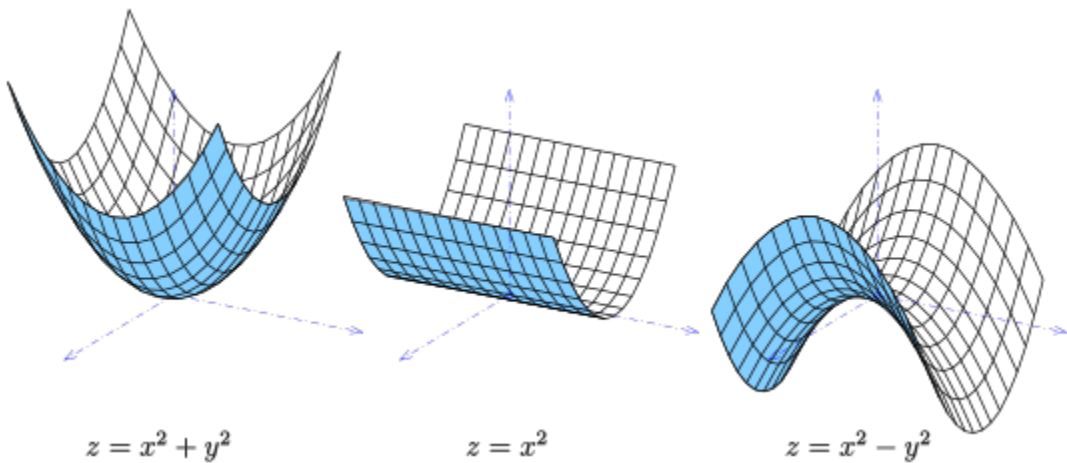


Figure 2.1. Three different types of bivariate quadratic polynomials (from left to right: elliptic, parabolic, and hyperbolic) (<https://en.wikipedia.org/wiki/Paraboloid>)

In the currently used methods, slope and curvature are calculated for the pixel centroid and do not describe topographic variability within a pixel. Given that slope and curvature can vary within a pixel, a true model should describe the properties of the entire cell rather than its centroid. So, an alternative method that considers the subpixel variations of elevation can provide a more accurate estimate of slope and curvature is required to develop. This research sidesteps the rigid pixel paradigm, considering sub-pixel variations (elevation, slope, and curvature) into basic DEM-

based geomorphometric measurements (e.g., elevation, and area) that can be used in more advanced types of spatial analysis (e.g., spatial interpolation, and proximity analysis).

2.2.4. Uncertainty in Surface Models

Digital Elevation Models (DEMs), like any other geospatial data, is subject to error. Errors are introduced in DEMs during construction, measurement and processing (Weibel and Heller 1993). DEMs contain both horizontal and vertical error, but the focus is usually on the vertical error (Fisher and Tate 2006). Vertical error is defined as the deviation of stated elevations from their actual elevations (i.e., ground truth measures) (El-Sheimy, Valeo, and Habib 2005). Actual elevation can be established by field-surveyed data, GPS measurements or a DEM of known higher quality. Although actual elevation measure also is subject to error, it is assumed to be ground truth. DEM vertical errors are categorized into gross errors, systematic errors, and random errors (Wise 2000). Gross errors (also called outliers and blunders) consist of outlier elevation values that are usually due to user error or equipment failure (Fisher and Tate 2006). These errors can be easily detected by visual inspection or statistical approaches (Hengl, Gruber, and Shrestha 2004). Systematic errors are consistent errors (bias) caused by a constant inaccuracy such as incorrect calibration or use of instruments. Random errors are statistical fluctuations caused by unknown and unpredictable changes, or random variation around a true value (Bolstad 2005). DEM vertical errors are not normally distributed in many cases, due to several reasons such as the incidence of systematic errors (i.e., the large positive autocorrelation of the vertical error in DEMs), outliers, and the non-stationary nature of vertical errors (Wood and Fisher 1993; Zandbergen 2011; Oksanen 2013). Consequently, the mean of vertical errors does not exactly equal zero in most cases (Fisher 1998).

A high quality DEM can be achieved by eliminating, reducing, and minimizing the errors

that can be introduced in different stages of terrain modeling. Terrain data can be broken down into three components: (1) deterministic variation (that can be estimated by several metrics, often by a constant mean trend), (2) spatially auto-correlated variation (a pattern of variation that diminishes with distance), and (3) random noise (spatially independent normally distributed residuals). This is based on Regionalized Variable Theory that assumes the value of a variable z is a realization of these three components (Calder and Cressie 2009). The first two components describe the trend and local variations in the terrain shape, and the third component describes remaining variation in the terrain not accounted for by the first two components.

DEM accuracy is an important factor for DEM producers and users. The most widely used method for assessing the accuracy of a DEM is evaluation by check points: a set of points are used as ground truth for checking the quality of the final model (Weibel and Heller 1993). DEM uncertainty is a function of several factors such as terrain roughness, interpolation method, source data (e.g., accuracy, density, arrangement), and the spatial resolution of the DEM (Shi, Wang, and Tian 2014; Reuter *et al.* 2009; Li, Zhu, and Gold 2004; Li, Zhu, and Gold 2004; Wilson and Gallant 2000; Weibel and Heller 1993). A DEM provides only one layer of elevation information and it is suggested by Hengl and Reuter (2008) that DEMs be provided in multiple layers containing information about the sub-grid properties and uncertainties in the data. For purposes of this dissertation, an additional source of uncertainty is introduced by the rigid pixel assumption.

The Root Mean Squared Error (RMSE) is a widely used error metric that expresses overall absolute accuracy of a DEM (Weng 2002; Hunter and Goodchild, 1997). This measure is computed as the average absolute deviation between the processed dataset and a benchmark. The RMSE has some advantages such as being easy to calculate and report, and it is an intuitive metric for comparing different models. But it provides a single global measure and does not represent the

spatial variation of error across a terrain surface (Fisher and Tate 2006). The RMSE also does not give a detailed information about various factors playing a role in DEM error (Hunter and Goodchild 1997). This metric also can be greatly affected by outliers, and it is recommended to be reported based on the 95% confidence interval (Zandbergen 2011). DEM errors are spatially autocorrelated and the RMSE cannot reveal which proportion of reported spatial variation are or are not correlated, nor to what degree. DEM errors also tend to vary by the land cover (highest RMSE for the forest area and lowest RMSE for the bare earth (Zandbergen 2011), and as a result it is not reliable for comparison of areas with different land cover. Therefore, RMSE is not an effective metric as DEM error is spatially variable, and correlated (Wilson 2018).

An error surface is commonly generated to examine DEM accuracy in a more spatially explicit way than with RMSE (Wechsler 2007). This surface is calculated based on the hypothesis that DEM error is spatially variable, spatially correlated and heteroscedastic (i.e., DEM errors are correlated with the morphometric characteristics of terrain) (Zhang and Goodchild 2002; Holmes, Chadwick, and Kyriakidis 2000; Fisher 1998). Such an error surface addresses the limitations of RMSE as a single metric to report the accuracy of DEM. It also helps to better understand the spatial distribution of DEM errors and DEM quality.

A spatially uniform error surface is the simplest error model generated based on randomly distributed noises with a mean of zero and standard deviation equal to RMSE (Hunter and Goodchild 1997; Sofia, Pirotti, and Tarolli 2013). In randomly distributed errors, values are completely independent of the values at neighboring cells. This case is unrealistic and is very seldom found in nature. Some degree of spatial autocorrelation is more common DEM errors. Spatially correlated random fields are used to simulate more realistic DEM error surfaces. A spatially correlated random fields can be generated in various ways. When data with higher

accuracy (i.e., check point elevations) is available, a spatially auto-correlated random field can be generated using Geostatistical techniques (i.e., correlograms, variograms or a sequential Gaussian simulation) (Darnell, Tate, and Brunsdon 2008; Oksanen 2006; Oksanen and Sarjakoski 2006; Holmes, Chadwick, and Kyriakidis 2000; Kyriakidis, Shortridge, and Goodchild 1999; Fisher 1998). But in lacking check point elevations, an unconditioned error surface can be generated. Spatial auto-regressive, pixel swapping or a Gaussian kernel method are available methods to simulate an unconditioned error surface (Wechsler 2007; Wechsler and Kroll 2006; Oksanen and Sarjakoski 2005; Ehlschlaeger 2002; Fisher 1998; Goodchild and Openshaw 1980). Finally, external topographic parameters can be used to model heteroscedasity of DEM error. DEM errors are expected to be affected by morphometric characteristics of terrain (Aryal *et al.* 2017; Salleh, Ismail, and Rahman 2015) and land cover type (Simpson, Smith, and Wooster 2017; Venzin 2013; Hodgson *et al.* 2005; Kraus and Pfeifer 1998). Slope, aspect, and vegetation canopy have been identified as significant predictors of error in SRTM DEMs (Shortridge, Fayne, and Rice 2017; Shortridge and Messina 2011). Least squares linear regression and geographically weighted regression can be used to model the heteroskedasity of DEM error (Erdoğan 2010; Hebeler and Purves 2009a; Hebeler and Purves 2009b; Carlisle 2005). The simulated DEM error surfaces are often used in a Monte Carlo approach to examine the effects of errors on the results (e.g., Shortridge, Fayne, and Rice 2017, Wechsler and Kroll 2006; Raafaub and Collins 2006; Aerts, Goodchild, and Heuvelink 2003; Ehlschlaeger 2002; Holmes, Chadwick, and Kyriakidis 2000; Goodchild 1992; Lee, Fisher, and Snyder 1992). In the Monte Carlo approach and the error propagation modeling, the original DEM and the parameters extracted from it are considered true values. DEM error surfaces are generated and added to the original DEM to make perturbed versions of the DEM. Parameters are extracted from the perturbed DEM and the residuals between

those and the original parameters are calculated. In this approach, the original DEM is considered error free.

The spatial distribution of DEM errors and the propagation of error to derived DEM parameters have been well documented in the literature (Shortridge, Fayne, and Rice 2017; Fisher 1998; Hunter and Goodchild 1997; Weibel and Brändli 1995; Wood 1994; Theobald 1989). Wechsler (2007) studies DEM errors in hydrological investigations. Shortridge (2001) characterizes DEM errors and its impact upon ecological applications. Veregin (1997) investigates the influence of DEM error on flow direction; Various DEM errors are simulated and added to the original DEM. The errors are generated within known ranges of RMSE, spatial autocorrelation and cross-correlation of DEM error and slope. He finds that multiple flow direction algorithms are less sensitive to DEM errors than the single flow (D8) direction algorithm. Aerts, Goodchild, and Heuvelink (2003) generate spatially correlated DEM error to investigate the propagation of error in site selection for a ski run using a Monte Carlo approach and sequential Gaussian simulation. Oksanen and Sarjakoski (2005) investigate error propagation in drainage basin delineation from DEMs using Monte Carlo simulation. Hengl and Reuter (2008) illustrate that errors propagate from the DEM to extracted parameters such as slope, Topographic Wetland Index (TWI) and soil redistribution.

2.2.5. Scale and Resolution

The notion of scale underlies much of the published research on terrain analysis and will form a prominent component of this dissertation research. DEM measurements (e.g., identifying critical points on a landscape, extracting terrain derivatives and morphometric parameters, extracting terrain features, and generalizing terrain surface) are known to be scale dependent (i.e., sensitive to DEM cell size) (Yang *et al.* 2014; Tarolli *et al.* 2009; Zhilin 2008; Zandbergen 2006;

Shary, Sharaya, and Mitusov 2005; Fisher, Wood, and Cheng 2004; Wood 1996; Hodgson 1995). Chang and Tsai (1991) show that when DEM resolution increases, there will be a bias towards lower slope values. So, DEM resolution should be chosen based on the scale at which features or processes under study become evident. Wood (2009) shows that a 3 by 3 focal window size on a 5 m resolution DEM is not appropriate for all geomorphological analysis, and a larger window size or a different DEM resolution should be used for example in identifying a terrace. Kienzle (2004) investigates the effect of DEM resolution (ranging from 100 to 5 m) on terrain derivatives, and concluded that the optimum resolution for estimating terrain derivatives is between 5 and 20 m.

Studies illustrate that the accuracy of a DEM decreases as the spatial resolution of DEM increases (Skidmore 2006, Gong *et al.* 2000). This happens because a coarser resolution DEM cannot capture the full complexities of the terrain surface. The impact of DEM resolution on topographic parameters is well-investigated (Grohmann 2015; Vaze, Teng, and Spencer 2010; Deng, Wilson, and Bauer 2007; Kienzle 2004). The accuracy of these parameters is usually measured based on a higher accuracy reference data. These studies have studied the impact of DEM error and DEM resolution on the extracted topographic parameters for the DEM pixel centroid. The error and variation of these parameter within a pixel influenced by DEM resolution has not been investigated.

Wood (1999) discusses three different ways to visualize terrain parameters calculated at various scales (here, measured over different spatial extents) that is called “visualizing scale dependency”. Every point has four dimensions (x, y, calculated parameter, and scale) that needs to be visualized. In one way, the parameter for each scale can be represented in a 2D raster. In an alternative way, the spatial dimensions can remain fixed and the parameter can be plotted for each

point over a range of scales, which is called a *scale-signature*. In another way, the mean and standard deviation of a parameter can be calculated over multiple scales and be represented in two 2D rasters. A similar concept of geometric measurements of line features across resolutions has been termed a *structure signature* (Buttenfield (1987, 1986, 1984)) and utilized to automatically distinguish among features as well as to automatically identify their geomorphometry.

Surface distance and area calculated from a regular gridded DEM depend on DEM resolution. Based on the Steinhaus Paradox, length increases with increased precision of measurement (Steinhaus 1960). Richardson (1961) found a consistent power law by plotting the log of line length against the log of the measurement sampling interval. Mandelbrot (1967) extended Richardson's work to demonstrate that the length of a geographical curve increases as the units of measurement get smaller. A similar paradox named the Schwartz Surface Area Paradox has been defined, noting that polyhedral approximations of area will tally to increasing magnitudes as the number of approximating polyhedra become smaller and fit a surface more closely (Feder 1988). These theories suggest that any measurement of length or area should be reported with the scale of measurement. In this research, surface-adjusted analyses are conducted in different scales. That is, surface-adjusted estimates are measured and compared across various DEM resolutions and based on different contiguity configurations to see in which scale surface-adjusted measurements make a difference in spatial modeling.

2.3. Spatial Analysis in Non-Euclidean Space

In addition to scale and resolution, another fundamental concept in modeling geographic space is Euclidean planar space wherein positional intervals are constant. Models defined in a Euclidean planar space are isotropic that consider a uniform planar space with identical values of a property in all directions. Non-isotropic geographic modeling is one Tobler's innovations in

geography and GIS (Tobler 1993). He inspires his ideas by five famous theoretical models in geography that simplify the real world based on isotropic geographic space: (1) agricultural land use modeled around the marketplace (Von Thünen 1975); (2) industrial location formulated using least cost path analysis (Weber 1909); (3) Central Place Theory, explaining the spatial distribution and pattern of human settlements in an urban system (Christaller 1933); (4) the Gravity Model of spatial interaction between two locations that is based on their size and proximity (Niedercorn and Bechdolt 1969); and (5) models of the diffusion and movement of an innovation across geographical space) (Hagerstrand 1968). Tobler states that the basic component of an isotropic geographic space is Euclidean distance. He incorporates time and cost distances between places into the above-mentioned theories and other geographic problems in order to demonstrate the challenges of non-isotropic geographic space. He poses the question of how a geographical circle of one hour travel radius can be formed, incorporating various factors such as location, time of day, transportation system, obstacles, and travel cost, to investigate the shape of this region in a spatial rather than temporal context. Tobler models the problem using differential calculus for distance on a manifold of variable curvature. He demonstrates the fact that the assumptions of Euclidean geometry do not satisfy non-isotropic applications in geographic space.

Tobler also encourage geographers to use a natural Earth-oriented geometry instead of Euclidean geometry (Tobler 1993). Tobler criticizes the published literature on the topic of spatial analysis for ignoring spherical-based analysis, and just focusing on planar calculations. He argues that a spherical coordinate system should be incorporated into spatial analysis to facilitate the analysis of global distributions. In this way, he tries to illustrate the benefit of “round earth thinking” instead of “flat earth thinking” for global analysis, asking the geospatial community to work toward an “Exploratory Global Analysis and Display System”. He suggests that in addition

to Euclidean geometry, the concepts of Riemann geometry should be taught and introduced. The focus of Riemann geometry is on curved surfaces instead of planar space. Solving spatial problems such as spatial interpolation, Voronoi partitioning, pattern and trend analysis, etc., on the sphere or ellipsoid are discussed and encouraged in his work.

Generally, Euclidean space and more specifically Euclidean distance is used in spatial analysis and GIS. However, Miller and Wentz (2003) discuss analysis in a non-Euclidean space. They argue that Euclidean models became the convention in an era when the spatial data and computation power was more limited, relative to present-day technology. Miller and Wentz (2003) propose alternative non-Euclidean geospatial measurement frameworks. This dissertation will test and evaluate surface-adjusted elevation, and area as an alternative geospatial measurement frameworks.

Distance measured on a terrain surface does not necessarily pass all three Euclidean metric criteria (positive distance, distance symmetry, and triangle inequality) or the parallel postulate (two parallel lines do not meet each other). Mathematically, for Euclidean distance $d(S_i, S_j) = \sqrt{(x_i - x_j)^2 + (y_i - y_j)^2}$, the metric criteria are as follows:

$$\text{Positivity:} \quad d(S_i, S_j) \geq 0 \quad (2.1)$$

$$\text{Symmetry:} \quad d(S_i, S_j) = d(S_j, S_i) \quad (2.2)$$

$$\text{Triangle inequality:} \quad d(S_i, S_j) + d(S_j, S_k) \geq d(S_i, S_k) \quad (2.3)$$

Figure 2.2 demonstrates how it is possible that the triangle inequality is not met for distances measured on a terrain surface. Planar distances in Figure 2.2 (a) meet all of the Euclidean metric criteria, but the surface distance in Figure 2.2 (b) does not meet the triangle inequality ($16.81 > 7.23 + 9.49$).

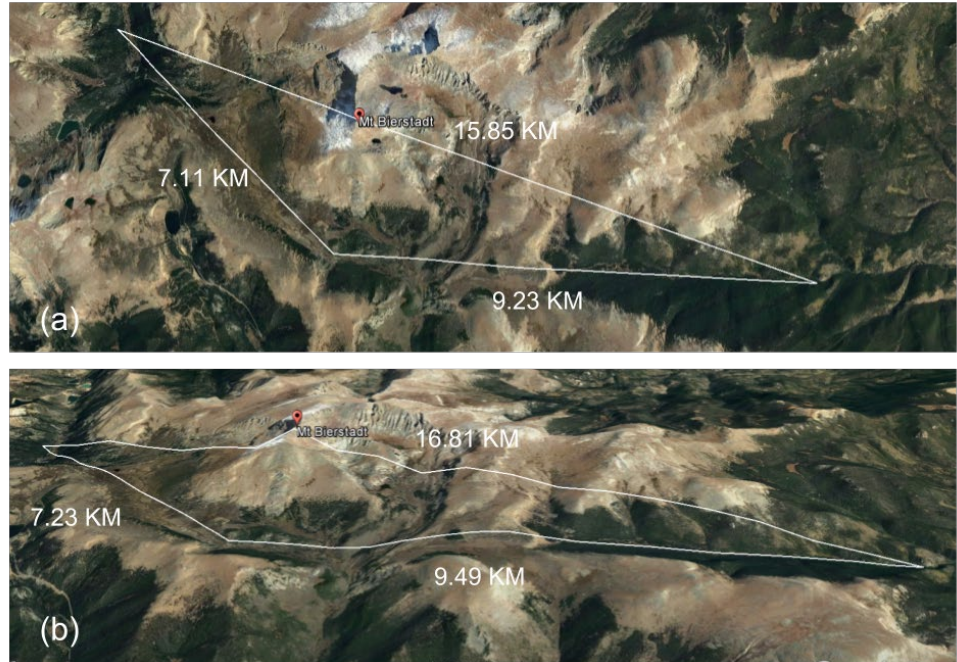


Figure 2.2. (a) Length of triangle edges are measured based on planar distance in the Euclidian space, and (b) surface distance adjusted to the terrain surface.

Figure 2.3 illustrates the parallel postulate. It can be seen that this criterion is satisfied always in Euclidean plane, but not necessarily satisfied on other types of manifolds. Various alternative geometries have been developed to deal with non-planar spaces.

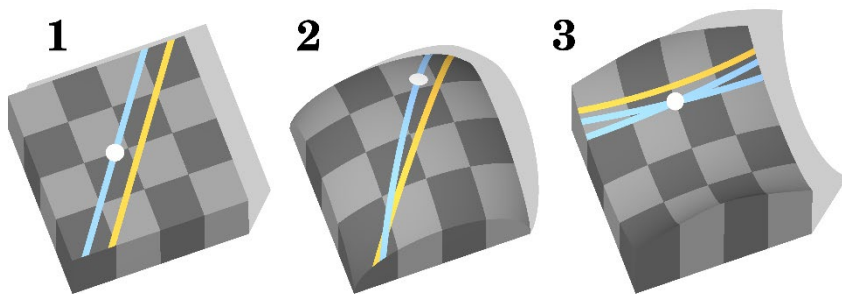


Figure 2.3. Parallel lines in Euclidean, elliptical and hyperbolic geometry (https://en.wikipedia.org/wiki/Parallel_postulate)

Autocorrelation and auto-covariance functions are based in distance and characterize the spatial dependence of processes. That is, these functions quantify the assumption that closer observations are more similar than those that are further apart (Tobler 1970). The straight-line or Euclidean distance used in these functions passes the metric criteria under the assumptions of stationarity and isotropy. Euclidean distance is easy to calculate, but it does not consider the slope and curvature of terrain. Therefore, surface-adjusted distance as a non-Euclidean distance can be considered to characterize spatial dependence as best as possible. However, it has been shown that using non-Euclidian distance does not necessarily pass metric criteria and might result in a non-valid variance-covariance functions. A valid variance-covariance matrix should be positive definite (Ver Hoef, 2018; Curriero 2006), in which eigenvalues are all real and positive. A variance-covariance matrix that is not positive definite contain zero or negative eigenvalues that leads to zero or negative determinants. Such a matrix cannot be inverted as it comprises dividing by zero, which is undefined. Therefore, this creates problems in different applications such as spatial interpolation that the variance-covariance matrix should be inverted.

There are several approaches in the literature for solving this problem. One substitutes spatial moving averages within a kernel convolution (Ver Hoef and Peterson 2010; Cressie *et al.* 2006; Krivoruchko and Gribov 2004)) and a second works with reduced rank Radial Basis Functions (generalized forms of splines, Wang and Ranalli 2007). Gneitling (2013) shows that geodesic distances (also non-Euclidean) limit kriging to exponential and spherical models. Crawford and Young (2008) apply isometric embedding or kernel convolutions. In isometric embedding, the coordinates are transformed to another geometry, keeping the distance between points as similar as possible to the original distances, and preserving topological adjacency. One commonly used isometric embedding technique is dimensionality reduction such as that used in

multidimensional scaling. Although, this technique satisfies the metric conditions, it has been shown that does not always ensure a positive definite variance-covariance function (Curriero 2006). Some variance-covariance models might result in a positive definite function even with non-Euclidean distance, but in other cases a negative variance-covariance function can result, even after using the isometric embedding technique (Crawford and Young 2008). Zou *et al.* (2012) use isometric embedding to address the problem that road network distance cannot guarantee that a matrix is positive definite. They conclude that the isometric embedding approach improves kriging interpolation accuracy.

Euclidean distance is the default assumption in many interpolation and geostatistical applications. However, several studies have been conducted on the use of non-Euclidian distance. For example, Greenberg *et al.* (2011) use least-cost path distances for the interpolation of water temperature in an inverse distance weighting interpolation. They illustrate that least-cost path distance results in a more realistic interpolation of water temperature by modeling their complex geographic connectivity (i.e., deltaic river system). In a different study, Little, Edwards, and Porter (1997) focus on kriging interpolation in estuarine streams. They suggest that distances between sites should be measured “as the fish swims”. Their results illustrate that kriging using in-water distances improves prediction accuracy. A third study (Boisvert and Deutsch 2011) investigates the use of shortest path distances in kriging. To ensure positive definiteness of the spatial covariance matrix, multidimensional scaling is used. Lu *et al.* (2014) modify geographically weighted regression method to use a non-Euclidean distance metric for exploring spatial heterogeneity. They conclude that the modified method improves the model fit and provides useful insights to better understand the complicated relationships in spatial data.

Surface-adjusted area will be examined in this research as an example of non-Euclidian

measurement. Area is usually measured on the plane. For example, the area of a land parcel, a forest patch or a wetland can be identified directly from land surveying or computed indirectly from a planar map using Euclidian coordinates. One key weakness of this approach is that the planar method used for calculating area does not account for the slope and curvature of the terrain, and can lead to under-estimation. Precious information may be lost when areas are systematically under-estimated. Hoechstetter *et al.* (2008) compare planar area versus surface area for several measurements such as patch area, patch perimeter, perimeter-area ratio, fractal dimension, shape index and terrain roughness for two different resolutions; and they conclude that terrain complexity significantly affects area and distance, but has only a small effect on shape measurements. Finding a suitable mathematical representation of the terrain surface is considered a challenge, and this research accounts for slope and curvature of the terrain.

2.4. Elevation Estimation from a Regular Gridded DEM

Some experiments are reported in the literature that model a terrain surface to estimate elevation from a regular grid DEM. Kidner, Dorey, and Smith (1999) test various interpolation methods to estimate elevations on regularized surfaces generated from six polynomial functions, and then densify these grids progressively. They conclude that higher order polynomials always lead to better results than linear polynomials for smooth mathematical surfaces. The application of their research to digital terrain models is questionable however, as they use smooth mathematical surfaces that do not realistically represent the irregularities and local complexities of real terrain.

In a later study, Kidner (2003) replicates the previous research, albeit on real DEMs generated from contour data with 25 m, 50 m, and 100 m intervals. DEMs are subsampled progressively by factors of 2, 4, and 8, and then the estimated elevations are interpolated back to the original resolution. Kidner concludes that a larger neighborhood and a higher order polynomial

that uses 9, 16 or 25 vertices always is more accurate than a bilinear interpolation that uses only four closest vertices. He finds that higher order polynomials result in up to 20% reduction in the RMS error. He does not use random sampling though, and he resamples a single DEM instead of working with independently compiled DEMs. Both factors confound the use of inferential statistical analyses and thus limit the robustness of his work. Essentially, his work is focused on resampling issues rather than on estimating elevations of off-center points in actual terrain. In another study, Rees (2000) resamples a DEM to coarser resolutions and then interpolates the resampled DEMs to the original resolution. He shows that a bicubic interpolation method is more accurate than a bilinear method. Rees does not use a full suite of interpolators, limiting his study to DEM resolutions of 50 m and 600 m.

Li (1993) and Li, Zhu, and Gold (2004) argue that linear interpolators (such as bilinear or triangular methods) are the least misleading and most reliable methods, and high-order polynomials can lead to dramatic oscillations that do not reflect actual elevations. These statements however are mentioned without empirical results or mathematical proofs. Shi and Tian (2006) combine bilinear and bicubic interpolation methods into a hybrid interpolator. They argue that a flat terrain can be modeled using a low-order polynomial, while a higher-order polynomial is more applicable to rough terrain. In their study, low-frequency information is modeled with bilinear interpolation and high-frequency information is estimated using bicubic interpolation. This research is not tested on real terrain and a hybrid parameter is selected for the entire terrain without accounting for local variations.

Liu, Hu, and Hu (2015) argue that terrain has some inherent characteristics that any interpolation method must take into account. One inherent characteristic is that each terrain point has only one recorded elevation. To preserve this property, the interpolation method should be

bijective. A bijective function creates a one-to-one relationship between the terrain surface and the surface modeled by the interpolation function. Higher order polynomials are not bijective because if a point locates on the boundary of two adjacent cells, its elevation can be estimated by two different polynomials. Linear and bilinear interpolations in contrast always satisfy the bijective requirement.

A second inherent property of terrain is that it is isomorphic, meaning that the relative magnitudes of elevation values are invariant. That is, “if point A is higher than point B in the terrain, the interpolated elevation of A remains higher” (Hu, Liu, and Hu 2009). This property is important for accurate drainage network extraction from a DEM. Bilinear and higher order polynomials are not isomorphic functions because they may not be monotonic (Liu, Hu and Hu 2015). Moreover, isomorphism is not always guaranteed due to the limitations of flow direction algorithms and the discretization of the terrain surface (Wilson 2018; O’Neil and Shortridge 2013). It should be noted that the interpolation methods that guarantee terrain properties do not necessarily result in minimal vertical error (Liu, Hu and Hu 2015).

2.5. Surface Area Estimation from a Regular Gridded DEM

Spatial measurements of area are employed to quantify the size of geographic features. However, most measurements are in planar Euclidian space that is dominated by the perception of paper maps (Goodchild 2010). Determination of areas on the plane, sphere and ellipsoid have been well-studied (Tobler 1963, Danielsen 1989, Usery *et al.* 2003, Sjöberg 2006). Spherical methods are used to calculate area of a geographical region on a sphere. The region is divided into a set of spherical triangles and based upon the geographic coordinates of its vertices the area is calculated (Kimerling, Buckley, and Muehrcke 2012). Pędzich and Kuźma (2012) propose a method for calculating the area of geodesic polygons on the ellipsoid. Area calculations on the ellipsoid are

complicated and the equal-area projection of the ellipsoid onto a plane is widely used. Berk and Ferlan (2018) investigate equal-area projections for the accurate area determination in the cadaster. Determination of areas on the plane, sphere and ellipsoid cannot represent the complex reality of a terrain surface (Tobler 1993; Goodchild 1992). With the advances in processing speed and increased availability of terrain data, planar area measurements can be adjusted to include the vertical component of the terrain surface to characterize area more realistically, which can improve spatial analysis and measurement (Buttenfield *et al.* 2016). Terrain surface is modeled in various ways for surface area calculations. Lidar point cloud can be used to model the landscape and to estimate terrain measurements (e.g., Petras, Newcomb, and Mitasova 2017; Blaschke, Tiede, and Heurich 2004). A voxel-based representation of space can be implemented to characterize terrain surface using lidar point cloud data (e.g., Jjumba and Dragićević 2016; Schilling, Schmidt, and Maas 2012, Mitasova *et al.* 2012). A triangular irregular network is used in various studies to model the terrain surface (Gold 2016a, Gold 2016b). A regular gridded DEM is used to estimate terrain measurements such as slope, curvature, surface distance and surface area (Hoechstetter, Thinh, and Walz 2006; Jenness 2004). This research aims to investigate surface area calculations from a regular gridded DEM.

Estimating the area of features is very important in geographic analysis. The area of a land parcel, a forest patch or a wetland can be computed directly from land surveying or from a map. When the method used for calculating area ignores the effects of topography and surface roughness, it does not account for the slope and curvature; and planar measurement can distort information when areas are systematically underestimated (Wilson 2018; Ying *et al.* 2014; Hoechstetter, Thinh, and Walz 2006).

For example, Xie *et al.* (2017) contend that surface area is quite different from ellipsoidal

areas in mountainous areas, and the ellipsoidal areas (i.e., area calculated based on distances on an ellipsoidal surface) do not meet the requirements of land and forestry surveys. Zhiming *et al.* (2012) illustrate that surface area is significantly larger than planar area in two different mountainous areas using a parametric T-Test. Monterroso *et al.* (2013) find that home-range (i.e., a density function that characterizes the probability of finding an animal in a specific area) estimates can be significantly biased when topography is ignored. Rogers *et al.* (2012) determine that the area of forest fire patches can be underestimated by as much as 20% when planar measurements are used. Jenness (2004) demonstrates that surface area will always exceed planar area, adding that the ratio of the two can provide a useful measure of terrain roughness, as the discrepancy increases between the two measures. He describes examples of how the true surface area of the landscape is very important in landscape analysis and studies of wildlife habitat. He *et al.* (2018) illustrate that the surface area for measuring forest biomass carbon storage and ecological compensation can increase measurements by as much as 10.13%.

The spatial nature of mountainous landscape structures is quantified using both planar and surface area to better understand how the landscape spatial pattern is affected by topography (Zhang *et al.* 2018). Many other authors point out that topography has a key role in the analysis of pattern and landscape structure, and slope and curvature have a significant impact on landscape measurements used in landscape ecology (Wu *et al.* 2017; Liu *et al.* 2017; Rogers 2012; Batista *et al.* 2012; Stupariu, Pătru-Stupariu, and Cuculici 2010; McGarigal, Tagil, and Cushman 2009; Hoechstetter, Thinh, and Walz 2006). Planar measurements are not relevant for analyzing landscape structure for habitat modeling, interlinked biotopes, erosion processes, microclimate, and analysis of forest stands (Walz *et al.* 2016). Kienzle (2010) finds significant area underestimation in hydrological modeling, especially in steep terrain. Hoechstetter *et al.* (2008)

compare planar area with surface area to characterize patch area, patch perimeter, perimeter-area ratio, and terrain roughness for two different resolutions (2m and 20m). They conclude that terrain complexity significantly affects area and distance calculations. The surface area calculation methods also are compared in Zhang *et al.* (2011) who conclude that when more than 30% of a region contains slopes greater than 18.2° , the difference between planar and surface area can exceed 5%. In this dissertation, the scale-, algorithm-, and topography dependence of surface area calculations are investigated.

Several available methods can determine surface area on terrain (Berry 2002, Jenness 2004, Xie *et al.* 2017). Surface area can be calculated simply as planar area / $\cos(\text{slope})$ (Berry 2002, Kundu and Pradhan 2003). Dorner, Lertzman, and Fall (2002) use this method to calculate surface area to account for non-uniform topography in landscape pattern analysis. Grohmann (2004) and Jenness (2004) calculate the ratio of surface area to planar area as a measure of terrain roughness. Jenness (2004) calculates the surface area in a regular grid DEM using a focal moving window by dividing each pixel into eight triangles. A Triangulated Irregular Network (TIN) can also be used to calculate surface area within each triangle (Xue *et al.* 2016). This method takes the slope of the terrain into account. TIN-based surface area calculations are preferable for vector data, while Jenness' method is preferable for raster data because the pixels in a raster surface area do not nest perfectly inside polygon boundaries. The surface area of vector data can be measured directly from the TIN surface or by generating the raster surface area and then clipping the raster cells using the vector polygon boundary (Xie *et al.* 2017). Zhang *et al.* (2011) compare the TIN-based method with Jenness' method for six mountain regions and conclude that the surface areas calculated from these methods are equivalent. Xue *et al.* (2016) argue that triangle-based surface area calculations are biased due to the nonlinear mapping of the length measurements from DEM that comprise

measurement errors. They propose a bias correction formula based on the variance of error in DEM to compute a more accurate estimate of the surface area. Therefore, the precision of DEM data is required to estimate bias but such information often is not available. Furthermore, DEM error has a complex structure and the variance of error or RMSE provide a single global measure and do not represent the spatial variation of error across a terrain surface.

A continuous surface also can be modeled to calculate surface area (Song, Chen, and Zhou 2013). One can apply continuous interpolation methods to reconstruct the three-dimensional (3D) surface of each pixel using contextual information from adjacent pixels (Ghandehari, Buttenfield, and Farmer 2017, Buttenfield *et al.* 2016). Each DEM cell is modeled with a polynomial function $z = f(x,y)$ whose surface area can be calculated with a double integral. In pilot work for this dissertation, the double integral method was tested on regular mathematical surfaces, but it proved computationally very slow. Even with the emergence of High Performance Computing (HPC), double integral methods for computing surface area are not yet feasible in terrain modeling processes simply because the basic computation of surface area remains overly time-consuming. Xue *et al.* (2018) approximate the double-integral formula using a Taylor series to reduce computational costs. A quadratic polynomial $(z(x,y) = a_0 + a_1 x + a_2 y + a_3 xy + a_4 x^2 + a_5 y^2)$ based on a least squares solution is used to reduce the effects of errors. Xue *et al.* argue that their proposed method is more accurate and robust due to the reduction of DEM errors. In general, interpolation methods create a continuous surface based on the DEM grid points. These surfaces are approximated at a specific spatial scale and so errors and uncertainty are inevitable (Schneider 2001, Goodchild and Haining 2004, Yao and Murray 2013). Li *et al.* (2018) investigate the approximated double integral method as well. They examine the truncation error (i.e., the error that results from using Taylor series as an approximation in place of an exact mathematical

function), concluding that the truncation error and absolute error are lower for finer DEM resolutions and lower terrain complexity.

2.6. Summary

In this chapter, a brief background of digital terrain modeling was discussed, focusing in turn on extracted parameters and features from a regular gridded DEM, widely used methods for digital terrain modeling, DEM errors, metrics used for reporting DEM accuracy, and scale and resolution in terrain modeling. These are reviewed to build a counter argument to the assumption that elevation is constant within each pixel. When topographic parameters such as elevation, slope and curvature are reported for the pixel centroid and their variation within a pixel is ignored, subsequent measurements such as landscape fragmentation or upstream drainage area can be biased, especially in higher slope or rough terrain. The spatial structure of DEM error has been well investigated in the literature, but the uncertainty introduced by the rigid pixel assumption has been neglected.

This dissertation will investigate how the surface-adjusted paradigm can improve the estimation of elevation and surface area in terrain modeling. Surface-adjustment relaxes the rigid pixel assumption and acknowledges sub-pixel variations of elevation, slope, and curvature. Specifically, this research aims to refine the methods for determination of elevation and area and to monitor reductions in error across spatial resolution and in terrain of varying roughness.

Chapter III

Cross-Scale Analysis of Sub-pixel Variations of Elevation in Digital Elevation Models

3.1. Introduction

The first surface-adjusted experiment of this dissertation is surface-adjusted elevation. This chapter relaxes the rigid pixel assumption, allowing for possible sub-pixel variations in slope and curvature for estimating elevation of off-centroid points from a regular gridded DEM. Different interpolation methods are compared to investigate sub-pixel variations of elevation in a regular gridded DEM. Tests are presented estimating elevation values for 20,000 georeferenced off-centroid random points from a regular grid DEM, using a variety of exact and inexact local deterministic interpolation methods, within contiguity configurations incorporating first and second order neighbors. The use of random sampling permits statistical inference to establish whether method or configuration differences are significant.

The analysis examines the accuracy of surface-adjusted estimations across a progression of spatial resolutions (10 m, 30 m, 100 m, and 1,000 m DEMs) and a suite of terrain types varying in latitude, altitude, slope, and roughness. The study areas of this research were selected based on the availability of lidar data because the methods proposed in this dissertation are compared and

validated against estimated elevations on a 3 m lidar data benchmark. Comparison among interpolation methods is intended to establish guidelines as to which provides the most accurate estimation at a particular resolution and for a particular type of terrain. The analysis also considers the balance between the increased computations needed to estimate surface-adjusted elevation against the improvement in accuracy.

3.2. Justification for the Research Approach

As discussed in the previous chapter, some experiments demonstrate that higher order polynomials outperform lower order polynomials, while others show the opposite outcome (Liu, Hu, and Hu 2015; Shi and Tian 2006; Li, Zhu, and Gold 2004; Kidner 2003; Rees 2000; Kidner, Dorey, and Smith 1999). The results may be contradictory because of several reasons: for example, some do not work on real terrain; some do not test a full suite of interpolators; some do not use random sampling; and some resample a single DEM instead of working with independently compiled DEMs. These inconsistencies present compelling reasons to justify the systematic empirical testing presented in this research. Each criticism has been considered in turn in preparing the research methodology for the current study, whose goal is to establish clear guidelines for interpolating off-center elevation values.

In response to the first criticism (not working on real terrain), DEMs from six different terrain types will be used to investigate how elevation varies within a pixel. Moreover, the set of mathematical surfaces used by Kidner, Dorey, and Smith (1999) were tested using a suite of interpolators. Results of this test replicate the conclusions of their work that bicubic interpolation is consistently more accurate than is bilinear interpolation. It should be noted that interpolation methods used in the surface-adjusted paradigm are only mathematical abstractions, and real terrain is rarely a smooth mathematical surface (Deng 2009; Florinsky 1998).

In response to the second criticism (not testing a full suite of interpolators), the research comparatively evaluates discrete and continuous local interpolators, incorporating exact and inexact estimation methods. Weighted average, linear, bilinear, biquadratic, bicubic, and least squares fitting are compared, along with different contiguity configurations that incorporate first and second order neighbors. Other interpolation methods such as Splines, Kriging, and Natural Neighbor are widely used for the interpolation of irregularly spaced points to generate a regular grid (Chen *et al.* 2014; Cressie 2015; Mitášová and Mitáš 1993; Cressie 1988). These methods however are not computationally efficient for estimating elevation, or slope, or curvature of a point from a regular grid DEM, and are not discussed this dissertation.

To avoid problems associated with the third criticism (lack of random sampling), the elevation of 20,000 points are sampled randomly from a DEM. The use of random sampling permits statistical inference to establish whether method or configuration differences are significant, comparing RMSE metrics between estimated elevations and a 3m lidar benchmark to assess differences among the various methods, configurations, and resolutions.

To address the fourth criticism (the use of resampled DEMs as opposed to independently compiled DEMs), this research examines DEMs independently compiled at 10 m, 30 m, 100 m, and 1000 m, using sub-pixel variations that can be directly validated from an independently compiled 3 m resolution lidar data benchmark.

3.3. Dataset and Study Areas

Six datasets were chosen based on maximizing the variation in terrain characteristics in latitude, altitude, precipitation, land use regimes and terrain roughness. An additional important criterion for dataset selection was the availability of 3 m resolution DEM based lidar data, which

is used for validation. While coarser resolution terrain data are available for the continental US, coverage at 3 m resolution is more limited. Six study areas will be tested, and one will serve to explain the research methodology. This same study area was utilized in a previously published pilot study (Ghandehari, Buttenfield, and Farmer 2017). Errors in the data and results were discovered after the pilot study was complete, and the data was downloaded again and the analysis re-run completely for the current results, generating different values in the statistical analysis than were published previously. The morphological characteristics of study areas are listed in Table 3.1. Figure 3.1 shows their location within the United States.

Table 3.1. The morphometric characteristics of all six study areas. Terrain surface roughness was calculated as the standard deviation of elevations in a 10 by 10 focal window of the 10 m DEM and is reported as its mean and standard deviation for the entire study area.

	Elevation (m)				Slope (°)		Roughness (m)		Study area size (Km ²)
	Maximum	Minimum	Mean	STD	Mean	STD	Mean	STD	
Washington	2,341.15	-0.68	445.04	438.55	15.29	14.39	8.24	7.92	4,533.35
Colorado	4,225.39	2,108.39	2,818.50	366.51	12.31	10.35	5.68	4.73	2,493.29
North Carolina	1,616.97	192.59	442.18	223.07	11.01	9.11	4.87	3.97	7,786.72
Nebraska	931.55	635.42	786.70	54.81	5.07	5.45	2.02	1.65	4,709.26
Texas	471.28	99.18	225.84	77.94	2.44	3.03	1.09	1.13	5,475.28
Louisiana	69.17	-4.87	13.81	12.26	0.92	1.53	0.35	0.44	5,307.17

The study area in North Carolina has its center at 35.798° N and 81.473° W. Its location at the southeast end of the Appalachian Mountains provides elevations ranging from 209 m – 1602 m. Its location where the Blue Ridge Mountains run down towards the coastal plains is a humid, hilly landscape, with annual precipitation averaging 51 inches (129.5 cm). The study area provides a mix of uninhabited land with smaller rural settlements.

The Washington study area is centered on 48.65° N and 122.16° W, near Bellingham. Its location near the northern tip of Puget Sound is cool and humid, with the Cascade Mountains

providing a range of elevation values (-1 m – 2362 m) and steep, rough terrain. Annual precipitation averages 41.9 inches (106.5 cm). The study area intermixes small coastal settlements with agricultural land. The Colorado study area (38.95 N, 106.20 W) lies in the dry High Plains area (precipitation averages 20.88 inches, or 53.04 cm) east of Aspen and Durango, dominated by cattle ranching and oil / gas exploration. A central flat area is rimmed by steeper slopes (2108 m – 4225 m).

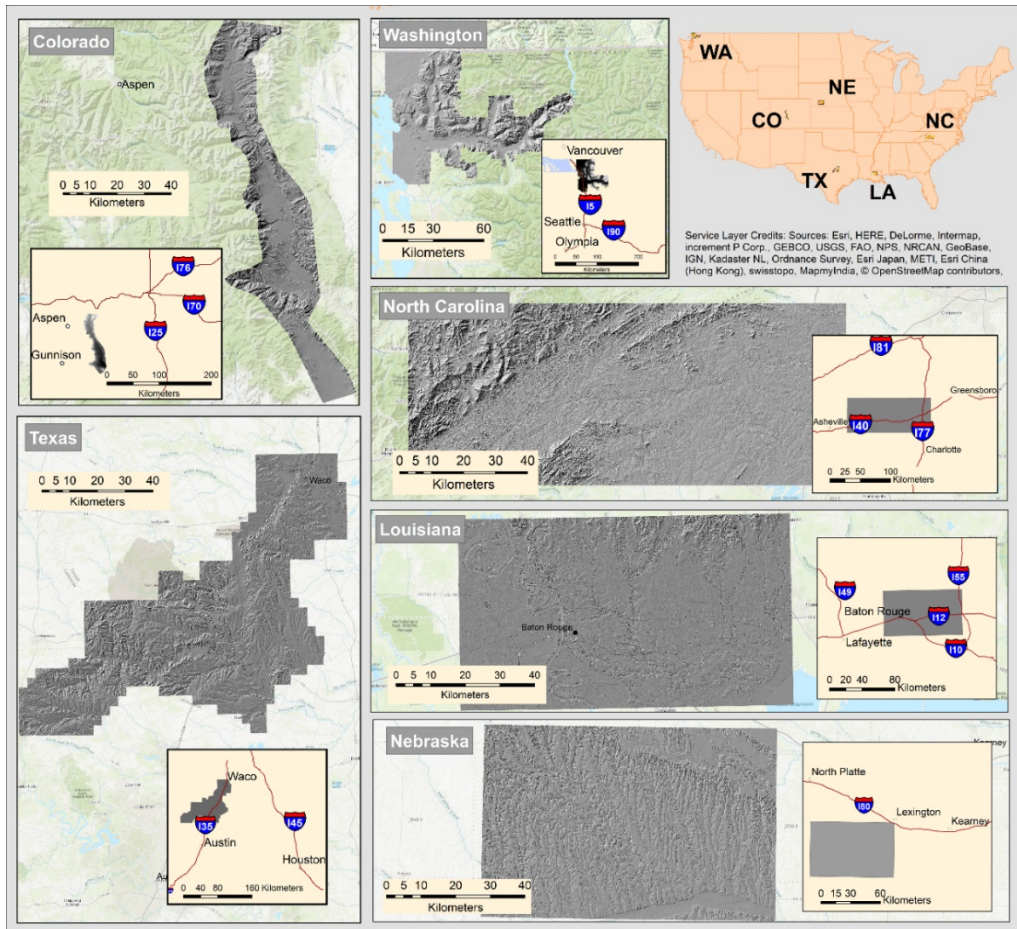


Figure 3.1. Six different study areas located in various terrain type and climate conditions.

The Nebraska study area (40.52° N, 100.26° W) has more uniform terrain whose elevation is lower (636 m – 938 m) but includes a uniform distribution of high frequency features evident in shallow stream channels dissecting the terrain. The land use is dominated by non-irrigated farming

and ranching and a transitional climate (average precipitation is 23.43 inches, or 59.51 cm). The Texas study area spans the area between Waco and Austin, a mix of urban and rural settlement. The precipitation regime is transitional, slightly wetter than Nebraska (32.80 inches or 83.31 cm rainfall), as well as lower and more uniformly flat (elevations 100 m – 468 m) than Nebraska. Louisiana is the fifth study area (30.51° N, 90.98° W), surrounding Baton Rouge and a segment of the Mississippi River. It is the most humid landscape, averaging 53.64 inches of precipitation annually. The landscape is agricultural with some pesciculture and oil and gas industrial activity.

DEM data will be tested at 10 m, 30 m, 100 m, and 1000 m resolutions, and compared against a 3 m lidar benchmark (Figure 3.2). Yellow points in Figure 3.2 are 20,000 randomly generated points to be used for the accuracy assessment of interpolated terrain elevations. The 3 m, 10 m, and 30 m resolutions are part of the USGS National Elevation Dataset (NED) and were downloaded from the National Map (<https://viewer.nationalmap.gov/basic/>). The USGS NED has seamless raster elevation data for the conterminous United States, Alaska, Hawaii, U.S. island territories, Mexico, and Canada. The 3 m, 10 m, and 30 m resolutions are independently compiled DEMs generated according to the methodology outlined in Gesch (2007). The accuracy of NED varies spatially due to the diversity of data sources. The overall absolute vertical accuracy of this dataset has an RMSE of 1.55 m estimated base on the geodetic control points of the National Geodetic Survey (NGS) that have millimeter- to centimeter-level accuracies (Gesch 2014). This RMSE is equivalent to 3.04 m in terms of the National Standard for Spatial Data Accuracy (NSSDA) at 95% confidence level. This RMSE is calculated based on the NED elevation value estimated at each NGS control point location using a bilinear interpolation. This assessment has been reported based on the April 2013 10 m version of the NED DEMs for the conterminous United States. The 3 m NED DEMs is generated from light detection and ranging (lidar) and other

high-resolution data sources. This dataset covers only some areas of the conterminous United States and small areas of Alaska. This dataset has been generate from numerous different lidar projects with varying specifications and there is no vertical accuracy reported for this dataset. It also should be noted that the NED DEMs has renamed to the 3DEP seamless bare earth DEMs (Jason M. Stoker 2018).

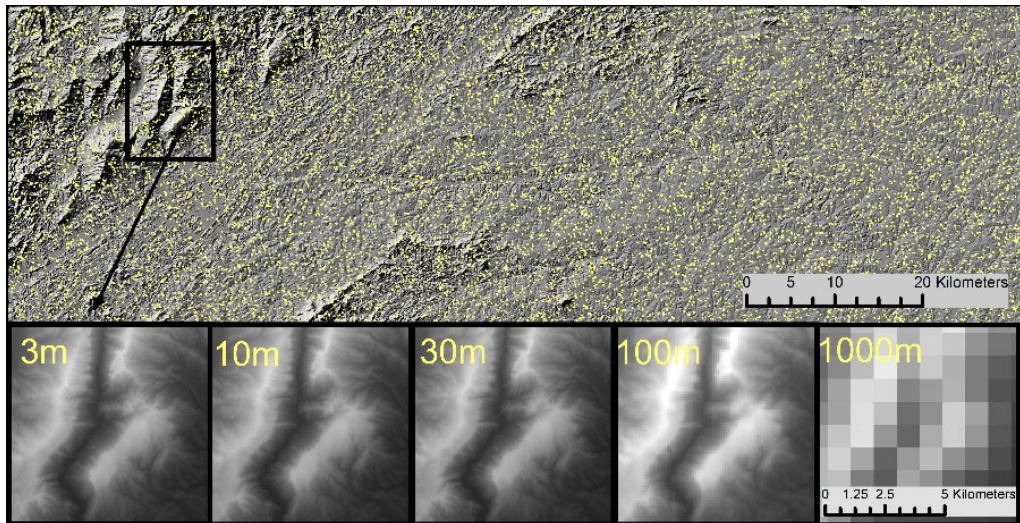


Figure 3.2. Study area in North Carolina used to demonstrate the research methods. The largest panel shows the full study area DEM (30 m resolution), with a sample of 20,000 randomly selected points shown in yellow. Lower panels show an inset at the 3 m (lidar validation) and four test resolutions, all labelled in meters.

The source for 100 m and 1000 m resolutions is the Shuttle Radar Topography Mission (SRTM) dataset (http://dds.cr.usgs.gov/srtm/version2_1/). The absolute vertical accuracy of this dataset has an RMSE of 4.01 m (Gesch *et al.* 2012). This accuracy is estimated based on the SRTM 30 m dataset using the NGS GPS bench mark control points. The NED and RRTM DEMs are projected in NAD 1983 UTM Zone 17N) coordinate system. It should be noted that the actual DEM resolutions are 1/9, 1/3, 1, 3, and 30 arc-seconds that are approximately 3 m, 10 m, 30 m,

100 m, and 1000 m, respectively.

3.4. Methods

Tests will estimate the elevation of 20,000 georeferenced random non-centroid points using different interpolation methods and contiguity configurations, across a progression of DEM resolutions. The tested methods differ in contextual information about surrounding pixels by varying the size and shape of the configuration neighborhoods. The output of those methods are evaluated against a 3 m lidar data benchmark. Note that, this research does not aim to provide a technique for resampling a DEM to finer resolutions. In fact, resampling a DEM to a finer resolution DEM does not capture the unpredictable variations in the terrain. This research aims to use and compare different interpolation methods for estimating elevation of arbitrary points from a regular grid DEM and monitor the reduction of error in different DEM resolutions.

Figure 3.3 diagrams the research workflow that involves a three-factor research methodology. The first factor refers to the four spatial resolutions (10 m, 30 m, 100 m and 1000 m). The second factor refers to the eight interpolation methods. The third factor indicates configurations of neighboring pixels to be tested. A range of contiguity configurations increases the number of pixels incorporated into elevation estimation. The second and third factors are not independent, since the interpolation method in some cases dictates the number of neighboring pixels. That is to say, tests for the least squares fitting and weighted average interpolators utilize a progression of configurations to establish not only the configuration that minimizes RMSE values but also to determine if increasingly large neighborhoods are associated with increasing or decreasing RMSEs, relative to Kidner's (2003, 1999) work. The other four interpolators test a single configuration of 3, 4, 9, and 16 neighboring pixels, respectively (Figure 3.3(b)).

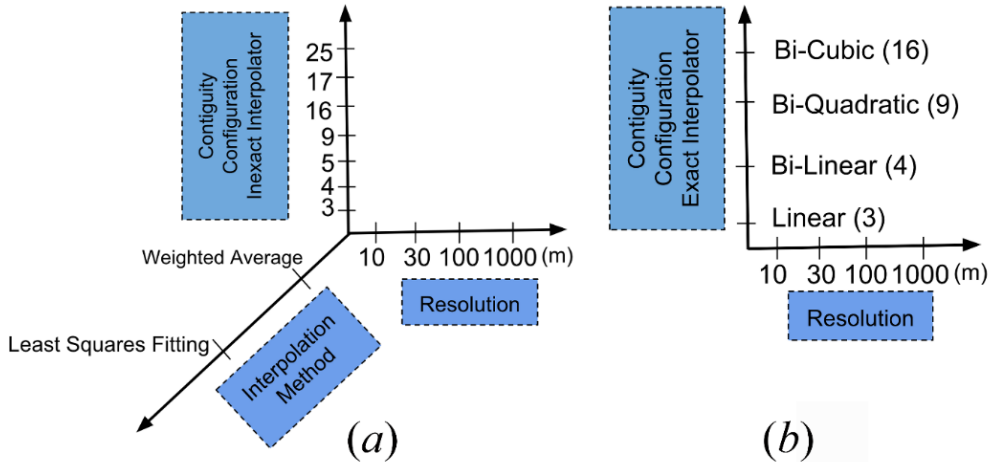


Figure 3.3. The research methodology compares estimates of DEM elevations spanning four common spatial resolutions, seven interpolation methods, and seven contiguity configurations of varying size and shape. (a) The least squares fitting and weighted average interpolation methods are tested in all contiguity configurations. (b) linear, bilinear, biquadratic, bicubic interpolation methods are exact interpolation methods and utilize 3, 4, 9, 16 neighboring pixels, respectively.

3.4.1. Interpolation Methods

Given a regular elevation grid within the defined neighborhood, different interpolation techniques will generate differing elevation estimates. The methods compared in this research include weighted average and least-squares polynomial fitting, which are inexact interpolators, and exact polynomial interpolators (linear, bilinear, biquadratic, and bicubic). Quadratic polynomials are further discussed as they are widely used for calculating slope and curvature from DEM. A Nearest Neighbor interpolator is used to estimate elevations from the lidar benchmark (3 m regular gridded DEM) for validation. It should be noted that the UTM coordinates cannot be directly used in polynomial fitting because large numbers might result in singularity (i.e., matrix is not invertible) in solving the equations. Therefore, these interpolation methods are solved for each individual pixel base on a local coordinate system centered on the central pixel (i.e., the central pixel has a coordinate of (0, 0)). The coordinates of random off-centroid points in the local

coordinate system are simply calculated by subtracting their UTM coordinates from the UTM coordinates of the central pixel. In what follows, different interpolation methods used in this research are further discussed.

- **Nearest Neighbor:** Each point represents a small area, a “region of influence” (i.e., the pixel) surrounded by a horizontal planar surface. Estimation proceeds by assigning the elevation of the centroid for whatever pixel the sampled point lies within. Although this approach is quite simple and easy to implement, it does not incorporate terrain derivatives and thus there is no surface adjustment. This method is used to estimate elevation from 3 m lidar data because the 3 m pixels are much smaller and therefore provide sufficiently precise estimates relative to the coarser resolutions.
- **Weighted Average:** This is a deterministic interpolator that computes an average elevation based on the elevation of neighboring pixel centroids. Distance to neighboring pixel centroids is commonly used as a weighting function, with shorter distances carrying larger weights. Weighted distance assumes that points that are closer together are more similar than those that are farther apart. Different distance functions can be used. The simplest and most common is the "Inverse Distance Weighting" (IDW) method, commonly used for continuous data such as terrain:

$$z(x, y) = \frac{\sum_{i=1}^n w_i z_i}{\sum_{i=1}^n w_i}; \quad w_i = \frac{1}{d_i^p} \quad (3.1)$$

where w_i and z_i represent the weight and elevation of each source point, respectively. Distance (d) is given an exponent (p) called distance power; and a larger exponent leads to progressively smaller weights at larger distances.

- **Exact Polynomial Interpolators:** This includes a set of deterministic methods whose estimates are based on a polynomial equation with varying terms and powers. By definition, the exact polynomial will generate a precise estimate of any original point. Polynomial equations with more terms create a surface with more freedom to undulate (Li, Zhu, and Gold 2004). Four different exact polynomial interpolators are used:

- 1) Linear: A triangle is generated from a three-term polynomial that creates a tilted plane based on the centroids of the nearest three pixels. Elevation is estimated based upon the position of each random off-centroid point within the tilted plane:

$$\mathbf{z} = a_0 + a_1 \mathbf{x} + a_2 \mathbf{y} \quad (3.2)$$

- 2) Bilinear: Like the linear polynomial, this is also a first order polynomial, but is based upon four known points. In contrast with linear interpolation, it utilizes a slightly larger neighborhood (Figure 3.4(c)):

$$\mathbf{z} = a_0 + a_1 \mathbf{x} + a_2 \mathbf{y} + a_3 \mathbf{x} \mathbf{y} \quad (3.3)$$

- 3) Biquadratic: A second order polynomial uses nine terms, generating a curved rather than planar surface. Nine closest pixel centroids are selected in the configuration:

$$\mathbf{z} = a_0 + a_1 \mathbf{x} + a_2 \mathbf{y} + a_3 \mathbf{x} \mathbf{y} + a_4 \mathbf{x}^2 + a_5 \mathbf{y}^2 + a_6 \mathbf{x}^2 \mathbf{y}^2 + a_7 \mathbf{x}^2 \mathbf{y} + a_8 \mathbf{x} \mathbf{y}^2 \quad (3.4)$$

$$+ a_8 \mathbf{x} \mathbf{y}^2$$

- 4) Bicubic: A third order polynomial increases the neighborhood to sixteen closest neighbors. This method calculates a surface having additional inflection points.

$$\begin{aligned}
z = & a_0 + a_1 x + a_2 y + a_3 xy + a_4 x^2 + a_5 y^2 + a_6 x^2y^2 + a_7 x^2y \\
& + a_8 xy^2 + a_9 x^3 + a_{10} y^3 + a_{11} x^3y^3 + a_{12} x^3y^2 + a_{13} x^2y^3 \\
& + a_{14} x^3y + a_{15} xy^3
\end{aligned} \tag{3.5}$$

- **Least Squares Fitting:** Least-Squares Polynomial Fitting is an interpolation method that minimizes the sum of squared errors using the Least-Squares technique. This is an inexact interpolator, and is not necessarily a better approximation of the terrain surface. A best-fitting surface can be linear or curved. Least squares fitting polynomials of order 1, 2, 3, 4, and 5 are used as follows:

$$\text{Order 1: } z = a_0 + a_1 x + a_2 y \tag{3.6}$$

$$\text{Order 2: } z = a_0 + a_1 x + a_2 y + a_3 xy + a_4 x^2 + a_5 y^2 \tag{3.7}$$

$$\begin{aligned}
\text{Order 3: } z = & a_0 + a_1 x + a_2 y + a_3 xy + a_4 x^2 + a_5 y^2 + a_6 x^2y \\
& + a_7 xy^2 + a_8 x^3 + a_9 y^3
\end{aligned} \tag{3.8}$$

$$\begin{aligned}
\text{Order 4: } z = & a_0 + a_1 x + a_2 y + a_3 xy + a_4 x^2 + a_5 y^2 + a_6 x^2y \\
& + a_7 xy^2 + a_8 x^3 + a_9 y^3 + a_{10} x^4 + a_{11} y^4 + a_{12} x^2y^2 \\
& + a_{13} x^3y + a_{14} xy^3
\end{aligned} \tag{3.9}$$

$$\begin{aligned}
\text{Order 5: } z = & a_0 + a_1 x + a_2 y + a_3 xy + a_4 x^2 + a_5 y^2 + a_6 x^2y \\
& + a_7 xy^2 + a_8 x^3 + a_9 y^3 + a_{10} x^4 + a_{11} y^4 + a_{12} x^2y^2 \\
& + a_{13} x^3y + a_{14} xy^3 + a_{15} xy^4 + a_{16} x^4y + a_{17} x^2y^3 \\
& + a_{18} x^3y^2 + a_{19} x^5 + a_{20} y^5 + a_{21} x^2y^2
\end{aligned} \tag{3.10}$$

Note that the first order polynomial shows an equation identical to the linear exact polynomial described above. The difference is that the linear exact method is based on the three-neighbor contiguity configuration, but the first order least squares fitting method is based on four-pixel and higher neighbor contiguity configurations. Least squares order two has been proposed by Evans (1980) for calculating slope and curvature. Least squares order three has been used by Haralick (1984) for step edge detection.

Quadratic Polynomials: Two kinds of quadratic polynomials are widely used for calculating slope and curvature from DEM; one is called partial quadratic model (Equation (3.4)) with nine coefficients that is an exact interpolation surface that passes through 9 sample points (Evans 1980), and the other is called full quadratic function (Equation (3.7)) with 6 coefficients that creates a non-exact smooth surface based on a least squares technique (Zevenbergen and Thorne 1987). Evans (2013) claims that the full quadratic function performs better in reducing the impact of DEM errors. Furthermore, the full quadratic function provides an error metric (e.g., standard deviation or RMSE). However, Zevenbergen and Thorne (1987) argue that the partial quadratic model works better for rugged terrain. Shary (1995) modified the full quadratic function in a way that the surface passes through the central point of the kernel. The Shary's calculations of elevation is as follows:

$$\mathbf{z} = z_5 + a_1 \mathbf{x} + a_2 \mathbf{y} + a_3 \mathbf{x} \mathbf{y} + (a_4 \mathbf{x}^2 / 2) + (a_5 \mathbf{y}^2 / 2) \quad (3.11)$$

Where the coefficients are as follows:

$$a_1 = (-z_1 + z_3 - z_4 + z_6 - z_7 + z_9) / (6 * w) \quad (3.12)$$

$$a_2 = (z_1 + z_2 + z_3 - z_7 - z_8 - z_9)/(6 * w)$$

$$a_3 = (-z_1 + z_3 + z_7 - z_9)/(4 * w^2)$$

$$a_4 = (z_1 + z_3 + z_7 + z_9 - 2 * (z_2 + z_8) + 3 * (z_4 + z_6) - 6 * z_5)/(5 * w^2)$$

$$a_5 = (z_1 + z_3 + z_7 + z_9 - 2 * (z_4 + z_6) + 3 * (z_2 + z_8) - 6 * z_5)/(5 * w^2)$$

Where z_1 to z_9 are the elevations of pixels inside the kernel (z_1 is the elevation of top-left pixel, and z_9 is the elevation of lower-right pixel in the kernel), z_5 is the elevation of the central pixel, and w is the pixel size.

3.4.2. Contiguity Configuration

Different contiguity configurations can be investigated based upon the number of neighbors (here 3, 4, 5, 9, 16, 17, 25). In this research, first (i.e., pixels on the border of a 3x3 kernel) and second order (i.e., pixels on the border of a 5x5 kernel) neighboring pixels are combined in different ways to configure the contiguity structure needed for different interpolation methods (Figure 3.4). Some interpolation methods are exact and can only be tested on one contiguity configuration. For example, the bilinear interpolation method is based upon four neighbors. The linear, bilinear, biquadratic, and bicubic interpolators are exact interpolators and use 3, 4, 9, and 16 neighboring pixels, respectively. On the other hand, as discussed in section 3.4, the weighted average interpolator can be tested on multiple contiguity configurations. For the weighted average, all possible configurations are tested to find the optimum number of neighboring pixels (that is, the configuration revealing the smallest RMSE). For the best fitting polynomial, all configurations except the 3-pixel configurations are tested; and the 3-pixel neighborhood is left out to insure inclusion of sufficient pixels in the least squares equation. It should be noted that in the least squares equations, an overdetermined system (more equations than

unknowns) is necessary. That is why the 3-pixel neighborhood is not tested for the best fitting polynomial. In the exact interpolators, the number of unknowns is equal to the number of equations and as a result there exist a single unique solution.

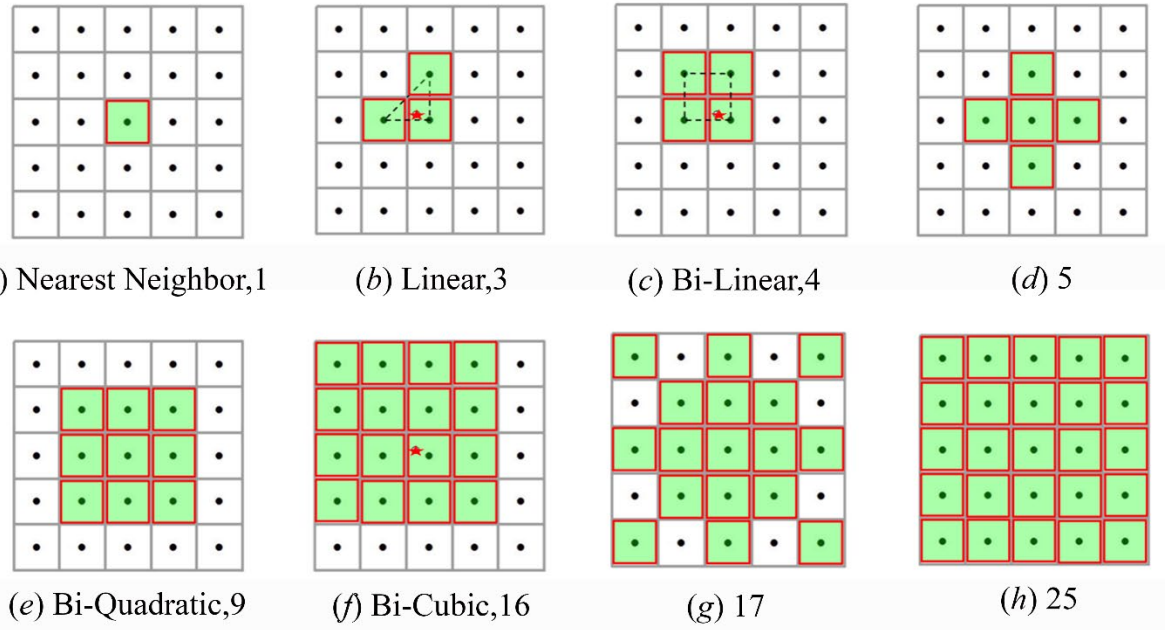


Figure 3.4. Contiguity configurations. The Nearest Neighbor configuration (a) will be used for validation. In (b), (c), and (f), the randomly sampled point is represented as a star and 3, 4, and 16 closest pixels are highlighted respectively. Based on the location of random point within the central pixel the contiguity configurations for the 3, 4, and 16 closest pixels are different. But, this is not the case for the other contiguity configurations. Weighted average and least squares fitting interpolators are tested using all configurations of 3 or more pixels to determine which neighborhood results in the smallest RMSE value.

3.4.3. Workflow and Processing

The workflow involves several steps. Each resolution DEM is processed one at a time. The 3 m benchmark DEM is loaded and a random sample of 20,000 points is generated, creating a shapefile containing coordinate positions in UTM meters, and elevations in meters extracted from the 3 m benchmark DEM and georeferenced on the test DEMs. At this point, the lidar DEM

is unloaded, and the shapefile is stored on disk. For each of the test DEMs, a nested loop processes each point for all DEMs and for all interpolation methods, then moves on to the next sampled point. Estimated elevations are added as new attributes in the original shapefile. Within the same nested loop, residuals (i.e., the difference between the interpolated elevation value and the corresponding 3 m lidar value) are calculated for each elevation (each sampled point). Once all sampled elevations have been estimated for all DEMs at all resolutions, the residuals are summarized by metrics described in the next section. The sequence of operations is as follows:

Cross-scale analysis of sub-pixel variation in DEMs using various interpolation methods

- (1) Load 4 Input DEMs (DEM10, DEM30, DEM100, DEM1000)
 - (2) Load benchmark (DEM3)
 - (3) Generate sample of 20,000 random points in the study area.
 - (4) For i in 20,000 random points:
 - For j in 4 Input DEMs:
 - For k in 6 interpolation methods:
 - Interpolate the elevation of point i based on the DEM resolution j using interpolation method k ($Elev_{ijk}$)
 - Compute $Residual_{ijk} = Elev_i$ of benchmark - $Elev_{ijk}$
 - (5) Accuracy Assessment (RMSE, Standard Deviation, etc.)
-

3.4.4. Accuracy Assessment

Accuracy assessment is conducted on the residuals. The residuals are calculated by subtracting the interpolated elevation value from the 3 m lidar value. Next, residuals are tested for normality (in preparation for statistical inference). Residuals are summarized by computing standard deviation (STD), Root Mean Square Error (RMSE), and Mean Bias Error (MBE).

$$\text{RMSE} = \sqrt{\frac{\sum_{i=1}^n e_i^2}{n}} ; \quad \text{STD} = \sqrt{\frac{\sum_{i=1}^n (e_i - e_{mean})^2}{n}} ; \quad \text{MBE} = \frac{\sum_{i=1}^n e_i}{n} \quad (3.13)$$

3.5. Results

3.5.1. Analysis of DEM Errors

Table 3.2 represents basic descriptive parameters of the residuals (mean, median, minimum, maximum, standard deviation, and 95th percentile—lower and upper bound) at different resolutions. These metrics are based on all sample points for the bilinear interpolation method. Negative mean values indicate overestimation at every resolution, increasing at coarser levels with increasing size discrepancy of test pixels relative to the 3 m lidar benchmark. The high values of minima and maxima are due to the occurrence of both positive and negative outliers. Two standard normality tests are run on the residuals — the Kolmogorov-Smirnov test and the Anderson-Darling test. The results of both tests verify that residuals are not normally distributed ($p\text{-value} < 2.2\text{e-}16$). Figure 3.5 illustrates the distribution of residuals for the bilinear interpolation method at various resolutions. Authors of other studies indicate that DEM vertical errors are usually not normally distributed due to small biases and outliers (Carlisle 2005; Fisher and Tate 2006; Höhle and Höhle 2009; Zandbergen 2011). It is clear that noise increases at coarser resolutions.

Table 3.2. Summary statistics of residuals for different resolutions for the bilinear interpolation method for North Carolina

Resolution	Mean (m)	Median (m)	Minimum (m)	Maximum (m)	Standard Deviation (m)	95th percentile lower bound (m)	95th percentile higher bound (m)
10	-0.01	-0.03	-18.76	15.82	0.91	-1.29	1.35
30	-0.01	0.00	-21.30	15.76	1.42	-2.17	1.37
100	-6.12	-4.70	-57.60	30.32	7.31	-20.41	2.51
1000	-5.41	-4.54	-187.21	191.11	29.35	-52.30	39.10

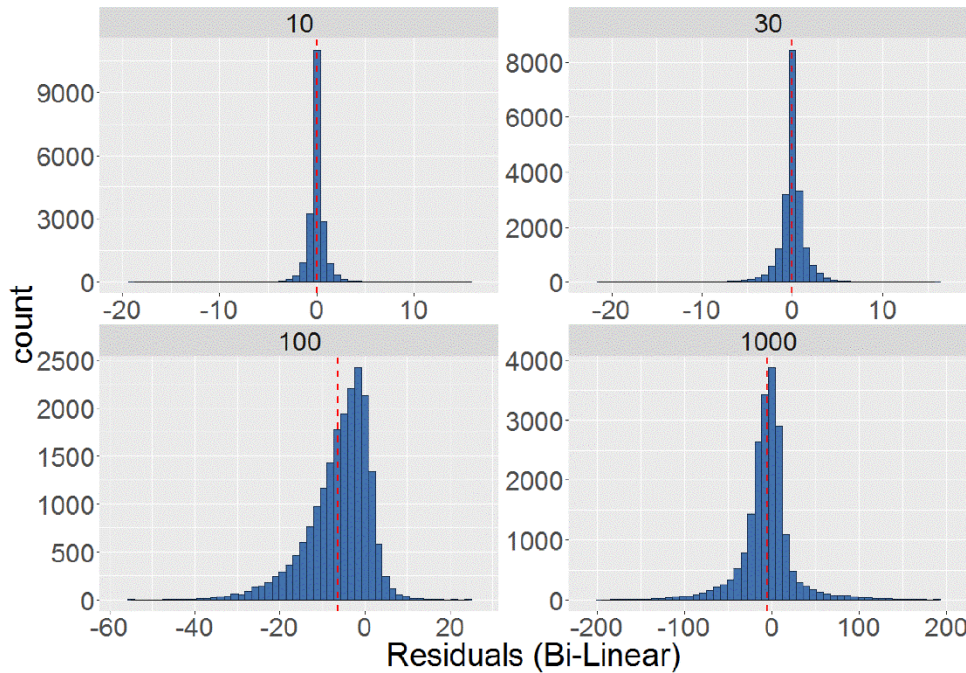


Figure 3.5. Distribution of residuals for the bilinear interpolation method in different resolutions for North Carolina

Outliers are an indication to inspect the spatial pattern of residuals more closely. Local Moran's I (Anselin 1995) was calculated for the residuals in order to visualize whether residuals with similarly high or low values are clustered. The residuals with a p -value smaller than 0.05 are considered significant. A map of North Carolina residuals display spatial heterogeneity that appears related to the varied character of terrain. The black triangle and ovals in Figure 3.6(b) highlight significant residuals resulting from bilinear interpolation and illustrate that many are situated in rougher terrain (in the northwest corner). These imply that terrain uniformity is an important factor needing further investigation, in accordance with other studies (Zhou, Liu, and Sun 2006).

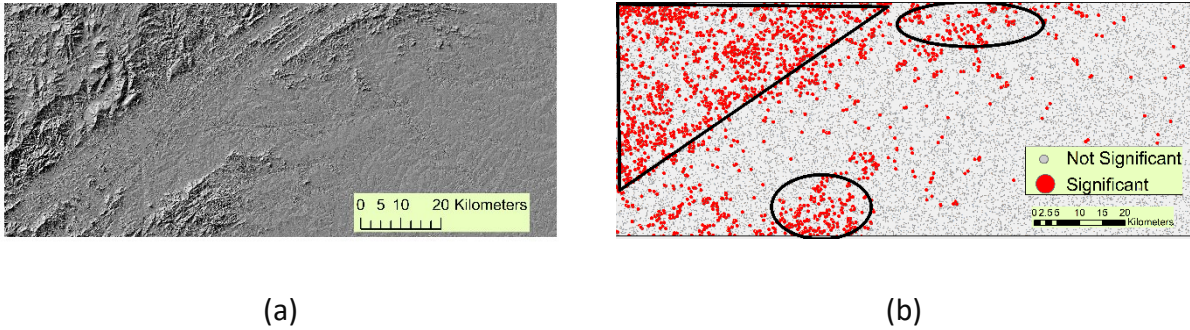


Figure 3.6. (a) Hillshade of North Carolina DEM, (b) Outliers of 20,000 residuals in 10 m DEM using the bilinear interpolation, with significant residuals enveloped in green. It is apparent that extreme residuals are situated in areas of roughest terrain.

Table 3.3 reports the correlation between the absolute of residuals and benchmark elevation, slope, aspect, curvature, local relief (the range of elevation in a 10 by 10 focal window), and roughness (the standard deviation of elevation in a 5 by 5 focal window) using the 30 m DEM as test data and the lidar benchmark as validation. All but one correlation coefficients are highly significant, though the high significance levels could be a consequence of the large number of sampled pixels. Slope has the highest correlation with the absolute of residual, indicating that DEMs could have greater errors in terrain with high slopes than with flatter slopes (Figure 10). A number of other authors also have reported that DEM error is positively correlated with slope (Hunter and Goodchild 1997; Carlisle 2005). In addition, there is a strong relationship between absolute of residuals and terrain roughness and local relief; and this also reflects the slope relationship, highlighted for all interpolators in Table 3.4. Although, the correlation between absolute of residuals and aspect is close to zero, there is a nonlinear relationship (i.e., curved pattern) between residuals and aspect (Figure 3.7). For the aspects smaller than 100° and larger than 300° , the majority of residuals are positive. The correlation between residuals and aspect is zero because Correlation can measure only the linear relationship between variables. Correlations tend to drop slightly at coarser resolutions for the interpolated residuals. For the

linear method, for example, correlations drop from 0.618 (10 m) to 0.411 (1000 m), although all are significant. This happens as a result of coarser resolution DEMs being unable to represent steep slopes. Mean slope of a DEM will tend to decrease as the resolution becomes increasingly coarse.

Table 3.3. The correlation and p-values between residuals and elevation, slope, aspect, curvature, local relief, and roughness for North Carolina (30 m DEM is used here). The *p*-values are so small that even at 4 or 5 decimal places they do not differ from zero.

Variable	Elevation (m)	Slope (°)	Aspect (°)	Curvature (cm)	Roughness (m)	Local relief (m)
Correlation	0.395	0.617	0.000	0.309	0.612	0.576
P-values	0.00	0.00	0.96	0.00	0.00	0.00

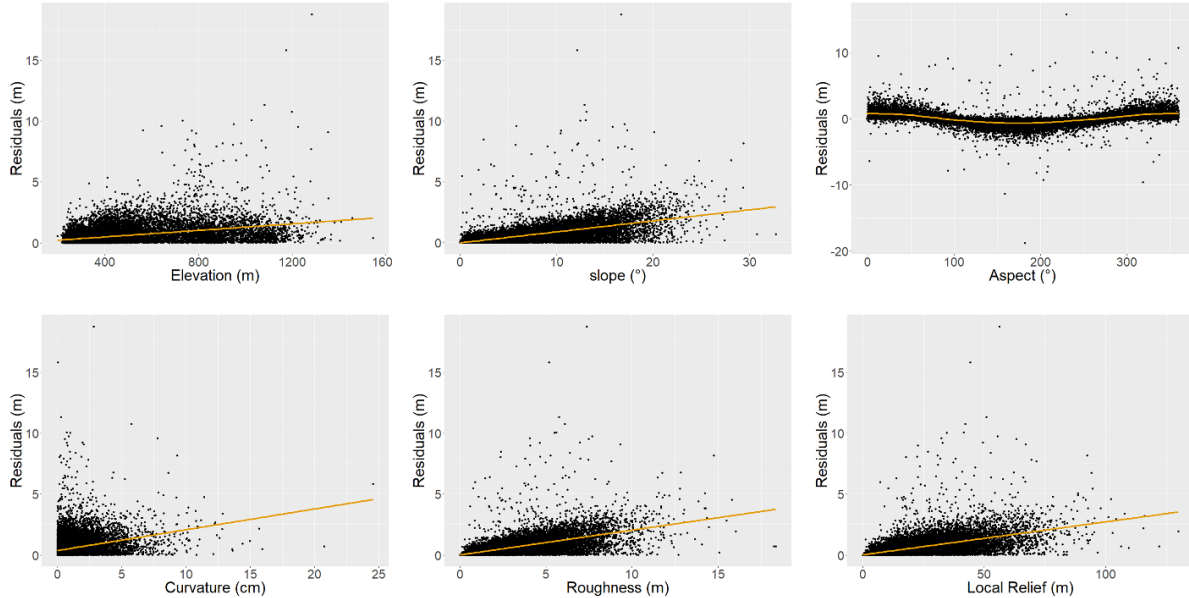


Figure 3.7. Residuals are plotted against elevation, slope, aspect, curvature, roughness, and local relief (10 m DEM and bilinear method is used here).

Table 3.4. Correlation between slope and residuals for different interpolation methods for North Carolina (10 m DEM).

Variable	Li3	BiLi4	WA4	BiQ9	BiC16
Correlation	0.618	0.618	0.617	0.622	0.621
P-values	0.00	0.00	0.00	0.00	0.00

3.5.2. Optimal Configuration for Weighted Average Interpolator

Table 3.5 shows the RMSEs resulting from the weighted average method for all contiguity configurations, and across all resolutions. The type of contiguity configuration appears to play a role in estimation errors. The 4 neighboring pixel configuration (Figure 3.4(c)) shows the lowest RMSE in all resolutions for this interpolator, and is chosen for the further analysis in Section 3.4.4. It should be noted that the 4 neighboring pixel configuration is also used in the bilinear interpolation. The range of RMSEs at each resolution is quite small. The 4 neighboring pixel configuration is a compromise between processing time and accuracy. Figure 3.8 graphs various distance powers (p in Equation 3.1) at different resolutions, and an exponent equal or close to 2.0 (i.e., Euclidean distance across the 4 pixels) gives the lowest RMSE values in all resolutions.

Table 3.5. RMSEs for the weighted average method using different number of neighbors in different resolutions for North Carolina; boldface indicates the lowest RMSE in each resolution

Contiguity Configuration	10 m	30 m	100 m	1000 m
WA3	0.93	1.54	9.65	30.42
WA4	0.92	1.48	9.64	30.23
WA5	0.97	1.79	9.90	31.23
WA9	0.96	1.77	9.98	31.49
WA16	0.95	1.83	10.13	32.36
WA17	0.97	1.92	10.21	32.40
WA25	0.98	2.08	10.44	33.43

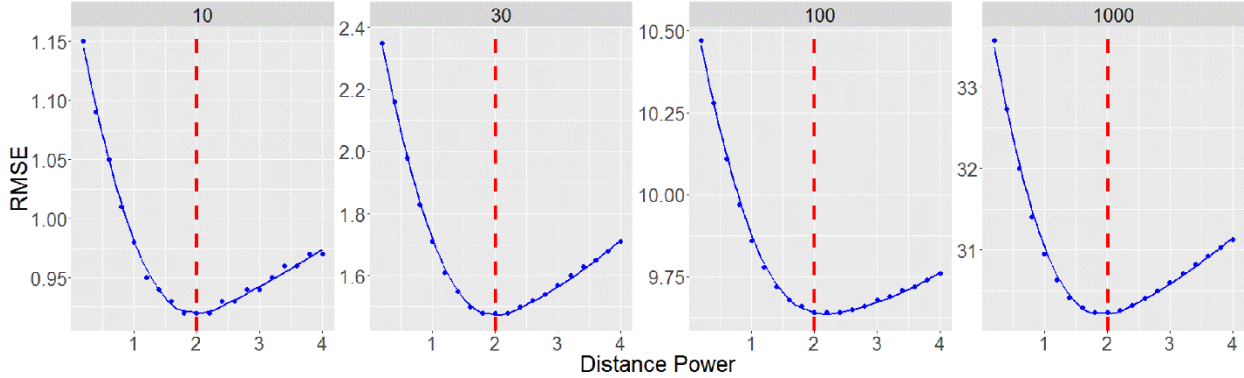


Figure 3.8. RMSE values of the weighted average method calculated for various distance powers ranging from 0.2 to 4.0 at each test resolution.

3.5.3. Optimal Configuration for Least Squares Fitting

Table 3.6 shows the RMSEs for the Least Squares Polynomial method. Different orders and configurations are tested. In the Table, the second order polynomial with a 9 neighbor pixel configuration shows the lowest RMSE at 10 m, 30 m, and 100 m resolutions. At 1000 m resolution, the first order polynomial with a 4 neighbor pixel configuration shows the lowest RMSE, with the second order 9-neighbor configuration showing the next lowest RMSE in the table overall. Comparing across resolutions for any given order polynomial, there is a general trend where RMSE increases with increasing numbers of neighboring pixels. This happens because increasing the order of polynomials forces a larger neighborhood configuration, which may introduce unwanted fluctuations in the generated surfaces.

Comparing each configuration across polynomial orders, a more confusing result emerges. For some configurations, the RMSE drops from 10 m to 30 m or 100 m resolution, and then rises. For example, the 16 pixel configuration at 1000 m resolution drops from 40.81 to 32.89 to 31.42 and then jumps to 47.06, the table's highest value. In contrast, the 25-pixel configuration drops steadily from 45.30 to 31.17 across all four resolutions.

It can be seen that 4, 9, 16, and 25 neighbors have the lowest RMSE for polynomial orders

1, 2, 3, and 4, respectively. This means that each polynomial has its own optimum contiguity configuration with respect to minimizing RMSE. This also implies that for compact neighborhoods a linear approach (i.e., first order polynomial) is sufficient for a good fit, and for 9 or higher pixel configurations a higher order polynomial works better than linear polynomials with higher degrees of freedom (i.e., more equations than unknowns) for the least squares equations at most resolutions. Linear surfaces cannot fit as well as second order polynomials, if 9 contiguity configurations is used. The polynomial order 2 with 9 neighbors (i.e., Evan's method discussed in Section 3.4.1) is selected as the optimum method for further analysis.

Table 3.6. RMSEs for the least squares fitting method using various polynomial orders and different number of neighbors in different resolutions for North Carolina. Boldface indicates the lowest RMSE in each resolution.

Polynomial order	Contiguity Configuration	10 m	30 m	100 m	1000 m
1	4	0.91	1.44	9.61	30.06
	5	0.92	1.67	9.95	31.04
	9	0.97	2.11	10.53	35.28
	16	1.09	2.94	11.69	40.81
	25	1.26	3.78	12.96	45.30
2	9	0.90	1.40	9.51	30.49
	16	0.92	1.68	9.91	32.89
	17	0.94	2.01	10.38	35.56
	25	1.09	2.05	10.43	35.88
3	16	0.91	1.51	9.69	31.42
	17	0.93	1.82	10.12	33.96
	25	0.93	1.88	10.21	34.54
4	16	1.01	1.94	9.95	47.06
	17	1.00	1.75	9.66	46.15
	25	0.91	1.46	9.58	31.17
5	25	1.05	2.18	10.24	49.65

3.5.4. Optimal Quadratic Polynomial Method

Table 3.7 illustrates the RMSEs for three different quadratic polynomials discussed in the previous section. It can be seen that the Zevenbergen and Thorne's method has the lowest RMSE,

and Sahry's method is slightly better than Evan's method. Therefore, the Zevenbergen and Thorne's method (biquadratic) is selected as the optimum method in all of the resolutions for further analysis. It should be restated that the quadratic polynomials use the 9 contiguity configuration.

Table 3.7. RMSEs for the quadratic Polynomials using different number of neighbors in different resolutions for North Carolina. Boldface indicates the lowest RMSE in each resolution.

	10 m	30 m	100 m	1000 m
Evan	0.90	1.40	9.51	30.49
Zevenbergen and Thorne	0.89	1.31	9.36	29.61
Shary	0.90	1.37	9.42	30.25

3.5.5. Analysis of Surface-Adjusted Elevations Methods

The surface-adjusted methods discussed so far are compared here. Table 3.8 shows the method comparison. Methods are ordered across the table columns by the number of pixels in each configuration. Only the optimal configurations selected for weighted average (WA), for least squares fitting, and for quadratic polynomials are included here, for comparison.

RMSEs evaluate the performance of various methods, and T-tests determine if differences between the RMSEs for different methods are statistically significant. To run the T-tests, bootstrapping tests on their corresponding residuals are conducted; for each RMSE, 1,000 residuals are selected at random from the 20,000 residuals on which the RMSE is based. This sampling process is repeated 1,000 times with replacement calculating one RMSE for each sample. Finally, a T-test is run comparing the calculated RMSEs of two methods at a time to see if differences are statistically significant. The results of these tests on the RMSEs of Table 3.8 are reported in meters. In this table, the lowest RMSE as well as RMSEs whose difference from the lowest RMSE is not statistically significant at a particular resolution are boldface. Standard

deviations of residuals remain relatively high (nearly equal magnitudes to the RMSEs) at finer resolutions, even at coarser resolutions where the Mean Bias Error (MBE) values are non-zero. Recalling that the vertical accuracy of DEMs is reported as 2.44 m and 4.01 m for the two data sources, it is likely that estimation method does not matter much for 10 m and possibly for 30 m resolution, but at 100 m and 1000 m resolution where MBE values diverge from zero, the biquadratic and bicubic polynomials generate the highest accuracy estimates of elevation.

Table 3.8. Accuracy assessment parameters for different interpolation methods in different resolutions for North Carolina. Columns show interpolation methods (left to right): Linear using 3 neighbors, bilinear using 4 neighbors, weighted average using 4 neighbors, biquadratic using 9 neighbors, and bicubic using 16 neighbors. Boldface indicates the lowest RMSE as well as RMSEs whose difference from the lowest RMSE is not statistically significant at a particular resolution. Values are rounded to the nearest whole centimeter.

		Li3	BiLi4	WA4	BiQ9	BiC16
10 m	RMSE	0.91	0.91	0.92	0.89	0.90
	MBE	-0.01	-0.01	-0.01	0.00	0.00
	STD	0.91	0.91	0.92	0.90	0.90
30 m	RMSE	1.43	1.42	1.48	1.31	1.29
	MBE	-0.01	-0.01	0.00	-0.01	-0.01
	STD	1.43	1.42	1.48	1.31	1.29
100 m	RMSE	9.60	9.59	9.64	9.36	9.38
	MBE	-6.22	-6.21	-6.22	-6.22	-6.22
	STD	7.32	7.31	7.36	7.01	7.02
1000 m	RMSE	30.03	29.84	30.23	29.61	29.10
	MBE	-5.42	-5.41	-5.37	-5.29	-5.38
	STD	29.54	29.35	29.50	29.13	28.59

RMSEs vary with DEM resolution and with interpolation method. Accuracy assessment parameters show a general trend of increasing RMSEs at coarser resolutions. The weighted average method shows highest magnitude errors for all resolutions. The bicubic method shows the lowest RMSEs at all resolutions, although RMSEs of the biquadratic method are statistically equivalent at 10 m and 100 m resolution. The results for North Carolina illustrate that higher order polynomials outperform weighted average, linear, and bilinear methods at coarse DEM

resolutions. At finer resolutions, the method used to estimate elevations matters less or not at all. It should be noted that the RMSE and STD are almost the same for 10 m and 30 m DEMs, and the MBE of residuals is almost zero at these two finest resolutions. Other authors (Fisher and Tate 2006; Fisher 1998; Hunter and Goodchild 1997) note similar findings. A two-sample Kolmogorov-Smirnov test and a Welch two sample T-test also show that interpolated elevations and elevations obtained from the benchmark appear to come from the same population for 10 m and 30 m DEMs.

3.5.6. Processing Time Comparison

Table 3.9 shows processing times in seconds to interpolate 20,000 off-centroid elevations for tested interpolation methods. The processing time is reported relative to the fastest method as well. Given that the same number of sampled points (20,000) was processed for all six study areas, these results apply to all six. Processing was performed on a computer with CPU Intel Core i7 (3.6 GHz) and 16 GB RAM installed. The code is written in 32-bit Python, version 2.7. In general, the assumption of non-rigid pixels carries an additional computational load, as it must incorporate not only elevation and pixel size, but also slope and curvature, in effect, adjusting for the changing terrain surface at sub-pixel resolutions. One goal of this research is to address the balance between the increased computations needed to measure surface-adjusted elevation against the improvement in precision.

Table 3.9. Processing time for different interpolation methods for North Carolina (10 m DEM).

	Li3	BiLi4	WA4	BiQ9	BiC16
Processing time for 20,000 sample points (seconds)	0.64	0.79	0.62	1.19	1.96
Relative processing time for 20,000 sample points (seconds)	1.03X	1.27X	X	1.91X	3.16X

The weighted average interpolator (WA4 in the Table) gives the fastest run time by far,

even though its neighborhood is essentially the same size as the bilinear (BiLi4). The bicubic method (BiC16) carries the highest processing time. To balance processing time with accuracy, a linear interpolator seems to be an optimal choice when accuracy is not the highest priority.

The processing time needed to generate these polynomial surfaces depends on the techniques used for solving the equations. To decrease the processing time of calculating polynomial surfaces, unknown coefficients can be solved in advance and be used directly in the implementation. Other than processing time, the computational complexity of each interpolation method can be reported. The computational complexity of the linear and bilinear polynomials are $O(n)$, the biquadratic polynomial is $O(n^2)$, and the bicubic polynomial is $O(n^3)$.

3.5.7. Results for Other Study Areas

In this section, the results of estimations are discussed for five other study areas to investigate how the results vary with different types of terrain. Table 3.10 represents the RMSE values for the remaining five study areas. The results are ordered based on terrain roughness (highest to lowest), and it can be seen that the RMSE values decrease from Washington (roughness = 8.24 m) to Louisiana (roughness = 0.35 m). As with North Carolina, T-tests indicate that some RMSEs are not statistically different, and these equivalencies are highlighted in the Table. Results show that in rougher terrain, bicubic and biquadratic methods outperform other interpolation methods in most DEM resolutions, while in flatter or smoother terrain (Texas and Louisiana) linear and bilinear methods perform with near equivalent accuracy in many cases. It can be seen that in these study areas as in North Carolina, the weighted average method generates the highest RMSE at most resolutions and in most study areas. Therefore, this method is not recommended to be used for elevation estimation when accuracy is a primary concern.

Table 3.10. RMSE values in meters for different interpolation methods in different resolutions for the remaining five study areas. Compare these values with those shown in Table 3.6 for North Carolina. Boldface indicates the lowest RMSE and those RMSEs whose difference from the lowest RMSE is not statistically significant at a given resolution.

Washington	Li3	BiLi4	WA4	BiQ9	BiC16
10 m	0.69	0.68	0.71	0.67	0.66
30 m	1.35	1.32	1.46	1.22	1.18
100 m	15.71	15.70	15.76	15.74	15.70
1000 m	63.74	63.17	63.93	63.32	61.36

Colorado	Li3	BiLi4	WA4	BiQ9	BiC16
10 m	0.37	0.37	0.40	0.35	0.35
30 m	1.01	1.01	1.11	0.93	0.89
100 m	7.82	7.80	7.87	7.52	7.53
1000 m	38.64	38.44	38.86	38.35	37.63

Nebraska	Li3	BiLi4	WA4	BiQ9	BiC16
10 m	0.23	0.23	0.24	0.21	0.20
30 m	0.74	0.73	0.75	0.66	0.64
100 m	3.61	3.61	3.62	3.51	3.51
1000 m	8.05	8.01	8.01	7.68	7.73

Texas	Li3	BiLi4	WA4	BiQ9	BiC16
10 m	0.20	0.19	0.20	0.19	0.19
30 m	0.43	0.42	0.44	0.40	0.39
100 m	3.85	3.85	3.86	3.86	3.85
1000 m	7.67	7.64	7.68	7.57	7.51

Louisiana	Li3	BiLi4	WA4	BiQ9	BiC16
10 m	0.13	0.13	0.13	0.12	0.12
30 m	0.29	0.28	0.29	0.28	0.27
100 m	7.77	7.77	7.77	7.85	7.83
1000 m	6.78	6.77	6.76	6.87	6.83

Louisiana is the only study area that bicubic interpolation produces the highest RMSEs for the coarser resolutions (100 m and 1000 m). Further investigation shows that the coarser resolution DEMs are noisier in Louisiana (Figure 3.9; compare this with Figure 3.10 for North Carolina). It can be concluded that higher order polynomials use more context to find the optimum surface representing terrain surface and may be unsuitable when DEM has some obvious errors.

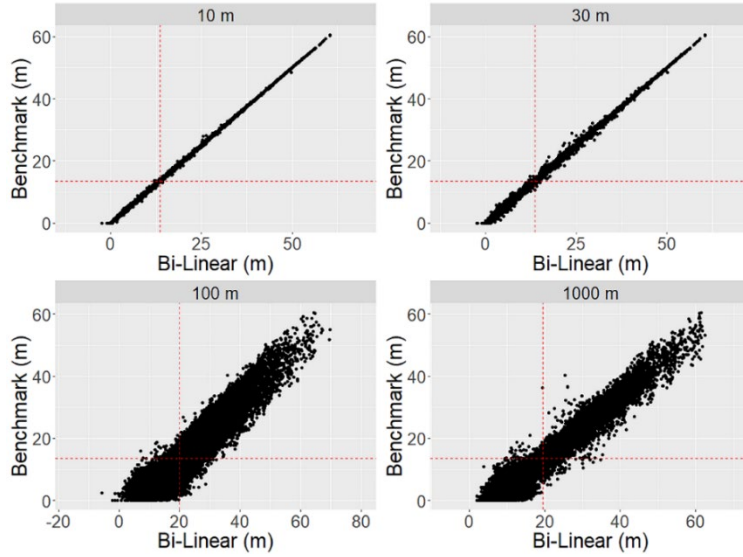


Figure 3.9. Estimated elevation using bilinear method versus the benchmark elevations in different resolutions for Louisiana. The red dotted lines show the mean of estimated values in the x axis, and lidar elevation values in the y axis.

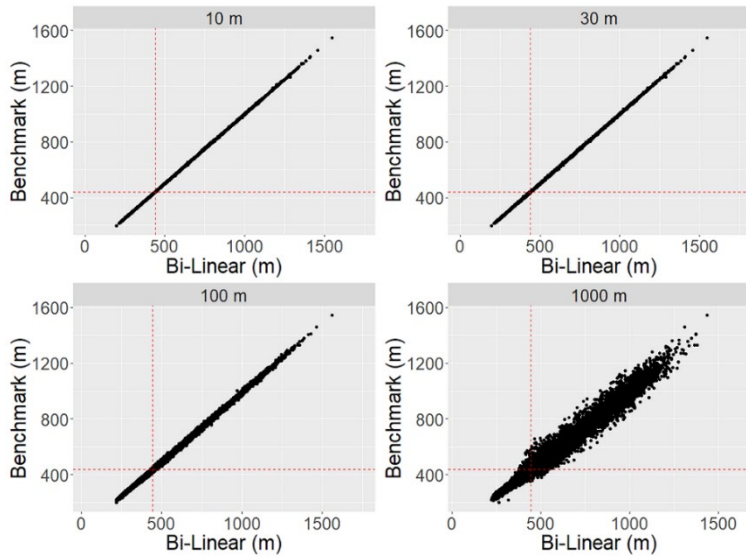


Figure 3.10. Estimated elevation using bilinear method versus the benchmark elevations at different resolutions for North Carolina. The red dotted lines show the mean of values in the x and y axis.

The next part of the analysis examines the performance of different interpolation methods in different slopes. Slope here is calculated based on the rise to run method using the values of the center cell and its eight neighbors (Bolstad 2005). First, random points in all study areas are merged

(120,000 points in total). Figure 3.11(a) illustrates the frequency distribution of slope values in 10 m DEM. This frequency distribution shows a long tail, meaning that slope is positively skewed. This graph indicates that a high percentage of DEM cells have a slope less than 10 degrees. Figure 3.11(b) shows that mean slope of a DEM will tend to decrease as the resolution becomes increasingly coarse.

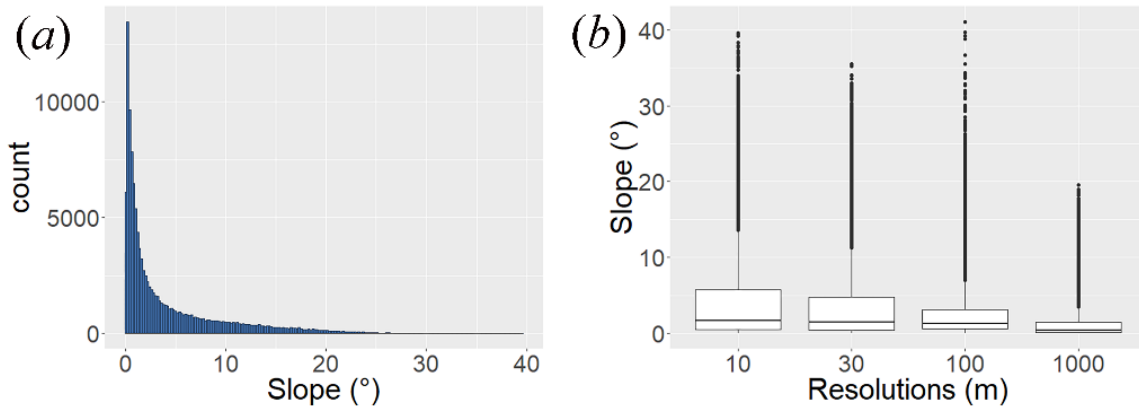


Figure 3.11. (a) Frequency distribution of slope values in 10 m DEM, and (b) the distribution of slope values in different resolutions

To investigate the performance of different interpolation methods, random points in all of the study areas are combined and are categorized into 4 different slope categories: flat ($0 \leq \text{slope} < 1$), gentle ($1 \leq \text{slope} < 10$), steep ($10 \leq \text{slope} < 20$), and very steep ($20 \leq \text{slope}$). Figure 3.12, illustrates the RMSEs for different interpolation methods in different slope categories and different DEM resolutions. RMSE values increase as slope increases. It can be seen that in higher slope categories and especially at 30 m resolution, the bicubic method outperforms other interpolation methods. In flat terrain and for all slope categories at 100 m, there is little or no difference in RMSE values of different interpolation methods for differing slope classes. The results for 100 m DEM might be related to the issues discussed for the courser DEM resolutions in Louisiana.

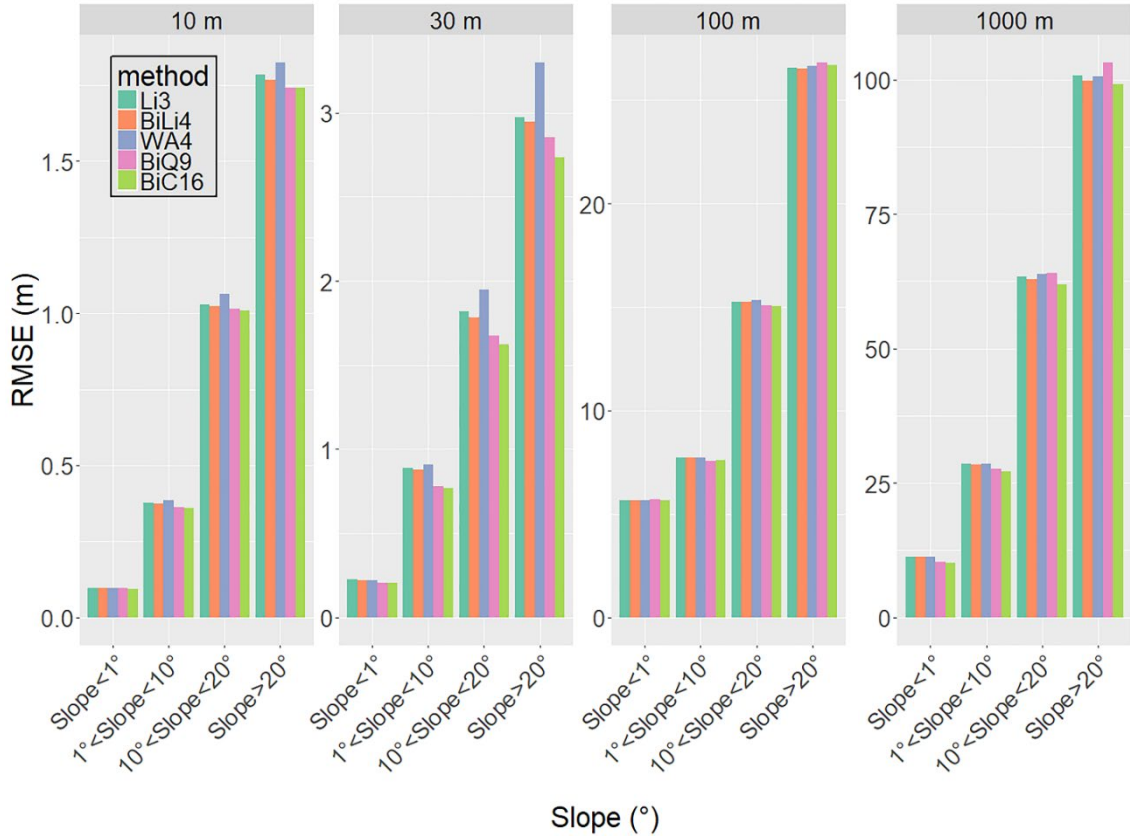


Figure 3.12. RMSE values for different interpolation methods in different slope categories and different DEM resolutions.

The performance of different interpolation methods in different terrain roughness is inspected in the next part of analysis. Roughness here is calculated based on the standard deviation of elevation in a 5 by 5 focal window. First, random points in all study areas are merged (120,000 points in total). Figure 3.13(a) demonstrates the frequency distribution of roughness values in 10 m DEM. Similar to the slope, the frequency distribution of curvature shows a long tail, meaning that roughness is positively skewed. It can be seen that most of DEM cells have a roughness less than 10 m as well. In contrast to slope, figure 3.13(b) shows that mean roughness of a DEM will tend to increase as the resolution becomes increasingly coarse. This is happening because a 5 by 5 focal window is used in all DEM resolutions and as a result roughness in coarser DEM resolution is calculated in a much larger area than the one calculated in finer DEM resolutions.

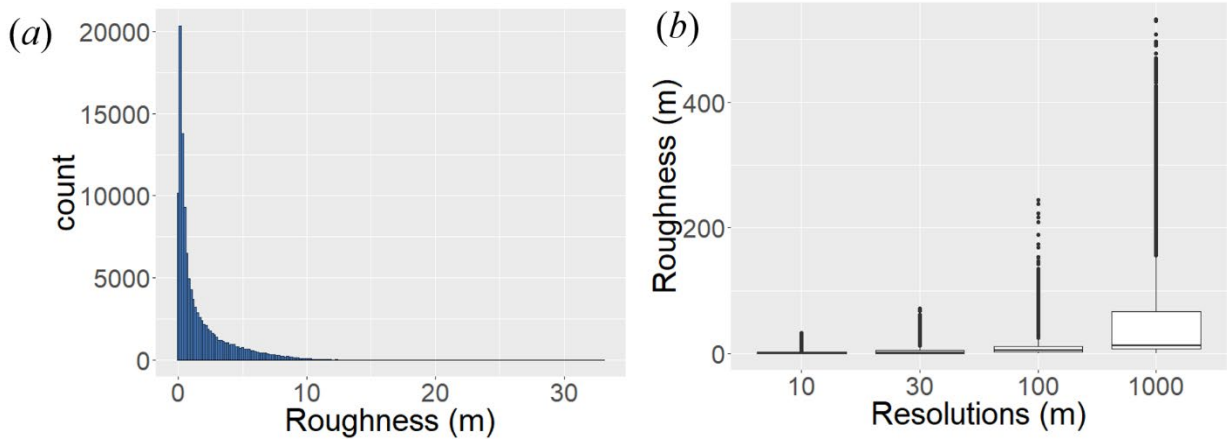


Figure 3.13. (a) Frequency distribution of roughness values in 10 m DEM, and (b) the distribution of roughness values in different resolutions

To investigate the performance of different interpolation methods, random points in all of the study areas are combined and are categorized into 4 different roughness categories: Smooth ($0 \leq \text{roughness} < 1$), slightly rough ($1 \leq \text{roughness} < 5$), intermediately rough ($5 \leq \text{roughness} < 15$), and highly rough ($15 \leq \text{roughness}$). Figure 3.15 illustrates the RMSEs for different interpolation methods in different roughness categories and different DEM resolutions. RMSE values increase as roughness increases. It can be seen that in higher roughness categories and especially at 30 m resolution, the bicubic method outperforms other interpolation methods. In flat terrain and for all roughness categories at 100 m, there is little or no difference in RMSE values of different interpolation methods for differing roughness classes.

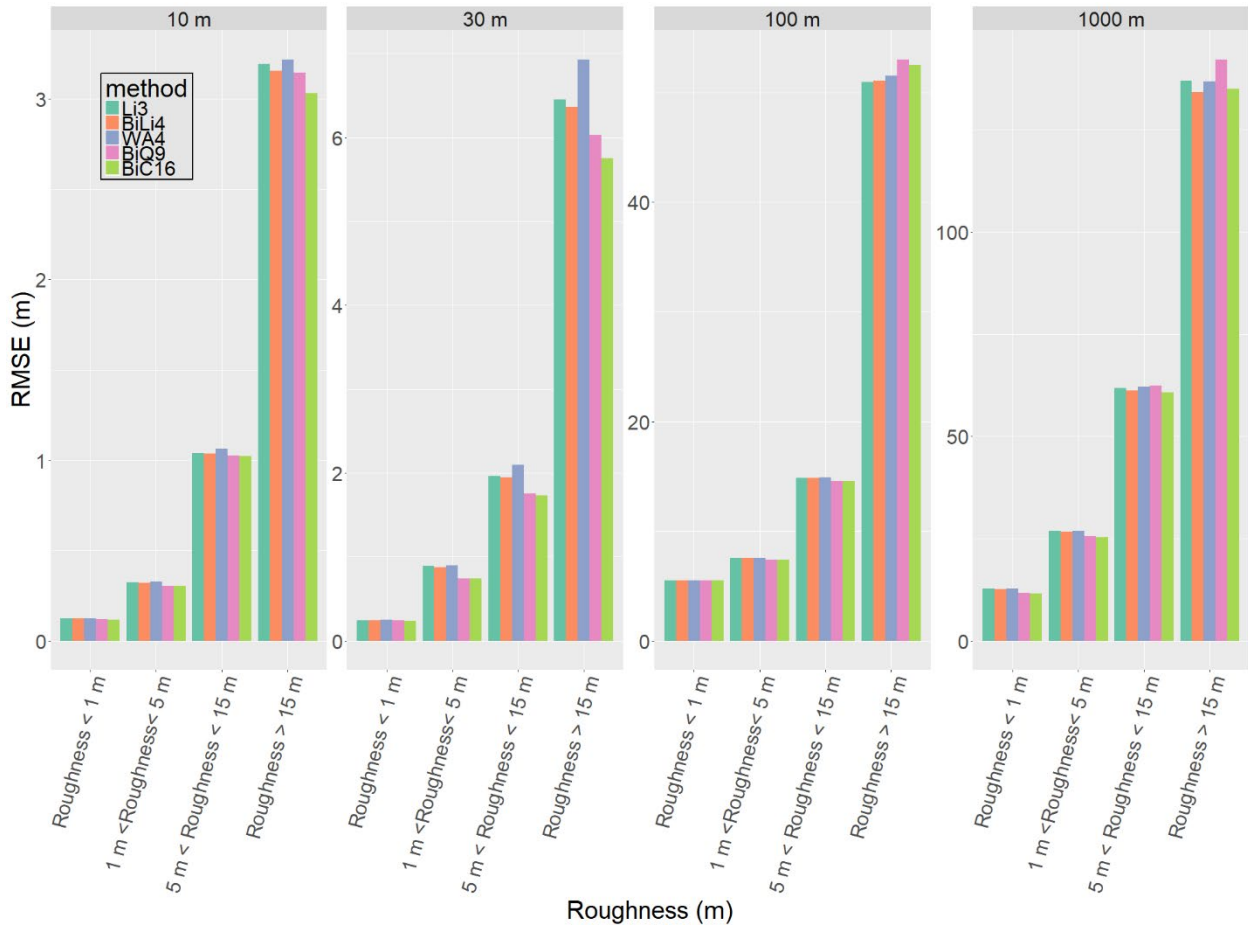


Figure 3.14. RMSE values for different interpolation methods in different roughness categories and different DEM resolutions.

3.6. Discussion and Summary

This chapter characterizes sub-pixel terrain fluctuations for the purposes of estimating elevation. The experiments demonstrate that the accuracy of elevation estimations varies with interpolation method, with spatial resolution, and with terrain type. Systematic comparison of a number of interpolation methods were applied to estimate off-centroid elevations, utilizing a series of increasingly large spatial neighborhoods across a progression of spatial resolutions. Findings confirm some previous work that concludes higher order polynomials are necessary to accurately interpolate sub-pixel resolutions.

The research employs realistic terrain (as opposed to regularized smooth manifolds), searching for a more accurate interpolated estimations of elevation using different interpolation methods and information from adjacent pixels. The research undertakes a systematic comparison among a selection of interpolation methods to estimate elevations from DEMs at off-centroid locations, utilizing a series of increasingly large spatial neighborhoods across a progression of spatial resolutions for six differing types of digital terrain.

Findings show that estimation errors increase at coarser resolutions, and that accuracy differences are less pronounced in flatter and smoother terrain. For the flattest and smoothest terrain (Louisiana and Texas study areas) significant differences in RMSEs occur at every resolution. Louisiana and Texas both display a mix of optimal interpolation accuracies, with linear and bilinear methods performing with equal or better accuracies compared to the polynomials and especially at coarser resolutions. However, these differences are in the magnitude of centimeters over terrain measured in meters; and in many modeling applications (except for civil engineering applications), the choice of interpolation method may not matter at all. In North Carolina, containing a mix of flat and rough terrain, accuracies at 10 m resolution also display significant differences, again in mere centimeters, although becoming more pronounced at 100 m and 1000 m resolutions. At all resolutions in rough terrain at the Washington, Colorado, and North Carolina sites, the bicubic and biquadratic methods generate the lowest RMSEs.

The two study areas with roughest terrain (Washington and Colorado) also exhibit significant differences at all resolutions, with weighted average producing the highest RMSEs at all resolutions. At 100 m resolution, results are mixed: the Washington RMSE values are statistically identical at all resolutions, while in other study areas, the higher order polynomials perform most accurately. Again, these RMSEs are reported in centimeter magnitudes for terrain

measured in meters, thus even significant differences might not matter in some modeling tasks. Results are consistent with the work of Shi and Tian (2006) and Schneider (2001) who also found differences in elevation estimation in smooth and rough terrain.

One must also consider processing time and balance it against accuracy, especially as researchers work with increasingly large data sets. Ideally, one would prefer an interpolation method that carries the lowest computational intensity. In this experiment, the weighted average method incurs the lowest processing time (0.62 seconds for 20,000 points), nearly two times faster than the biquadratic and more than three times faster than the bicubic polynomial. If accuracy is a primary goal and data volumes are small, then biquadratic and bicubic methods may prove the best choice in rough and/or non-uniform terrain. For smooth and uniform terrain and/or very large volume data sets, the linear or bilinear methods could be the better choice, especially at finer resolutions, where accuracies appear to be less method-dependent and data volumes increase exponentially.

These findings should lead to more realistic estimation of elevation on DEMs, and contradict the conclusions of other authors whose interpolation of smooth manifolds was thought to transfer consistently to actual terrain. This work also advances understanding of how spatial error changes across resolutions, a cross-scale terrain analytics component that at present is not well understood.

Chapter IV

A Systematic Evaluation of Scale-, Algorithm-, and Topographic-Dependence of Surface Area Computations in Digital Terrain

4.1. Introduction

The measured area of a polygon is an integral and fundamental part of any spatial database and plays a significant role in many geographic analyses and applications. Area is commonly measured in Euclidean space ignoring the variations in the actual terrain height. As argued in previous chapters, planar area computations ignore the slope and curvature of the terrain and result in under-estimation, particularly as pixel size increases or in uneven terrain. Calculating surface area using a regular DEM can overcome this issue by considering localized variations on the terrain surface. This chapter investigates the scale-, algorithm-, and topographic-dependence of DEM-based surface area calculations. One can make a compelling argument that for any individual pixel, the improvement in measurements can be relatively small; however, the additive effects across the study area can become significant.

The method of dividing each DEM pixel into eight triangles is commonly used to calculate surface area (Jenness, 2004). Triangles are formed by connecting the 8 surrounding pixels. The surface area of individual triangles takes centroid elevation into account. The surface area of the central pixel is equal to one quarter the summed area of all 8 individual triangles. In this dissertation, this method is revised and is called modified Jenness method. In the modified Jenness

method, the connecting vector between pixel centroids are bisected creating 8 smaller triangles that fit inside the pixel in question. The trick is to estimate the elevation at each of the surrounding points located on the central pixel's boundary. The elevation of triangle vertices are estimated using different interpolation methods. These methods are compared and validated against the surface area measured based on a 3 m lidar DEM benchmark. The surface area is not directly calculated on the 3 m lidar data benchmark. The benchmark is only used to obtain the elevation at each of the generated vertices in the modified Jenness method located on the central pixel's boundary.

Surface area is estimated using a series of increasingly complex discrete interpolation methods, applied to digital terrain compiled independently at five different spatial resolutions. Different DEM resolutions are tested to establish rates of under-estimation for progressively larger pixels. Various terrain types also are tested to evaluate error magnitudes for different surface area estimation methods. Measurements based on the planar area in rough terrain are thought to be less accurate results than the measurements in flat terrain.

4.2. Surface Area Calculations

Surface area can be calculated simply as: planar area / cos(slope) (Berry 2002, Kundu and Pradhan 2003), which will be called the slope method in this chapter. In the slope method, each DEM cell is regarded as an inclined plane (Figure 4.1) that its surface area can be calculated as:

$$SA = \frac{P^2}{\cos(\theta * \pi * 180)} \quad (4.1)$$

Where p is pixel size. Slope (θ) as the rate of change of elevation from the center cell is commonly calculated using the following discrete method:

$$\theta \text{ (degrees)} = (\tan^{-1} \sqrt{(\frac{dz}{dx})^2 + (\frac{dz}{dy})^2}) * 57.29578 \quad (4.2)$$

The elevation values of the center cell and its eight neighbors determine the partial derivatives in the x and y directions (Figure 4.1(a)). A third-order finite difference method (Horn 1981) is used to calculate the partial derivatives.

$$\begin{aligned} \frac{dz}{dx} &= \frac{(H3 + 2 * H6 + H9) - (H1 + 2 * H4 + H7)}{8 * P} \\ \frac{dz}{dy} &= \frac{(H1 + 2 * H2 + H3) - (H7 + 2 * H8 + H9)}{8 * P} \end{aligned} \quad (4.3)$$

Where H is the elevation of the corresponding centroids.

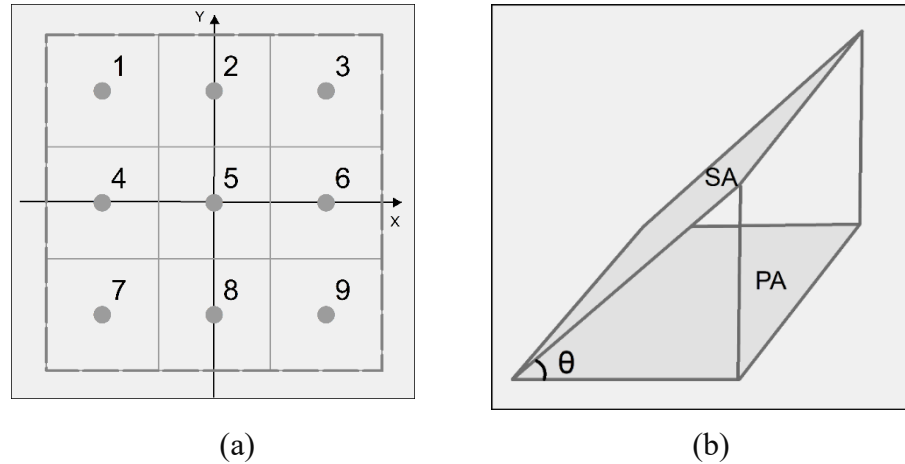


Figure 4.1: (a) a 9*9 cell window is used to calculate the surface area of the pixel including point 5. Slope of the central pixel is calculated based on the central pixel and the eight surrounding pixels. (b) Surface area (SA) is equal to the planar area (PA) divided by the cosinus of slope (θ).

In another approach, the surface area of each pixel in a regular grid DEM is calculated by dividing each DEM pixel into eight triangles using a focal moving window (Jenness 2004). In each pixel, all of the triangles between the pixel and adjacent pixels are constructed (Figure 4.2(a)). The

vertices of each triangle have differing elevations taken from respective pixel centroids. The 3D lengths for the sides of these 8 triangles can be calculated using the Pythagorean Theorem, incorporating slope because of each vertex's unique elevation value. The area of each triangle given the lengths of sides a , b , and c is calculated as $\sqrt{s(s-a)(s-b)(s-c)}$, where $s = \frac{a+b+c}{2}$.

Finally, surface area of the central pixel is equal to one quarter the summed area of all 8 individual triangles:

$$SA = \frac{1}{4} (SA_{\Delta 541} + SA_{\Delta 512} + SA_{\Delta 523} + SA_{\Delta 536} + SA_{\Delta 569} + SA_{\Delta 598} + SA_{\Delta 587} + SA_{\Delta 874}) \quad (4.4)$$

Where Δ is symbol for triangle (for example, $\Delta 541$ means triangle 541 illustrated in Figure 4.2(a)).

This research modifies the method proposed by Jenness for calculating surface area from a DEM and is called modified Jenness method. In Jenness's original method, each pixel centroid is linked to the pixel centroid of the 8 surrounding pixels to generate 8 triangles. In the modified Jenness method proposed in this dissertation, each connecting vector is bisected creating 8 smaller triangles that fit inside the pixel in question (Figure 4.2(b)). In this way, a new set of vertices is created on the pixel boundary. The trick is to estimate the elevation at each of the surrounding points located on the pixel boundary. The elevations of new vertices are estimated using five different interpolation methods. The 3 m lidar DEM is used to capture the actual elevations of the 8 estimated points, and to compute a validation surface area value. The surface area values computed using different interpolation methods are compared with the lidar-based surface area to find the interpolation method that is closest to the lidar-based surface area. It should be noted that the lidar DEM is only used to capture the actual elevations of the new vertices generated in the modified Jenness method. The surface area cannot be directly measured on the 3 m lidar DEM for

validation because each DEM resolution is independently compiled and so its pixels are not aligned with the pixels in the 3 m lidar DEM.

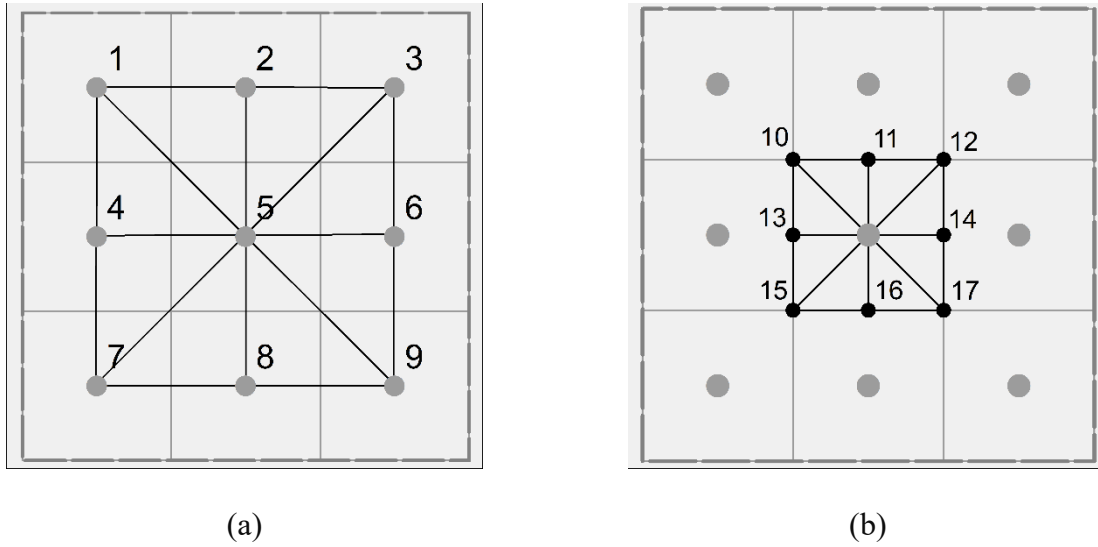


Figure 4.2. (a) Jenness's original method; each triangle facet is created from the pixel centroids; one is the centroid of the central pixel (5), and the other two are the centroids of two adjacent grid cell. (b) Modified method proposed in this research; first, the eight triangles fitting inside the central pixel are generated; points 10 to 17 are the new vertices created on the central pixel's boundary. Each triangle facet is created from three points; one is the centroid of the central pixel (5), and the other two are the points created on the central pixel's boundary. The elevation of each new vertex located on the central pixel's boundary is estimated based on different interpolation methods. The true elevation of these vertices are directly obtained from the 3 m lidar DEM.

It should be mentioned that the modified Jenness method is the contributions of this dissertation for calculating surface-adjusted area from a regular gridded DEM. The modified Jenness method is tailored to each interpolation method (Ghandehari and Buttenfield 2018). As discussed, each interpolation method can be used to estimate the elevation of new generated vertices located on the central pixel's boundary. Figure 4.3 illustrates an example that how the bilinear interpolation method is used to estimate the elevation of new vertices. For example, for the highlighted triangle in the Figure 4.3(a), the elevation of vertices 10 and 13 are unknown and

can be interpolated from the surrounding pixel centroids. The bilinear surface is constructed from the four closest centroid (here, 1, 2, 4, and 5), and as a result the elevation of vertices 10 and 13 can be estimated from the generated bilinear surface. The surface area of other triangles are calculated the same way using the corresponding bilinear surface. So, the interpolation methods are used to estimate the elevation of new generated vertices, and as a result for surface area calculations.

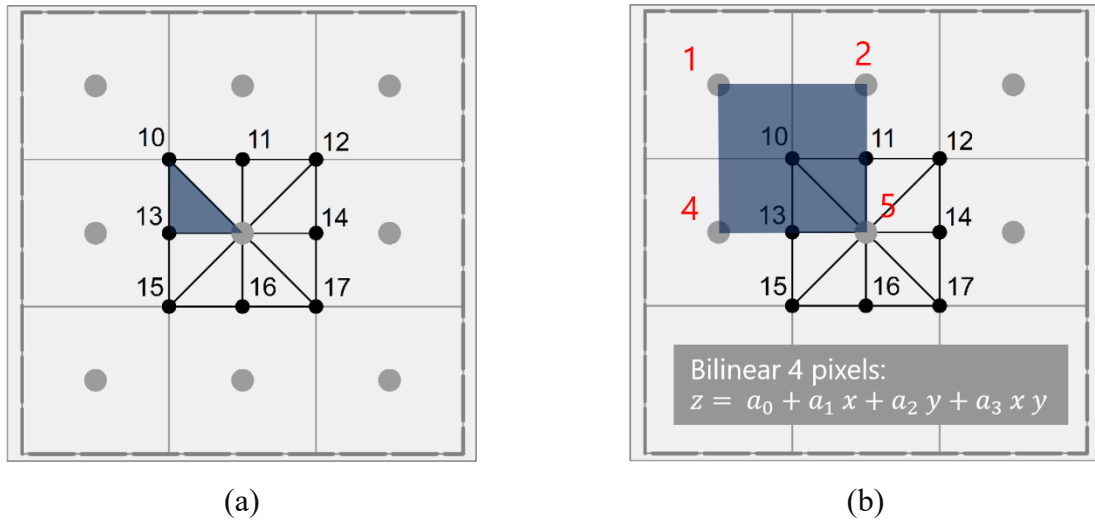


Figure 4.3. An example to illustrate the role of interpolation methods in the modified Jenness method proposed in this research: Points 1, 2, 4, and 5 in (b) with known elevation are used to calculate the bilinear surface. This bilinear surface is used to interpolate the elevation of unknown points 10 and 13 in the high-lighted triangle in (a).

4.3. Interpolation Methods used in the Modified Jenness Method

Interpolation methods are commonly used to reconstruct the surface of each pixel using contextual information from adjacent pixels. As discussed in the previous chapters, some studies establish that higher order polynomials outperform lower order polynomials, while others show the opposite conclusion. Therefore, one surface adjustment method cannot be the optimal method in all DEM resolutions and under all geographic conditions. This research investigates in which DEM resolutions and under what geographic conditions surface-adjusted area make a difference

in spatial modeling.

In the Modified Jenness Method, Interpolation methods are used for estimating the elevation of triangle vertices used for surface area calculations. Given a regular elevation grid within the defined neighborhood, different interpolation techniques will generate differing elevation estimates. The methods compared in this research include weighted average and discrete polynomial surfaces (linear, bilinear, biquadratic, and bicubic), both of which are exact interpolators. Different contiguity configurations are used in the interpolation methods. The linear, bilinear, weighted average, biquadratic, and bicubic interpolators use 3, 4, 4, 9, and 16 neighboring pixels, respectively. As discussed, these interpolation methods are used to interpolate the elevation of unknown triangle vertices created on the central pixel's boundary in the modified Jenness method. The interpolation surfaces are not used as a continuous surface in the double integral formula discussed in Chapter 2 for surface area calculations.

4.4. Workflow and Processing

Four different DEM resolutions (from 10 m to 1,000 m pixel sizes), six different methods, and six study areas across the conterminous United States are used in this research. The results are validated against direct elevation measurements on 3 m lidar DEM. The workflow involves several steps. First, the 3 m lidar DEM is loaded. Then each resolution DEM is input one at a time to calculate the corresponding surface area raster. For each of the test DEMs, a nested loop processes each pixel for all interpolation methods and the benchmark. Estimated surface area for each interpolation method is recorded into a new raster. At the end, one surface area raster is generated for each resolution and each interpolation method. Surface area raster for each method is subtracted from the surface area raster calculated based on the 3 m benchmark DEM in order to calculate one RMSE for each method in each resolution.

Coding and statistical analysis are conducted in Python using open source modules (GDAL, Geopandas, numpy, scipy, and multiprocessing). Amazon Web Services (AWS) is needed to handle large sets of DEM data and increase the speed of this research using high performance computers. In one study area, as an example, there are 25,500,000 pixels in the 10 m DEM. The surface area for each pixel should be calculated based on six different methods. This process is compute-intensive and very time-consuming, and the code needs to be parallelized to speed up the process. A virtual server on AWS is used with 32 CPUs and 224 GB of RAM. This instance concurrently calculates the surface area of 32 rows of DEM. Also, all of the computations are carried out in RAM and very large numpy arrays are saved in memory.

Here is the strategy to process larger data sets in AWS. A single DEM at a single resolution is partitioned into strips covering 5 rows and all columns to create a task pool (Figure 4.5). The justification for 5 rows is that the interpolation methods using 3rd order polynomials require 5*5 neighborhoods. Once uploaded, each strip is processed by one CPU to estimate surface area by all interpolation methods, storing the results in a numpy array. Therefore, the strips can be executed concurrently to calculate the surface area for the entire DEM. The calculated surface area raster for all methods and DEM resolutions are saved onto disk and are subsequently downloaded for validation against the surface area calculate based on the 3 m lidar DEM .

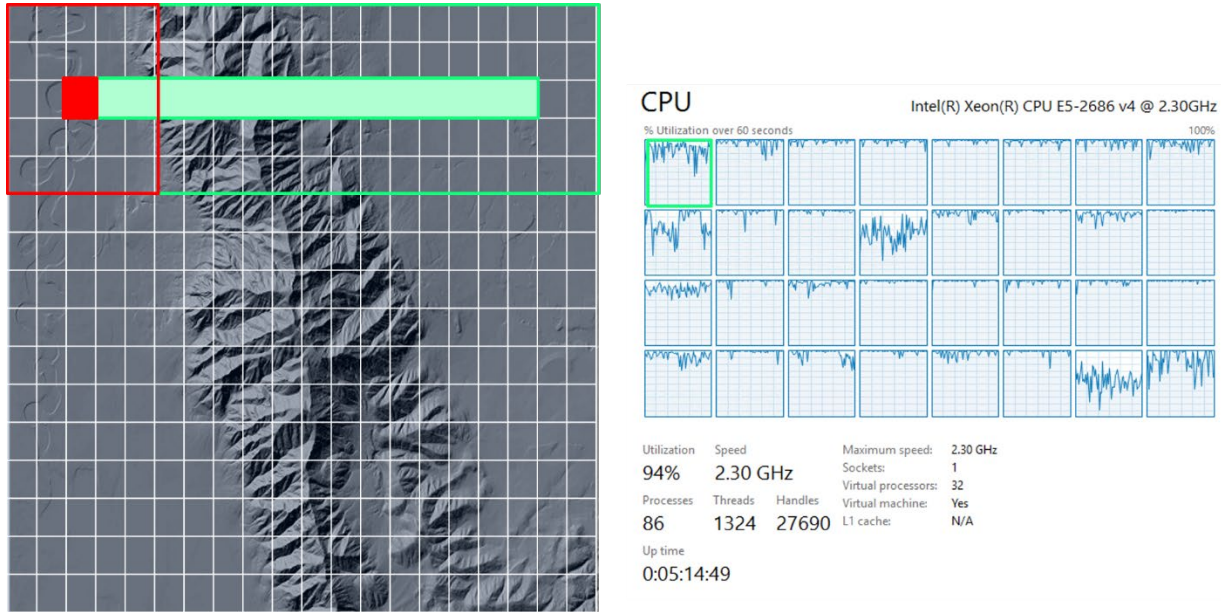


Figure 4.5. An AWS virtual server with 32 CPUs and 224 GB of RAM in used to concurrently calculate the surface area of 32 rows. Red box moves as a focal window across row to calculate the surface area of pixels in the first row in the highlighted CPU. This process is conducted in parallel in all 32 CPUs to concurrently calculate the surface area of 32 rows.

4.5. Results

4.5.1. Areal Characteristics of the Six Data Sets

Data sets used in this chapter are the same as the previous chapters. Areal characteristics of the six data sets are discussed here. Figure 4.4 illustrates the percentage of planar area stratified by slope in each study area; planar area raster and slope raster were calculated for each study area and the slope raster categorized into six different classes. Then, the zonal statistics was used to calculate the percentage of planar area in each slope class. The range slope in Washington is close to uniform across slope classes. In Colorado, North Carolina, Nebraska, and Texas, the range of slope between 1° to 10° has the highest coverage. In Louisiana, about 80% of the terrain has a slope of less than 1° . In Colorado and North Carolina the range of slope between 1° to 20° has the highest coverage. In Nebraska and Texas, slope of less than 1° has the second highest coverage.

Figure 4.5 shows the mean of difference between surface area and planar area categorized based on slope in each study area; planar area raster were subtracted from the surface area raster and the mean of differences in each slope class were calculated. This graph illustrates the relationship between terrain slope and the difference between surface area (calculated based on Jenness's method) and planar area. As expected, there is a general trend of increase in the mean difference between surface area and planar area at higher slopes. The trend and values are similar in all of the study areas because the mean difference between surface area and planar area has not been standardized. The results in Figure 4.4 and 4.5 are obtained from 10 m DEM. The surface area is calculated based on Jenness's method. Other methods are not investigated here because these graphs aim to simply illustrate the trend of area stratified by slope in various terrain types, so the selected surface area method does not matter.

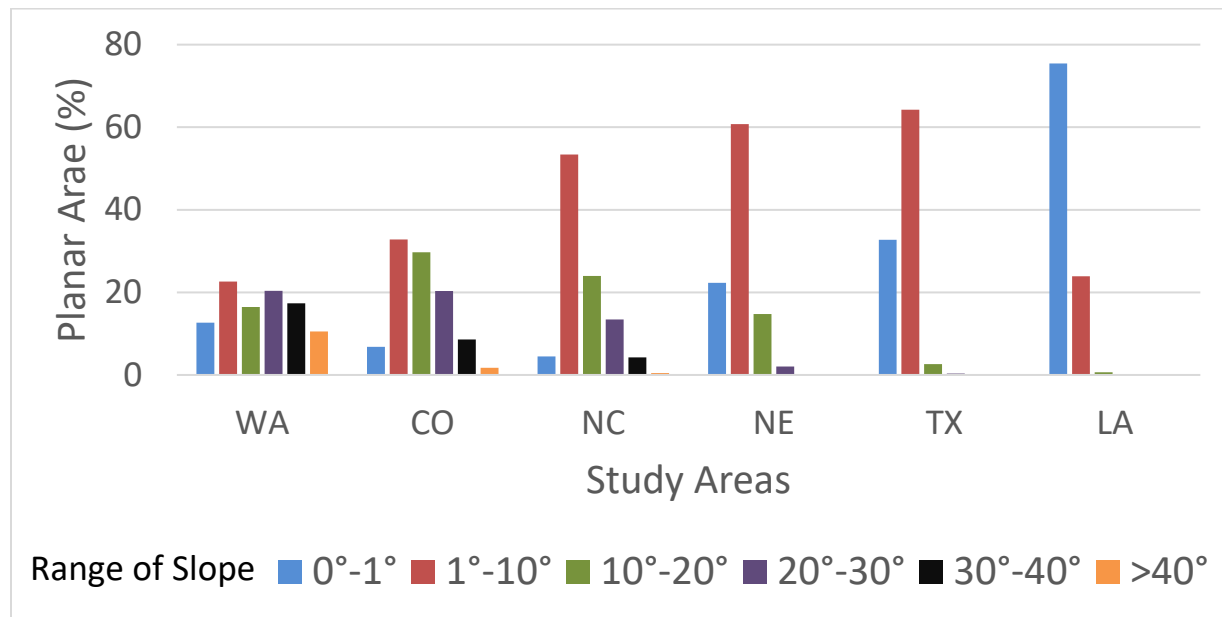


Figure 4.4: The percentage of planar area categorized on slope in each study area (10 m DEM is used)

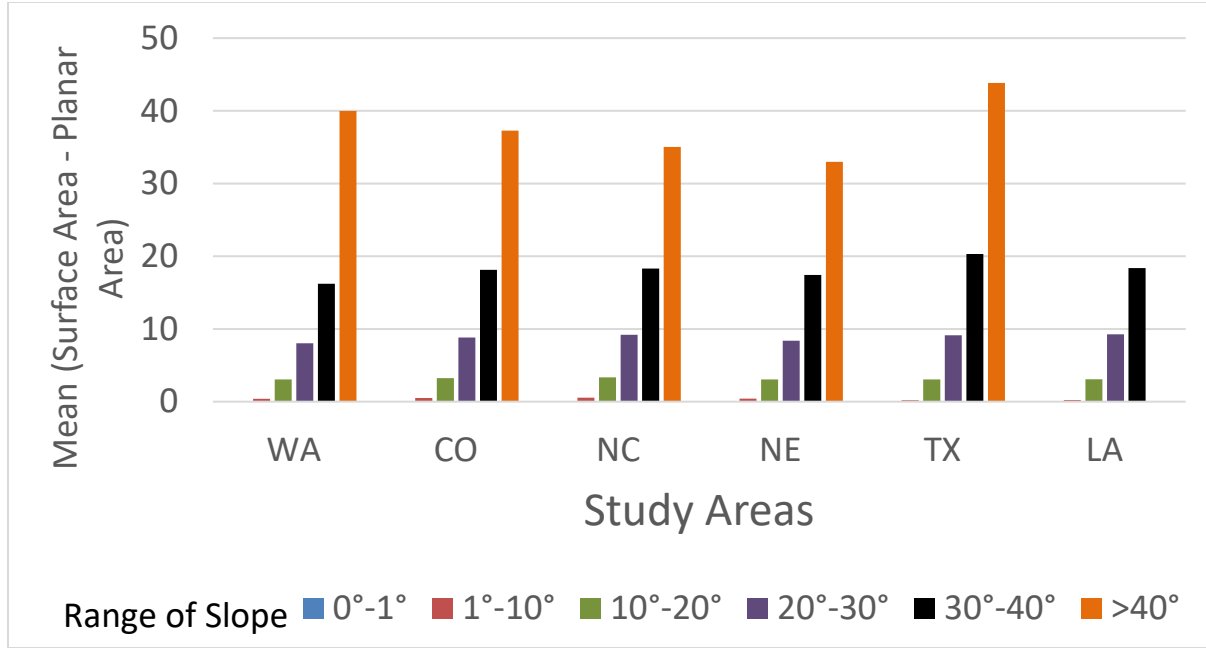


Figure 4.5: The mean of difference between surface area and planar area categorized on slope in each study area (10 m DEM is used)

4.5.3. Analysis of Surface Area Measurements

As discussed in the previous chapter, Jenness method employs the elevation of 8 surrounding pixels to generate 3D triangles and calculate the surface area of the central pixel. In this research, the Jenness method was modified to improve the accuracy of surface area estimation. In the modified method, 3D triangles located inside the central pixel are generated and the elevation of vertices located on the central pixel's boundary are estimated using an interpolation method. In this section, surface area calculated based on different methods are compared.

Table 4.1 shows the method comparison based on the RMSE of surface area calculations for six study areas at various DEM resolutions. Surface areas are computed for a planar solution in each table to provide a baseline “worst case” comparison. Also, the surface area calculated based on the local slope at each DEM cell (i.e., the Slope method) is reported. The original (unmodified) Jenness method is also reported. Here, only the modified Jenness method based on

the linear interpolation (called Linear3 in the table) is discussed to determine if the modification (that adds some processing time) is warranted.

Similar to the previous chapter, T-tests regulate if difference between the RMSEs of different methods are statistically significant. To run the t-tests for two RMSEs, 1,000 random pixels are selected from the residuals on which the RMSE calculation is based. This random sampling process is repeated 1,000 times with replacement and each time one RMSE is calculated for that 1,000 random samples. The boldface in Table 4.1 illustrates the lowest RMSE and the RMSEs that their difference from the lowest RMSE is not statistically significant in each DEM resolution.

Table 4.1. RMSE values (sq. m.) for planar, slope, Jenness and modified Jenness method (here, linear interpolation) at different resolutions for 6 study areas. Boldface indicates the lowest RMSE and the RMSEs that their difference from the lowest RMSE is not statistically significant.

Washington	10 m	30 m	100 m	1000 m
Planar	13.695	104.784	790.141	43,265.816
Slope	4.297	34.359	394.108	29,894.168
Jenness	4.032	29.195	375.898	21,739.666
Linear3	3.854	27.765	388.559	22,343.145

Colorado	10 m	30 m	100 m	1000 m
Planar	8.298	61.614	457.065	20,039.174
Slope	2.829	21.959	220.494	14,871.395
Jenness	2.507	17.682	193.281	11,866.118
Linear3	2.387	17.086	191.879	11,885.051

North Carolina	10 m	30 m	100 m	1000 m
Planar	7.163	53.960	380.230	12,003.862
Slope	2.225	20.581	235.759	10,370.065
Jenness	1.924	15.043	207.241	8,652.469
Linear3	1.866	14.872	206.327	8,634.967

Nebraska	10 m	30 m	100 m	1000 m
Planar	2.773	16.372	78.373	639.683
Slope	1.372	11.447	70.379	605.736
Jenness	1.141	8.750	66.390	569.497
Linear3	1.064	8.593	66.364	569.904

Texas	10 m	30 m	100 m	1000 m
Planar	1.987	11.763	65.334	1,029.190
Slope	1.020	6.767	49.179	938.384
Jenness	0.886	5.680	45.096	851.475
Linear3	0.824	5.348	44.206	844.650

Louisiana	10 m	30 m	100 m	1000 m
Planar	0.5830	2.674	8.718	42.616
Slope	0.4020	2.256	8.453	39.471
Jenness	0.330	1.867	9.445	36.458
Linear3	0.318	1.837	9.911	36.731

In all study areas, the linear method shows lowest RMSEs at most resolutions, and the planar and slope methods show the highest RMSEs. Similar to the elevation experiment in the previous chapter, Louisiana is the only study area that the slope method produces the lowest RMSEs

for 100 m resolution. Therefore, it can be confirms that the 100 m DEM data in Louisiana has a problem. The results illustrate that the modified linear-based method outperform the Jenness method in most of the DEM resolution and terrain types. Therefore, the modified Jenness method is selected as the optimum method for surface area calculations for further analysis. In the next section, the modified Jenness method will be examined based on different interpolation methods.

4.5.2. Analysis of Surface Area Measurements based on the Modified Jenness Method

In this section, surface area measurements based on the modified jenness method is investigated. The elevation of vertices generated in the modified jenness method can be estimated based on different interpolation methods. The linear, bilinear, weighted average, biquadratic and bicubic interpolations methods are compared in this section. Table 4.2 illustrates the statistical properties of surface area rasters calculated based on the modified Jenness method using different interpolation methods in different DEM resolutions for the North Carolina. The extent of rasters at different resolutions are not exactly aligned, so the sum of surface area in these rasters cannot be compared strictly across resolution. But, in general, it can be seen that the sum of area is decreasing by moving from fine to course resolution. The Bicubic method has higher values in 10, 30, and 100 m resolution, except median. In 1000 resolution, the linear method has higher values than bicubic. Also, the linear method has higher medians in all resolutions. The weighted average method has the lowest values in all DEM resolutions. The minimum value for all of the methods are the same in 10, 30, and 100 m resolutions, as there is at least one pixel in the study area with the slope of zero.

Table 4.2. Summary statistics of surface area rasters for the modified Jenness method using different interpolation methods in different resolutions for North Carolina.

10 m	Mean Sq. m.	Std. Dev. Sq. m.	Min Sq. m.	Max Sq. m.	Median Sq. m.	Sum Sq. km.
Linear3	90.525	5.187	87.259	411.895	88.261	8,324.136
Bilinear4	90.4937	5.115	87.259	388.283	88.257	8,321.188
Wtd Average4	89.043	2.852	87.259	311.358	87.813	8,187.846
Biquadratic9	90.402	5.066	87.259	391.671	88.188	8,312.787
Bicubic16	90.543	5.274	87.259	424.353	88.243	8,325.752

30 m	Mean Sq. m.	Std. Dev. Sq. m.	Min Sq. m.	Max Sq. m.	Median Sq. m.	Sum Sq. km.
Linear3	810.453	38.698	785.339	2,390.637	793.609	8,267.189
Bilinear4	809.758	37.475	785.339	2,213.052	793.454	8,260.101
Wtd Average4	799.701	21.872	785.339	1,654.637	790.167	8,157.516
Biquadratic9	807.892	36.326	785.339	2,267.461	792.271	8,241.072
Bicubic16	810.673	39.726	785.339	2,392.441	793.479	8,269.438

100 m	Mean Sq. m.	Std. Dev. Sq. m.	Min Sq. m.	Max Sq. m.	Median Sq. m.	Sum Sq. km.
Linear3	7,177.178	184.598	7,067.959	13,811.917	7,099.766	8,101.886
Bilinear4	7,173.883	179.149	7,067.959	13,075.770	7,098.559	8,098.166
Wtd Average4	7,130.485	101.586	7,067.959	11,288.363	7,087.218	8,049.177
Biquadratic9	7,164.808	174.936	7,067.959	13,305.991	7,092.541	8,087.922
Bicubic16	7,178.504	191.111	7,067.959	13,987.038	7,099.293	8,103.383

1000 m	Mean Sq. m.	Std. Dev. Sq. m.	Min Sq. m.	Max Sq. m.	Median Sq. m.	Sum Sq. km.
Linear3	708,787.812	4,185.199	706,837.375	757,248.187	707,072.562	7,531.579
Bilinear4	708,607.375	3,710.965	706,839.812	748,064.437	707,054.781	7,529.662
Wtd Average4	708,072.562	2,844.051	706,838.062	748,009.562	706,987.281	7,523.979
Biquadratic9	708,157.000	2,914.196	706,838.437	742,863.812	706,988.031	7,524.876
Bicubic16	708,754.750	4,091.762	706,839.937	752,138.687	707,074.687	7,531.228

Table 4.3 shows the RMSEs to evaluate the performance of the modified Jenness method using different interpolation methods. Error magnitudes vary with DEM resolution and with interpolation method within each table, with higher RMSEs overall for Washington in rough terrain and lower RMSEs for Louisiana in flatter and smoother terrain. In other words, terrain non-

uniformity causes more discrepancy with the benchmark. The general trend in either table is that RMSE values increase to varying degrees moving from finer to coarser DEM resolutions. In all study areas, the bicubic interpolation shows lowest RMSEs at most resolutions, and weighted average method show the highest RMSEs. Linear method shows the next lowest RMSEs at most of the resolutions. The Linear method also has a RMSE with values statistically similar to the bicubic method in most of the DEM resolutions. Therefore, higher order polynomials do not appear to outperform lower order polynomials for surface area calculations.

Table 4.3. RMSE values (sq. m.) the modified Jenness method using different interpolation methods at different resolutions for 6 study areas. Boldface indicates the lowest RMSE and the RMSEs that their difference from the lowest RMSE is not statistically significant.

Washington	10 m	30 m	100 m	1000 m
Linear3	3.854	27.765	388.559	22,343.145
Bilinear4	3.939	28.785	381.837	22,961.992
WtdAverage4	7.149	55.526	516.876	29,095.031
Biquadratic9	3.969	30.074	386.471	26,272.572
Bicubic16	3.693	26.118	385.719	22,067.410

Colorado	10 m	30 m	100 m	1000 m
Linear3	2.387	17.086	191.879	11,885.051
Bilinear4	2.464	17.711	195.622	12,284.397
Wtd Average4	4.526	33.634	296.526	14,807.516
Biquadratic9	2.537	19.146	205.202	13,521.696
Bicubic16	2.270	16.372	187.988	11,902.850

North Carolina	10 m	30 m	100 m	1000 m
Linear3	1.866	14.872	206.327	8,634.967
Bilinear4	1.922	15.455	210.426	8,899.853
Wtd Average4	3.992	30.097	277.748	9,802.203
Biquadratic9	2.016	17.242	220.189	9,660.688
Bicubic16	1.810	13.958	202.475	8,655.975

Nebraska	10 m	30 m	100 m	1000 m
Linear3	1.064	8.593	66.364	569.904
Bilinear4	1.127	9.035	66.967	575.486
Wtd Average4	1.769	11.608	71.273	595.990
Biquadratic9	1.181	9.941	68.526	591.068
Bicubic16	0.969	8.178	65.944	569.425

Texas	10 m	30 m	100 m	1000 m
Linear3	0.824	5.348	44.206	844.650
Bilinear4	0.872	5.655	45.209	862.605
Wtd Average4	1.276	7.855	53.141	913.090
Biquadratic9	0.898	5.947	46.397	899.804
Bicubic16	0.782	5.137	43.096	848.091

Louisiana	10 m	30 m	100 m	1000 m
Linear3	0.318	1.837	9.911	36.731
Bilinear4	0.333	1.915	9.360	37.029
Wtd Average4	0.422	2.147	8.917	38.817
Biquadratic9	0.355	2.061	8.770	38.123
Bicubic16	0.303	1.828	9.778	36.420

4.5.3. Processing Time Comparison

Table 4.4 compares processing times and accuracy for different methods used in this research to calculate surface area. These times are reported for a small subregion in the North Carolina dataset illustrated in Figure 4.6. The processing time depends on the number of pixels

and the method used for surface area calculations. Terrain type does not change the processing time, and there is no reason for choosing a rough terrain in Figure 4.6. The processing time is reported relative to the fastest method. The simple slope method gives the fastest run time and is the proper method, if the ultimate goal is fast processing. On the other hand, as expected, the bicubic method has the highest processing time. The bicubic method has the lowest RMSE, but it was illustrated that the results obtained from the linear method is statistically equivalent to bicubic in most of the cases. Therefore, bicubic and linear methods are the proper methods if the ultimate goal is accuracy. It can be seen that using interpolation methods carries an additional computational load. It can be seen that the linear method about two times slower than Jeness, but bicubic is five times slower than Jennens method. Therefore, the Jenness and linear methods seems to be an optimal choice to make a balance between the increased computations needed to measure surface area against the improvement in precision. It should be noted that the planar method has not been reported in this table as it takes a fraction of a second to calculate.

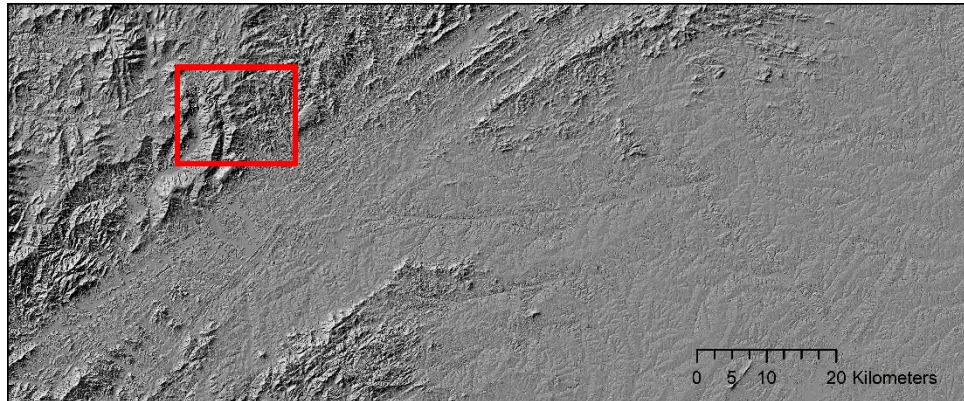


Figure 4.6. A subset in North Carolina selected for processing time comparison including 2,682,091 pixels in the 10 m DEM.

Table 4.4. Relative processing time and RMSE for different surface-adjusted methods for 10 m DEM resolution. Processing time and RMSE of different methods are reported relative to slope method (lowest processing time) and bicubic method (lowest RMSE), respectively.

	Slope	Jenness	Linear3	Bilnear4	Wtd Average4	Biquadratic9	Bicubic16
Processing time in seconds	5.59	25.03	52.21	53.34	41.34	46.62	116.49
Relative processing time	X	4.47X	9.30X	9.54X	7.39X	8.33X	20.83X
Relative RMSE	1.27Y	1.12Y	1.06Y	1.10Y	2.49Y	1.14Y	Y

4.6. Discussion and Summary

Planar area introduces errors that vary with terrain roughness, slope, and DEM resolution. Errors might be ignored for individual pixels but can propagate dramatically for measurements that encompass many pixels or where pixel sizes become quite large, corrupting terrain-based measurements and spatial modeling outcomes. Advances in processing speed force scientists to reconsider the assumption of planar area and the need to acquire an accurate measurement of area. Differences between planar area and surface area can be expected to vary with the size of geographic footprint, DEM resolution, the algorithm used for estimating surface area, terrain roughness, and landscape conditions. This chapter compares surface area measurements using different methods across a progression of spatial resolutions and a suite of terrain types varying in latitude, altitude, slope, and roughness. The analysis also considered the balance between the increased computations needed to measure surface-adjusted area against the improvement in accuracy.

This research employs realistic terrain surface geometries using different interpolation methods and the information from adjacent pixels for purposes of incorporating terrain slope and curvature into surface area computations. Findings from this research indicate that bicubic polynomials have the lowest RMSEs, but do not improve the accuracy of estimating surface area

on DEMs by a large percent in comparison to linear and bilinear methods. The Linear method has an RMSE with values statistically similar to bicubic method in most of the DEM resolutions. The bilinear interpolation performs slightly less accurately than do linear method. Furthermore, the accuracy of surface area estimations have a relation with terrain roughness, i.e, the accuracy is lower in rough terrain.

Chapter V

Surface-Adjusted Frameworks for Estimating Elevation and Area from a Regular Gridded DEM

5.1. Introduction

The rigid-pixel paradigm assumes that land surface is flat and uniform within each pixel. The research reported in previous chapters illustrated how this assumption leads to errors in measurements from a regular gridded DEM. In this dissertation, a surface-adjusted paradigm formed the basis for two experiments, i.e., surface-adjusted elevation discussed in Chapter 3 and surface-adjusted area discussed in Chapter 4. The elevation of 20,000 randomly generated points within each study area were examined in the surface-adjusted elevation experiment and the modified Jenness method was proposed and examined in the surface-adjusted area experiment. Different interpolation methods (i.e., linear, bilinear, weighted average, biquadratic, and bicubic) and the information from adjacent pixels were examined to confirm the effectiveness of surface-adjusted methods for estimating elevation and area from a regular gridded DEM. The analysis examined the sensitivity of surface-adjusted measurements to different terrain types (flat versus hilly or mountainous; smooth versus rough, and uniform versus non-uniform) across a progression of spatial resolutions (10 m, 30 m, 100 m, and 1000 m). The statistical analysis and summary error metrics in Chapter 3 and 4 illustrated the accuracy of elevation and area estimates based on different interpolation methods, terrain types, and DEM resolutions. A general trend was observed

of increasing RMSEs at coarser resolutions and/or rough terrain. The bicubic method showed the lowest RMSEs in many but not all DEM resolutions and terrain types, and RMSEs for linear and bilinear interpolations were either statistically equivalent or very close to the bicubic in many cases, especially in the surface area calculations. In this chapter, these results are further discussed to propose two frameworks for surface-adjusted elevation and surface-adjusted area.

The proposed frameworks in this chapter will facilitate the selection of appropriate methods for estimating elevation and surface area from a regular gridded DEM based on resolution, and terrain type. The choice of surface-adjusted method is discussed from three different perspectives; to achieve the highest accuracy, to attain the fastest computations, or to achieve a balance between the increased computations needed to measure surface-adjusted elevation and area against the improvement in precision. Finally, the limitations of the proposed frameworks are discussed.

5.2. Conceptual Surface-Adjusted Framework

Statistical metrics used in the previous chapters illustrated that the interpolation method, DEM resolution, and terrain type are the main factors that should be considered in surface-adjusted measurements. The frameworks proposed in this chapter are based on these factors. Various interpolation methods and DEM resolutions used in this research are represented in Figure 5.1 as a conceptual framework. The following discussion is intended to guide others in navigating this conceptual space to utilize appropriate interpolation methods to estimate elevations and surface area in various types of terrain, prioritizing accuracy, processing speed, or a balance of the two.

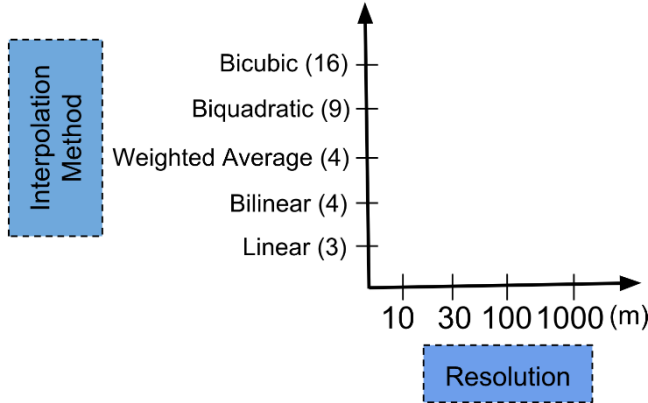


Figure 5.1. The conceptual surface-adjusted framework spanning four spatial resolutions, and five interpolation methods. Numbers in parentheses refer to the size of the local neighborhood used for interpolation.

Interpolation methods were evaluated by estimating terrain elevations at off-center pixel locations, and estimating surface area of each DEM pixel, as two possible applications of the surface-adjusted approach. Five interpolation methods were examined, i.e., linear, bilinear, weighted average, biquadratic, and bicubic. The bicubic method showed the smallest RMSEs in many DEM resolutions and terrain types, and the results of linear, and bilinear were statistically equivalent to bicubic in many cases. The weighted average method illustrated the highest RMSEs in almost every case, but displayed fastest processing times. In this chapter, these results are further discussed to propose frameworks for the surface-adjusted elevation and the surface-adjusted area.

Some researchers argue that a flat or uniform terrain can be modelled effectively using a lower-order polynomial, while a higher-order polynomial is more applicable to rough terrain (Shi and Tian 2006). The results of this dissertation confirm this finding. Furthermore, it was observed that RMSE values decrease to varying degrees moving from rough and non-uniform terrain to smooth and uniform terrain. In this chapter, the morphometric characteristics of study areas are investigated to see under what geographic conditions surface-adjusted methods make a difference

in elevation and area measurements. Slope, roughness, and uniformity are taken into consideration as the most important morphometric characteristics in surface-adjusted measurements. Terrain roughness is quantified based on the standard deviation of elevation in a 5 by 5 window. Table 5.1 reports slope and roughness statistics for each study area. It was discussed in Chapter 3 that these two morphometric characteristics have the highest correlation with the residuals calculated in the elevation experiment. Values for slope and roughness show strong association with each other, as well as with overall uniformity of terrain. Study areas are ordered in the table based on the mean of slope. In developing frameworks for this chapter, Washington, Colorado, and North Carolina with average slopes greater than 10° and average roughness greater than 4 m are considered rough terrain. Nebraska, Texas, and Louisiana are considered smooth terrain. Terrain uniformity is used as another terrain characteristic in this chapter. It has not been quantified in this research, but the DEMS visualized in Figure 3.1 show that the rough terrain study areas contain both mountainous and flat terrains. North Carolina is the most non-uniform study area. Washington and Colorado are mountainous and are relatively non-uniform. On the other hand, Texas and Louisiana display nearly flat and comparatively uniform terrain. Nebraska is the most uniform study area, with very small (high-frequency) features dispersed evenly across the DEM.

Table 5.1. The morphometric characteristics of all six study areas used in this research.

Study area	Slope ($^{\circ}$)		Roughness (m)		Uniformity
	Mean	STD	Mean	STD	
Washington	15.29	14.39	8.24	7.92	Non-uniform
Colorado	12.31	10.35	5.68	4.73	Non-uniform
North Carolina	11.01	9.11	4.87	3.97	Very non-uniform
Nebraska	5.07	5.45	2.02	1.65	Very uniform
Texas	2.44	3.03	1.09	1.13	Uniform
Louisiana	0.92	1.53	0.35	0.44	Uniform

5.3. Surface-Adjusted Elevation Framework

The results of the surface-adjusted elevation are presented in Table 5.2 in a simple way to be used as a guideline for choosing the appropriate interpolation method in a DEM resolution and terrain type. In this table, the lowest RMSE as well as the RMSEs whose difference from the lowest RMSE is not statistically significant at a resolution range. Cells whose RMSEs are significantly higher than the lowest RMSEs are shown with a plus sign, and the table value for these cells reports the magnitude of the difference. The RMSE values that differ significantly from the optimum but are closest to it (effectively, the second lowest RMSE values) have cells shaded in pale orange.

The magnitude of differences in the tables (hundredths of a meter) are on the order of 1 or 2 centimeters at finest resolutions, rising above 60 meters (for Washington state) at coarsest resolution. So, for example, in Washington State, the bicubic interpolator at 10 m resolution estimates elevation values with an RMSE of 66 cm, and the second-most accurate interpolator is biquadratic, with an RMSE of 67 cm (1 cm higher). As terrain becomes more uniform (that is, in Nebraska, Texas and Louisiana), the magnitude of RMSE values drops overall to a range of errors just under 8 meters for worst case estimation. The Louisiana 100 m DEM shows higher RMSEs than the 1000 m DEM for the linear interpolators and (as discussed in an earlier chapter) this may be due to compilation issues for this particular DEM that are not possible to confirm. The non-uniform terrain in the other three study areas reflect larger ranges of RMSEs 3.7 times higher for North Carolina, 4.8 times higher for Colorado, and 7.9 times higher for Washington. Clearly, the estimation of elevation in non-uniform terrain is subject to higher levels of uncertainty, and this cautions against using a single interpolator in such circumstances, or as Shi and Tian (2006) advise, adopting a hybrid solution involving more than one interpolation algorithm.

While each interpolation method performs differently based on DEM resolution and terrain

type, some patterns are common to more than one study area. For example, RMSE values increase from finer to coarser resolutions, except for Texas, where RMSEs for 100 m estimations are more accurate than for 30 m estimates. Differences among study areas are also apparent. In Washington at 100 m, all five interpolators show equal accuracy in estimating elevations; and in North Carolina at 10 m the five interpolators are equal or nearly equal in accuracy.

Table 5.2. Surface-adjusted elevation RMSE values reported as differences from highest accuracy. Dark orange shading shows the lowest RMSE for any interpolator at a given resolution. Multiple dark orange cells indicate that multiple interpolators generated RMSE values that do not differ significantly from the optimum value. Pale orange shows the lowest RMSE in each resolution that does differ significantly from the optimum.

(1) Washington

Resolution	Li3	BiLi4	WA4	BiQ9	BiC16
10 m	+0.03	+0.02	+0.05	+0.01	0.66
30 m	+0.14	+0.14	+0.18	+0.04	1.18
100 m	15.70	15.70	15.70	15.70	15.70
1000 m	+2.38	+1.81	+2.57	+1.96	61.36

Colorado

Resolution	Li3	BiLi4	WA4	BiQ9	BiC16
10 m	+0.02	+0.02	+0.05	0.35	0.35
30 m	+0.12	+0.12	+0.22	+0.04	0.89
100 m	+0.30	+0.28	+0.35	7.52	7.52
1000 m	+1.01	+0.81	+1.23	+0.72	37.63

North Carolina

Resolution	Li3	BiLi4	WA4	BiQ9	BiC16
10 m	0.89	0.89	+0.03	0.89	0.89
30 m	+0.14	+0.13	+0.19	+0.02	1.29
100 m	+0.24	+0.23	+0.28	9.36	9.36
1000 m	+0.93	+0.74	+1.13	+0.51	29.10

Nebraska

Resolution	Li3	BiLi4	WA4	BiQ9	BiC16
10 m	+0.03	+0.03	+0.04	+0.01	0.20
30 m	+0.10	+0.09	+0.11	+0.02	0.64
100 m	+0.10	+0.10	+0.11	3.51	3.51
1000 m	+0.37	+0.33	+0.33	7.68	7.68

Texas

Resolution	Li3	BiLi4	WA4	BiQ9	BiC16
10 m	+0.01	0.19	+0.01	0.19	0.19
30 m	+0.04	+0.03	+0.05	+0.01	0.39
100 m	3.85	3.85	+0.01	+0.01	3.85
1000 m	+0.16	+0.13	+0.17	+0.06	7.51

Louisiana

Resolution	Li3	BiLi4	WA4	BiQ9	BiC16
10 m	+0.01	+0.01	+0.01	0.12	0.12
30 m	+0.02	0.27	+0.02	0.27	0.27
100 m	7.77	7.77	7.77	+0.08	+0.06
1000 m	6.76	6.76	6.76	+0.11	+0.07

Given the vertical accuracy of 10 m and 30 m DEMs and the accuracy in most of the GIS projects, it can be concluded that the lower order polynomials (i.e., linear and bilinear) are preferable to be used in any terrain type when a fine DEM resolution is used. In 100 m DEM, the results are not consistent. In Washington and Texas, bicubic is performing statistically the same

as linear and bilinear method. In Colorado, North Carolina, and Nebraska, bicubic method outperforms linear and bilinear with RMSE differences of 30 cm, 24 cm, and 10 cm, respectively. In 1000 m DEM, bicubic strongly outperform linear and bilinear methods in rough and non-uniform terrain with RMSE differences of about 2 m, 1m and 90 cm. In smooth and uniform terrain, bicubic cannot be the best choice in any resolution due to the small RMSE differences.

Table 5.2 can be used as a workflow for estimating surface-adjusted elevation in terrain of varying roughness and uniformity. The table distinguishes priorities of accuracy and speed. When the accuracy of surface-adjusted elevation is the ultimate goal, the bicubic method is the best choice when DEM resolution is coarse, and terrain is rough or non-uniform. In fine DEM resolutions, and/or smooth and uniform terrains, linear or bilinear methods provide the highest accuracy. The weighted average method has the highest RMSE in four study areas, except for Nebraska and Louisiana, where both terrains flat and uniform. But, it was observed that this method is the fastest surface-adjustment method. Therefore, when the speed of computations is the highest priority, the rigid-pixel paradigm (i.e., the nearest centroid approach) or the weighted average method can be used. This might be an appropriate choice if one is performing a rough estimation for example when working in the field, or to determine a worst-case accuracy prior to performing more intensive computations. Given that most applications will warrant a strategy that balances accuracy and the added computational time, the linear and bilinear methods provide the best choices in estimating the elevation of off-centroid points from a regular gridded DEM.

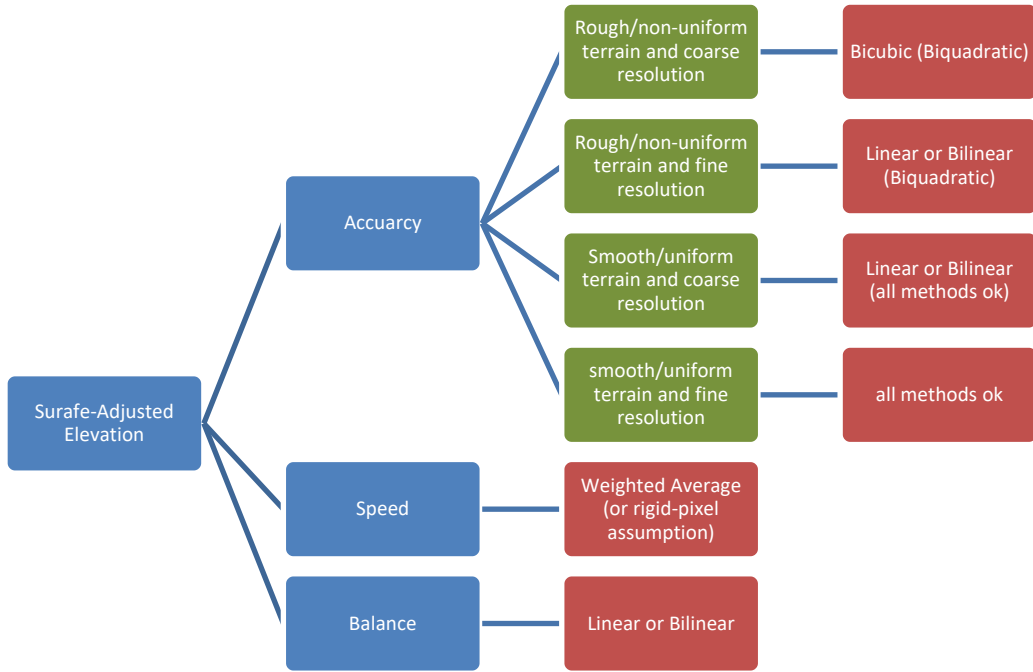


Figure 5.2. Surface-adjusted elevation workflow. Blue boxes indicate overall strategy, gray boxes identify various terrain types, and orange boxes display the best choice for an interpolation method in each situation (with secondary choices in parentheses).

5.4. Surface-Adjusted Area Framework

This section discusses the results of area measurements presented in Chapter 4 in order to provide guidelines for surface-adjusted area measurements. Different methods were discussed for calculating surface area on a regular gridded DEM. The slope method was discussed as the simplest method for calculating surface area by considering one slope angle for each DEM pixel. The Jenness method was examined as one of the most widely used methods for surface area calculations. This method was modified in the dissertation research and a comparison illustrated that the modified Jenness method outperforms the original Jenness method. The modified Jenness was used to compare different interpolation methods for estimating surface area. Table 5.3 illustrates the results of these comparisons. These results are transformed from Table 4.3 and are presented in the same manner as Table 5.2. Dark orange shows the lowest RMSE and the RMSEs that are not statistically different from the lowest RMSE. All other table values are reported as

differences from the optima (shown with a plus sign). Pale orange indicates the method with the lowest RMSE that does differ significantly from the most accurate values.

Table 5.3. Surface-adjusted area RMSE values reported as differences from highest accuracy. Dark orange shading shows the lowest RMSE for any interpolator at a given resolution. Multiple dark orange cells indicate that multiple interpolators generated RMSE values that do not differ significantly from the optimum value. Pale orange shows the lowest RMSE in each resolution that does differ significantly from the optimum.

Washington						Colorado					
Resolution	Li3	BiLi4	WA4	BiQ9	BiC16	Resolution	Li3	BiLi4	WA4	BiQ9	BiC16
10 m	3.69	+0.25	+3.46	+0.28	3.69	10 m	2.27	+0.19	+2.26	+0.27	2.27
30 m	+1.65	+2.67	+29.41	+3.96	26.12	30 m	16.37	+1.34	+17.26	+2.77	16.37
100 m	385.72	385.72	+131.16	385.72	385.72	100 m	187.99	+7.63	+108.54	+17.21	187.99
1000 m	+275.7 4	+894.5 8	+7,027.6 2	+4,205.1 6	22,067.4 1	1000 m	11,885.0 5	+399.3 5	+2,952.4 7	+1636.6 5	11,885.0 5

North Carolina						Nebraska					
Resolution	Li3	BiLi4	WA4	BiQ9	BiC16	Resolution	Li3	BiLi4	WA4	BiQ9	BiC16
10 m	1.81	+0.11	+2.18	+0.21	1.81	10 m	+0.10	+0.16	+0.80	+0.21	0.97
30 m	+0.91	+1.50	+16.14	+3.28	13.96	30 m	+0.42	+0.86	+3.43	+1.76	8.18
100 m	+3.85	202.48	+75.29	+17.71	202.48	100 m	65.94	+1.02	+5.29	+2.58	65.94
1000 m	8,634.9 7	+264.8 9	+1,167.2 4	+1,025.7 2	8,634.9 7	1000 m	569.43	+6.06	+26.57	+21.64	569.43

Texas						Louisiana					
Resolution	Li3	BiLi4	WA4	BiQ9	BiC16	Resolution	Li3	BiLi4	WA4	BiQ9	BiC16
10 m	0.78	+0.09	+0.49	+0.12	0.78	10 m	0.30	+0.03	+0.12	+0.05	0.30
30 m	5.14	+0.52	+2.72	+0.81	5.14	30 m	+0.01	+0.09	+0.32	+0.23	1.83
100 m	43.10	+2.11	+10.05	+3.30	43.10	100 m	+1.14	+0.59	+7.91	8.77	+1.01
1000 m	844.65	+17.96	+68.44	+55.15	844.65	1000 m	36.42	36.42	+2.40	+1.70	36.42

It can be seen that the bicubic, linear and bilinear methods have the lowest or second lowest RMSEs in most of the DEM resolutions and terrain types. It is also apparent from the tables that, in contrast with surface-adjusted estimates of elevation, RMSE values for surface area estimation do appear to vary much across terrain type or resolution. The weighted average method has the highest RMSEs in all cases, except in estimating surface area for the 100 m DEM in Louisiana where it shows second highest accuracy. The biquadratic method performs more accurately than

the weighted average method, but does not provide higher accuracy than other methods, contrary to research findings (discussed in Chapter 4) estimating surface areas for regularized polynomial manifolds. For achieving the highest accuracy generally, both the bicubic and linear methods are performing best in different DEM resolutions and terrain types, with bilinear performing nearly as well.

Figure 5.3 summarizes the results of Table 5.3 to provide a simpler workflow for choosing the best surface-adjusted area estimation method in different terrain types. If the goal is to reach the highest accuracy in the surface area measurements, the bicubic or linear methods (with modified Jenness) can be used, with bilinear as a second-best choice. The planar area or the slope methods discussed in Chapter 4 have the lowest accuracy in estimating area, but are the best choice when the speed of computations is a primary priority. The original Jenness method is faster than any of the five tested interpolation methods, so while it is four times slower than the planar or slope methods, it is included as a second-best choice. In most situations, a balance is needed between processing time and accuracy. Given the extra computational time needed for the bicubic method the linear interpolation using the modified Jenness method is the appropriate choice to balance speed with accuracy, for calculating surface area from a regular gridded DEM.

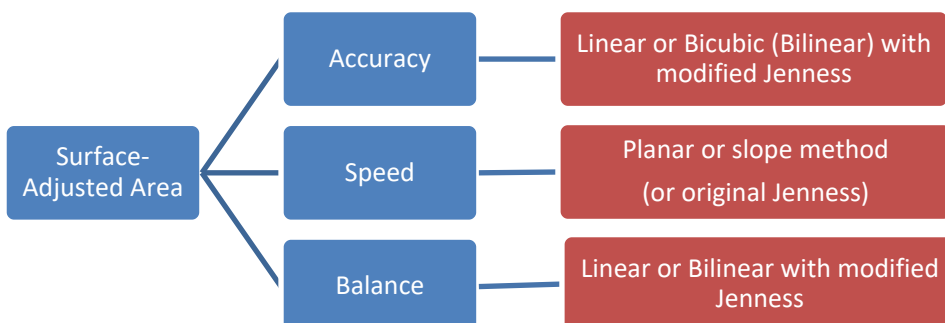


Figure 5.3. Surface-adjusted area workflow. Blue boxes indicate overall strategy, gray boxes identify various terrain types, and orange boxes display the best choice for an interpolation method in each situation (with secondary choices in parentheses).

5.5. A Proposed Framework for the Surface-Adjusted Elevation and Surface-Adjusted Area

RMSE values of elevation and area estimates were investigated in the previous sections to establish the basic of a surface-adjusted framework. Figure 5.4 presents a proposed framework for surface-adjusted elevation and surface-adjusted area. These frameworks illustrate that where each terrain type provides a justifiable reason for using a particular interpolation method at a particular resolution. In the surface-adjusted elevation framework, for the finer DEM resolutions, all methods perform similarly in a smooth/uniform terrain., and the linear and bilinear interpolation methods perform better in the rough/nonuniform terrain. In the same framework, for the courser DEM resolutions, the linear and bilinear interpolation methods perform better in a smooth/uniform terrain, and the bicubic and biquadratic interpolation methods outperform other methods in the rough/nonuniform terrain. The framework for the surface-adjusted area is simpler. The linear and bicubic outperform other methods in all terrain types and DEM resolutions. That is, the linear method can be used for surface area calculation in all situations to achieve the highest accuracy, and also to make a balance between processing time and accuracy.

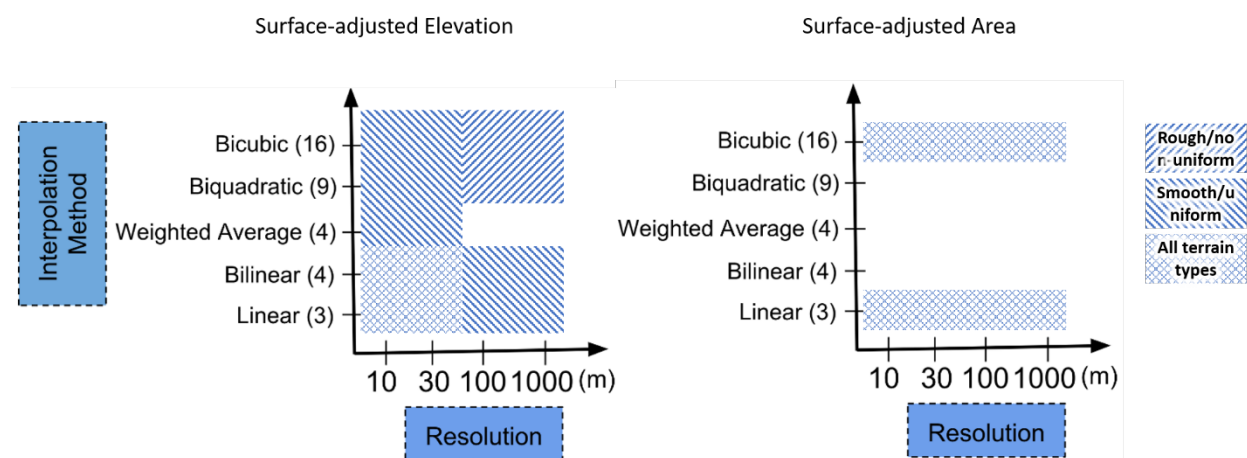


Figure 5.4. The proposed framework for surface-adjusted elevation and surface-adjusted area

5.6. Limitations of the Proposed Frameworks

The proposed workflows and framework for the surface-adjusted elevation and the surface-adjusted area presented in this chapter have some limitations. First, terrain type was proposed to be one of the most important factors in choosing an appropriate surface-adjustment method. Slope, roughness and uniformity were used as the main morphometric characteristics of the terrain. Slope and roughness were quantified for each study area and illustrated that the slope and roughness are highly correlated with residuals. However, terrain uniformity was not quantified for each study area. Geostatistical techniques such as variogram analysis can be used to further understand the uniformity of each study area.

Furthermore, other terrain characteristics such as land cover type, and settlement disturbance might be investigated as well to have a more comprehensive land type classification for the surface-adjusted framework. Moreover, the results were discussed based on the overall terrain characteristics of each study area. Each study area is a combination of different terrain types, but uniformity was not inspected in this research. One way to resolve issues of uniformity would investigate the study areas at the pixel level. That is, the pixels for all of the study areas could be isolated from their respective DEMs and then categorized based on the terrain characteristics of each pixel and its surrounding. This could be accomplished using decision trees or some other form of machine learning.

A different limitation to the study is that data sets used in this research were limited to four spatial resolutions. Choosing a surface-adjusted method and understanding its accuracy for a DEM resolution that was not tested might be based on the overall trend of RMSEs in the presented results. RMSE results show a trend of increasing with coarser resolutions, but exceptions do occur, which may relate to terrain type, compilation methods, or data production standards, all of which

lie beyond the control of the DEM use case. Besides, if someone uses a DEM resolution of 10 m, 30 m, 100 m, or 1000 m, but with a different vertical accuracy, the proposed framework for selecting an appropriate strategy cannot be totally assured. The DEMs used in this research were independently compiled DEMs from the NED and SRTM data archives. The accuracy metrics of surface-adjusted measurements can differ if a DEM from another source is used.

Finally, one must consider the effects of resampling on DEM results. All of the study areas in this dissertation were original and independent compilations, due to findings from pilot research showing that resampled DEMs display quite different patterns of texture, uniformity, and proportion of high- to low-frequency detail. Resampling remains a common processing step in many DEM applications, especially with the emergence and wider availability of lidar data. An interesting use case for future work might involve resampling lidar data to different DEM resolutions and compare interpolations from resampled data at varying spatial resolutions in order to separate the influence of DEM compilation and DEM resampling.

5.6. Summary

The appropriate surface-adjustment method is different for alternate purposes in the literature. For example, Li, Taylor, and Kidner (2005) employ elevations of points from a regular gridded DEM to refine GPS estimates in a vehicle navigation experiment using bilinear and bicubic interpolation methods, finding little or no difference in RMSE values at 10 m and 50 m resolutions. Wood (1998) models the continuity of pixel surfaces in DEMs using biquadratic interpolation for calculating slope and curvature. He prefers this interpolation method to linear interpolators because the first and second order properties (i.e., slope and curvature) can be calculated from the biquadratic function. Wood (1996) argues that this model provides a successful compromise between accuracy and the number of points required to generate the surface. Wood

(1998) also uses these models to identify and extract features on a DEM. Quadratic-based algorithms are recommended for calculating curvature as well (Evans 2013; Schmidt, Evans, and Brinkmann 2003; Florinsky 1998; Shary 1995). The findings of this dissertation also illustrate that appropriate surface-adjustment methods for estimating elevation and area differ, and they depend to a certain degree on terrain type and DEM resolution. Higher order polynomials seem to produce more accurate estimates for rough and non-uniform terrain, or for coarse DEM resolutions. On the other hand, linear and bilinear interpolation methods have faster computational times, and (especially for estimating surface area) are as accurate or more accurate as higher order polynomials in smooth and uniform terrain and in finer DEM resolutions.

In this chapter, two frameworks were proposed for estimating surface-adjusted elevation and surface-adjusted area. These frameworks can be used to guide selection of interpolators for estimating elevation and surface area from a regular gridded DEM. These frameworks are based on DEM resolution, terrain type, and interpolation method. Therefore, each surface-adjusted estimation task should be investigated in the context of these variables, since no single interpolation method provides the most appropriate estimation strategy in every case.

Chapter VI

Discussion and Conclusions

6.1. Surface-Adjusted Terrain Measurement: Why is it Important?

The current paradigm in GIScience for characterizing terrain assumes that the land surface is flat and uniform within each pixel, ignoring slope and curvature. This rigid-pixel paradigm is widely adopted in many if not most geospatial analyses. The paradigm served a useful purpose historically, until processing capabilities and data storage capacities advanced to a degree where such simplifying assumptions are less of a pragmatic necessity. In those situations, compelling reasons to understand the progression of errors that might occur when estimating elevations from digital terrain include common applications such as routing, modelling natural hazards risks, and monitoring habitat fragmentation.

This research employed realistic surface geometries of terrain, incorporating slope and curvature in estimating elevation and surface area. The incorporation of slope and curvature leads to *surface-adjusted* terrain metrics. The research is possible because of advances in processing speeds and newly available access to high performance computing (through Amazon Web Services), and the research is scientifically important because terrain derivatives (elevation, distance, area, and volume) underlie many spatial modeling tasks. The availability of fine resolution lidar-based DEMs provides a benchmark against which to gauge interpolated estimates,

but it is important to remember that lidar availability is sparse in rural areas and in developing regions, thus it is useful to develop guidelines for understanding the progression of errors across spatial resolutions, interpolation methods, neighborhood configurations, and terrain heterogeneity. Finally, it is important to recognize that the assumption of non-rigid pixels carries an additional computational load, as it must incorporate not only elevation and pixel size, but also slope and curvature, in effect, adjusting for the changing terrain surface at sub-pixel resolutions. The balance between the increased computations needed to measure surface-adjusted elevation against the improvement in precision was addressed as well.

6.2. Research Objectives and Methodology

The research reported in this dissertation was proposed along three objectives, including: 1) cross-scale analysis of sub-pixel variations of elevation in digital elevation models; 2) cross-scale analysis of surface area computations; and 3) the statistical properties of DEM error across resolution and terrain type.

A suite of six DEMs were examined that span several dimensions (flat versus hilly or mountainous; smooth versus rough, and uniform versus non-uniform). Each study area were analyzed with 4 DEM resolutions of 10 m, 30 m, 100 m, and 1000 m; and these were validated against another independently compiled 3 m lidar-based DEM as the benchmark. Data were downloaded from USGS and from SRTM. The data were selected on the basis of variety in the three dimensions as well as the availability of a lidar benchmark.

Five discrete (averaging) and two continuous (polynomial) estimation methods were utilized to estimate elevation and then surface area, including planar, least squares, weighted average, linear, bilinear, biquadratic, and bicubic interpolation. The planar method was utilized on

the lidar benchmark due to its relatively fine resolution, and to avoid introducing interpolation artifacts into the interpolation during the validation of interpolation tests.

Statistical analysis compared residuals against 3 m lidar data as well as computing summary error metrics such as RMSE values, Mean Average Error, and interpolated extrema. A correlation analysis compared terrain slope, aspect, curvature, roughness and uniformity. Computational benchmarks were compared to establish relative processing times as well as guidelines on error propagation across scales.

6.3. Research Questions and Answers

The research questions mentioned in Chapter 1 are reexamined to further argue the findings of this dissertation:

Research question 1: How can surface-adjusted elevation and surface-adjusted area be most accurately estimated from a DEM? What is the best mathematical model to reconstruct the surface of a DEM cell to estimate elevation, and surface area?

To answer this question, elevation of 20,000 randomly generated points within each study area were estimated and examined using different interpolation methods that employed different contiguity configurations. The estimated elevations were compared with the corresponding elevation of the pixel centroid (i.e., residuals analysis) to investigate sub-pixel variations in elevation. The sub-pixel variation of elevation becomes significant, especially in rough terrain and in coarser DEM resolutions. The estimated elevations were compared with the lidar benchmark (i.e., using RMSE and other metrics) to assess the accuracy of different interpolation methods.

Results in Chapter 3 illustrated that the bicubic and biquadratic interpolations performed with lower RMSEs than linear and bilinear methods at coarse resolutions and in rough or non-

uniform terrain. The biquadratic and bicubic methods had RMSE values that were statistically equivalent in most DEM resolutions. The weighted average method showed highest magnitude errors estimating elevations for all resolutions. In terms of accuracy, higher order polynomials improve elevation estimation on a regular grid DEM.

Surface area measurements based on different polynomial functions were tested in Chapter 4. To perform the estimates of surface area, pixel neighborhoods were partitioned into 8 triangular facets whose vertex elevations were estimated by the same seven interpolation methods utilized in Chapter 3. A discrete approximation of surface area incorporating slope of the 8 facets was used to estimate surface areas. Findings indicated that the bicubic and linear methods performed with essentially equal accuracy in all DEM resolutions and terrain types. When estimating surface area, the weighted average method performed with the smallest standard deviation at every resolution although mean and median estimates were never the most accurate. This implies that the weighted average introduced a systematic bias that was inaccurate but highly consistent.

Research question 2: *How does the accuracy of surface-adjusted elevation and surface-adjusted area vary with changing spatial resolution? And does this vary with the method of surface adjustment, and/or terrain roughness?*

DEM error is spatially variable, spatially autocorrelated and heteroscedastic. In this research, DEM vertical errors are not normally distributed, and extreme errors tend to situate in rougher terrain. Errors introduced by the rigid pixel assumption depend largely on DEM resolution and terrain type. Comparing terrain derivatives such as slope, aspect, curvature and terrain roughness, slope shows the highest correlation with DEM errors; and DEM errors in rough terrain are correlated at a larger distance than the errors in flat terrain.

Four different DEM resolutions (10 m, 30 m, 100 m, and 1,000 m) were analyzed. Error

magnitudes of estimated elevation and surface area varied with DEM resolution. A general trend of increase in the RMSEs at coarser resolutions were observed because as pixel sizes increase, the interpolator is less able to make a precise estimate of elevation. And because elevations must be interpolated to estimate surface area, a similar pattern is observed for both types of estimation.

The study area in Washington is composed of the roughest terrain with 438.55 m as the standard deviation of elevation, 15.29° as the mean slope and 8.24 m as the mean roughness. The study area in Louisiana, on the other hand, has the flattest terrain with 12.26 m as the standard deviation of elevation, 0.92° as the mean slope and 0.35 m as the mean roughness. The RMSE of estimated elevations and surface areas decreases from rough and uneven terrain to smooth and flat terrain. That is, terrain type has an impact on the performance of different interpolation methods in estimating both elevation and surface area. Therefore, the surface-adjusted measurements make a greater difference in steeper and rough terrain. These findings are tempered somewhat at coarser resolutions, where larger pixels tend to damp down both roughness and slope.

Research question 3: *What computational cost does the surface-adjusted paradigm add to computations for estimating elevation and surface area? And does the added cost vary with resolution and geographic conditions?*

One goal of this work was to establish a balance between processing time and improvements in accuracy, to assist geospatial scientists in understanding the rate at which uncertainty increases when modeling terrain of a particular roughness at specific resolutions in areas where lidar data or when high performance computing may not be available.

For estimating elevation, the weighted average, linear and bilinear interpolators give the fastest run time, while the bicubic method shows the highest processing time. If accuracy is a primary goal and the data volumes are small, then biquadratic and bicubic methods may be the

best choice. For large volume data sets, the linear polynomials are likely the better choice. For estimating surface area, Jenness's method is the fastest and bicubic is the slowest. To make a balance between the increased computations needed to measure surface area against the improvement in accuracy, Jenness and linear methods seem to be optimal choices. The processing time depends on the number of pixels and the method used for elevation or surface area calculations. DEM resolution and terrain type does not change the processing time.

6.4. Limitations of the Experiments on Surface Adjustment

The surface adjustment project in this dissertation has some limitations discussed in the following:

- The 3 m lidar DEM is used as a benchmark in this research. Pixels in the lidar data are considered flat to avoid introducing interpolation during the validation of interpolation tests. Therefore, slope and curvature of pixels in the lidar data are ignored. Due to the relatively small pixel size of lidar data, this error can be negligible; but, it might be worth testing against a point cloud lidar data to evaluate this error.
- Surface area cannot be compared through different independently compiled DEM resolutions. That is, the extent of rasters at different resolutions are not exactly aligned and so the sum of surface area in these rasters cannot be compared. Figure 6.1 illustrates the extent mismatching occurring in 100 m and 1000 m DEMs in North Carolina. Therefore, resampling the lidar DEM to courser resolutions in order to have the same extent in all DEMs might be a solution for this issue.

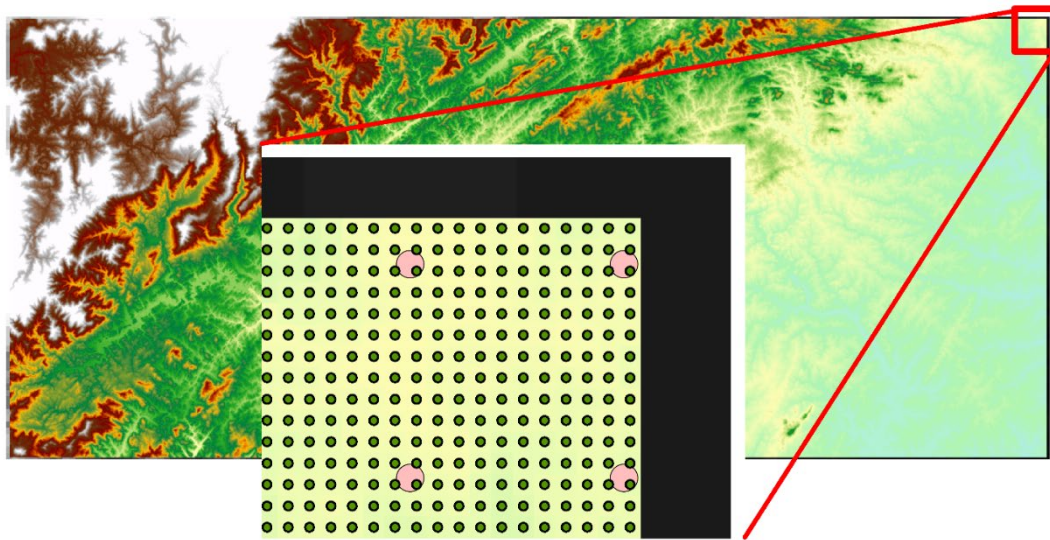


Figure 6.1. Mismatching of 100 m and 1000 m DEMs in North Carolina. The green and pink circles show the pixel centroids in the 100 m and 1000 m DEMs, respectively.

- Independently compiled DEMs from different sources (NED at 10 and 30 m, SRTM at 100 and 1000 m) are used in this dissertation. The performance of different interpolation methods used for elevation and area estimation is partly capturing the effects of different resolutions and partly the effects of different source data. Therefore, it is not clear whether the changes at the coarsest resolution is due to the resolution or the change of source data. It would be more informative to consider those effects separately by using the 3 m lidar as the source data at all resolutions, and consider the changes when different source data is used. Furthermore, data from different sources that have the same resolution can be used to investigate the impact of DEM vertical accuracy on the surface-adjusted methods.
- For testing the surface-adjusted elevation, 20,000 random points were generated. The elevation of each individual random point was estimated based on different interpolation methods in each resolution. Although terrain is highly spatially autocorrelated and thus

elevations are spatially dependent, random points were treated as individual points in each resolution. There are a subtle issue in this experiment. Comparing the errors derived from the same number of points but different resolutions ignores different autocorrelative structures in the data. Having a constant sampling intensity is appropriate for "across-methods" comparison, but to have a cross-scale comparisons, an optimum sample size can be derived for each resolution.

- Terrain uniformity in each study area was not investigated in this research. Some of the study areas are a combination of both homogenous and non-homogenous terrain. RMSE was reported for each interpolation method as the overall accuracy of subpixel elevation estimation of that interpolation method for the entire study area. DEM errors are spatially autocorrelated and the RMSE is not an effective metric to evaluate a spatially variable, and correlated measure.

6.5. Conclusions and Future Work

Terrain models play an important role in geosciences and engineering. They are used in numerous applications such as planning of road and canals construction, analyzing drainage and catchment area, locating radio networks, flight simulation and virtual battlefield exercises, delineating natural hazards zones, predicting the spread of forest fires, and simulating floods. Surface-adjusted models presented in this dissertation refine terrain modeling and improve its applications, and as a result benefit environment, society, and safety. Furthermore, the surface-adjusted paradigm provides an alternative to non-Euclidean geospatial measurement frameworks. Guidelines developed for surface-adjusted metrics will benefit rural communities and developing regions where lidar data is not available, to generate reliable model results for precise and robust environmental characterization.

This research contests a prevailing paradigm for terrain-based analyses, which forms the foundation for nearly all environmental models. An understanding of uncertainty in the rigid-pixel paradigm is especially necessary for environmental scientists to determine how inaccuracy leads to uncertainty in their models. This work fills a critical gap in the literature regarding errors in estimating elevation, and surface area in terrain modeling. Results of this research are needed to improve the scientific value of models that are widely used in most environmental applications.

Spatial analysis is commonly conducted in Euclidean space, and the slope and curvature characteristics of terrain surface are ignored. With advances in computer processing speed and increased data availability, the scientific community must address limitations of existing modeling methods to provide decision-makers the best possible information about critical environmental issues including biophysical and anthropogenic factors and interactions. This work develops a set of terrain-adjusted metrics incorporating terrain slope and curvature that can reduce estimation errors in spatial analysis. In this research sub-pixel variations in DEMs through different resolutions were investigated in order to develop the foundation of surface-adjusted computations on DEMs, resulting in more realistic analysis in terrain models.

Part of this dissertation was related to the computation of surface area in terrain. Surface area is an important element in modeling hydrologic processes such as flow accumulation or erosion, in landscape processes such as fuel loads for wildfire, and even in basic characterizations of terrain roughness. At present, terrain metrics are most often calculated under the assumption that values of elevation and slope in DEM pixels are uniform, and that within-pixel variations can be ignored to simplify processing and modeling. In spite of advances in processing speeds and availability of finer resolution data (e.g. lidar) the convention persists, since errors remain small so long as pixels remain small. In parts of rural North America and in developing nations however,

lidar and other fine resolution data is not widely available.

Additionally, as applications such as disaster response, climate change, or predictive models of human and natural landscape change emerge that span continents or the entire globe, the errors introduced in surface area metrics can become dramatic. The outcomes of this dissertation demonstrate that using surface area instead planar area can significantly improve the accuracy of spatial metrics. For localized areas or for very small pixel sizes, the amount of imprecision is insignificant, but can increase with larger pixel size and/or across regional or global expanses, as in the case with models of climate change, sea level rise, and other modeling applications, where pixels can span dozens to hundreds of kilometers.

In ongoing research, Buttenfield *et al.* (2016) are comparing surface-adjustment methods for calculating terrain distance. Future work to identify critical modelling data resolutions and landscape conditions under which surface-adjustment improves model outcomes will advance terrain-based computational modelling, as for example in weighted flow accumulation, debris flow extents, and similar areal metrics. Furthermore, this work will assess the impacts of surface adjustment on environmental models (e.g., least cost path calculation, land cover fragmentation, and flood inundation models) that use elevation, distance, and area metrics. The future work also will advance understanding of how spatial error propagates through processing stages and across resolutions.

BIBLIOGRAPHY

- Aerts, J. C., M. F. Goodchild and G. Heuvelink (2003). Accounting for Spatial Uncertainty in Optimization with Spatial Decision Support Systems. *Transactions in GIS* 7(2): 211-230.
- Aryal, R. R., H. Latifi, M. Heurich and M. Hahn (2017). Impact of Slope, Aspect, and Habitat-Type on Lidar-Derived Digital Terrain Models in a near Natural, Heterogeneous Temperate Forest. *PFG—Journal of Photogrammetry, Remote Sensing and Geoinformation Science* 85(4): 243-255.
- Bai, R., T. Li, Y. Huang, J. Li and G. Wang (2015). An Efficient and Comprehensive Method for Drainage Network Extraction from DEM with Billions of Pixels Using a Size-Balanced Binary Search Tree. *Geomorphology* 238: 56-67.
- Band, L. E. and I. Moore (1995). Scale: Landscape Attributes and Geographical Information Systems. *Hydrological Processes* 9(3-4): 401-422.
- Batista, T., P. Mendes, L. Carvalho, C. Vila-Viçosa and C. P. Gomes (2012). Suitable Methods for Landscape Evaluation and Valorization: The Third Dimension in Landscape Metrics. *Acta Botanica Gallica* 159(2): 161-168.
- Berk, S. and M. Ferlan (2018). Accurate Area Determination in the Cadaster: Case Study of Slovenia. *Cartography and Geographic Information Science* 45(1): 1-17.
- Berry, J. (2002). Beyond Mapping Use Surface Area for Realistic Calculations. *Geo World* 15: 20-21.
- Blaschke, T., D. Tiede and M. Heurich (2004). 3d Landscape Metrics to Modelling Forest Structure and Diversity Based on Laser Scanning Data. *International Archives of the Photogrammetry, Remote Sensing and Spatial Information Sciences* 36(8/W2): 129-132.
- Boisvert, J. B. and C. V. Deutsch (2011). Programs for Kriging and Sequential Gaussian Simulation with Locally Varying Anisotropy Using Non-Euclidean Distances. *Computers & Geosciences* 37(4): 495-510.
- Bolstad, P. (2005). *GIS Fundamentals: A First Text on Geographic Information Systems*. Eider Press, White Bear Lake, Minnesota.

- Burrough, P. A., R. A. McDonnell and C. D. Lloyd (2015). *Principles of Geographical Information Systems*. Oxford University Press, Oxford, United Kingdom.
- Buttenfield, BP. (1987). Automatic Identification of Cartographic Lines. *The American Cartographer* **14**(1): 7-20.
- Buttenfield, B. P. (1986). Digital Definitions of Scale-Dependent Line Structure. *Proceedings, AUTO-CARTO, London* **1**: 497-506.
- Buttenfield, B.P. (1984). *Line Structure in Graphic and Geographic Space*. Ph.D. dissertation, University of Washington.
- Buttenfield, B. P., M. Ghandehari, S. Leyk, L. V. Stanislawska, M. Brantley and Y. Qiang (2016). Measuring Distance “as the Horse Runs”: Cross-Scale Comparison of Terrain-Based Metrics. *Proceedings 9th International Conference on Geographic Information Science, GIScience 2016*, Montreal, Canada: 37-40
- Calder, C. and N. A. Cressie (2009). Kriging and Variogram Models. *International Encyclopedia of Human Geography* **1**: 49-55.
- Carlisle, B. H. (2002). *Digital Elevation Model Quality and Uncertainty in DEM-Based Spatial Modelling*. Ph.D. dissertation, University of Greenwich, London, UK.
- Carlisle, B. H. (2005). Modelling the Spatial Distribution of DEM Error. *Transactions in GIS* **9**(4): 521-540.
- Chang, K.-t. and B.-w. Tsai (1991). The Effect of DEM Resolution on Slope and Aspect Mapping. *Cartography and Geographic Information Systems* **18**(1): 69-77.
- Chen, C., Y. Li, X. Cao and H. Dai (2014). Smooth Surface Modeling of DEMS Based on a Regularized Least Squares Method of Thin Plate Spline. *Mathematical Geosciences* **46**(8): 909-929.
- Chen, C., Y. Li and H. Dai (2011). An Application of Coons Patch to Generate Grid-Based Digital Elevation Models. *International Journal of Applied Earth Observation and Geoinformation* **13**(5): 830-837.

- Chen, C., X. Wang, C. Yan, B. Guo and G. Liu (2016). A Total Error-Based Multiquadric Method for Surface Modeling of Digital Elevation Models. *GIScience & Remote Sensing* **53**(5): 578-595.
- Chorley, R. J., D. E. Malm and H. A. Pogorzelski (1957). A New Standard for Estimating Drainage Basin Shape. *American Journal of Science* **255**(2): 138-141.
- Christaller, W. (1933). Die Zentralen Orte in Süddeutschland: Eine Ökonomisch-Geographische Untersuchung Über Die Gesetzmässigkeit Der Verbreitung Und Entwicklung Der Siedlungen Mit Städtischen Funktionen. University Microfilms.
- Clarke, K. C. and B. E. Romero (2017). On the Topology of Topography: A Review. *Cartography and Geographic Information Science* **44**(3): 271-282.
- Coveney, S. (2013). Association of Elevation Error with Surface Type, Vegetation Class and Data Origin in Discrete-Returns Airborne Lidar. *International Journal of Geographical Information Science* **27**(3): 467-483.
- Crawford, C. A. G. and L. J. Young (2008). Geostatistics: What's Hot, What's Not, and Other Food for Thought. *Proceedings of the 8th International Symposium on Spatial Accuracy Assessment in Natural Resources and Environmental Sciences*, Shanghai, PR China: 8-16.
- Cressie, N. (1988). Spatial Prediction and Ordinary Kriging. *Mathematical Geology* **20**(4): 405-421.
- Cressie, N. (2015). *Statistics for Spatial Data*. John Wiley & Sons, New York.
- Cressie, N., J. Frey, B. Harch and M. Smith (2006). Spatial Prediction on a River Network. *Journal of Agricultural, Biological, and Environmental Statistics* **11**(2): 127–150.
- Curriero, F. C. (2006). On the Use of Non-Euclidean Distance Measures in Geostatistics. *Mathematical Geology* **38**(8): 907-926.
- Czarnecka, B. and Ł. Chabudziński (2014). Assessment of Flora Diversity in a Minor River Valley Using Ecological Indicator Values, Geographical Information Systems and Digital Elevation Models. *Open Life Sciences* **9**(2): 220-231.
- Danielsen, J. (1989). The Area under the Geodesic. *Survey review* **30**(232): 61-66.

- Darnell, A. R., N. J. Tate and C. Brunsdon (2008). Improving User Assessment of Error Implications in Digital Elevation Models. *Computers, Environment and Urban Systems* **32**(4): 268-277.
- Deng, Y. (2009). Making Sense of the Third Dimension through Topographic Analysis. In: T.A. Warner, M.D. Nellis, and G.M. Foody (Eds.) *The SAGE Handbook of Remote Sensing*, London, UK.
- Deng, Y., J. P. Wilson and B. Bauer (2007). DEM Resolution Dependencies of Terrain Attributes across a Landscape. *International Journal of Geographical Information Science* **21**(2): 187-213.
- Dorner, B., K. Lertzman and J. Fall (2002). Landscape Pattern in Topographically Complex Landscapes: Issues and Techniques for Analysis. *Landscape Ecology* **17**(8): 729-743.
- Ehlschlaeger, C. R. (2002). Representing Multiple Spatial Statistics in Generalized Elevation Uncertainty Models: Moving Beyond the Variogram. *International Journal of Geographical Information Science* **16**(3): 259-285.
- Ehlschlaeger, C. R. and A. Shortridge (1996). Modeling Elevation Uncertainty in Geographical Analyses. *Proceedings of the International Symposium on Spatial Data Handling: Advances in GIS research I*, 12–16 August 1996, Delft, Netherlands: 9B.15-9B.25.
- El-Sheimy, N., C. Valeo and A. Habib (2005). *Digital Terrain Modeling: Acquisition, Manipulation, and Applications*. Boston, Artech House.
- Endreny, T. A. and E. F. Wood (2001). Representing Elevation Uncertainty in Runoff Modelling and Flowpath Mapping. *Hydrological processes* **15**(12): 2223-2236.
- Erdog˘an, S. (2010). Modelling the Spatial Distribution of DEM Error with Geographically Weighted Regression: An Experimental Study. *Computers & Geosciences* **36**(1): 34-43.
- Evans, I. (1990). General Geomorphometry. In: Goudie, A.(Red.) *Geomorphological Techniques*, London: Unwin Hyman.
- Evans, I. (1998). What Do Terrain Statistics Really Mean. In: Lane, S. N., K. S. Richards, and J. H. Chandler (eds.) *Landform Monitoring, Modelling and Analysis*, Wiley, Chichester, UK: 119-138.

- Evans, I. S. (1972). General Geomorphometry, Derivatives of Altitude, and Descriptive Statistics. *Spatial Analysis in Geomorphology*: 17-90.
- Evans, I. S. (1980). An Integrated System of Terrain Analysis and Slope Mapping. *Zeitschrift für Geomorphologie* **36**: 274-295.
- Evans, I. S. (2013). Land Surface Derivatives: History, Calculation and Further Development. *Proceedings of Geomorphometry*: 16-20.
- Favorskaya, M. N. and L. C. Jain (2017). Digital Modelling of Terrain Surface. *Handbook on Advances in Remote Sensing and Geographic Information Systems*, Springer, Cham: 205-250.
- Feder, J. (1988). *Fractals*. Plenum Press, New York.
- Fisher, P. (1991). First Experiments in View- Shed Uncertainty: The Accuracy of the Viewshed Area. *Photogrammetric Engineering & Remote Sensing* **57**(10): 1321–1327.
- Fisher, P. (1998). Improved Modeling of Elevation Error with Geostatistics. *GeoInformatica* **2**(3): 215-233.
- Fisher, P., J. Wood and T. Cheng (2004). Where Is Helvellyn? Fuzziness of Multi-Scale Landscape Morphometry. *Transactions of the Institute of British Geographers* **29**(1): 106-128.
- Fisher, P., J. Wood and T. Cheng (2005). Fuzziness and Ambiguity in Multi-Scale Analysis of Landscape Morphometry. In: Petry F.E., Robinson V.B., Cobb M.A. (eds) *Fuzzy Modeling with Spatial Information for Geographic Problems*, Springer, Berlin, Heidelberg: 209-232.
- Fisher, P. F. and N. J. Tate (2006). Causes and Consequences of Error in Digital Elevation Models. *Progress in Physical Geography* **30**(4): 467-489.
- Florinsky, I. (2016). *Digital Terrain Analysis in Soil Science and Geology*. Elsevier Academic Press, Amsterdam.
- Florinsky, I. V. (1998). Accuracy of Local Topographic Variables Derived from Digital Elevation Models. *International Journal of Geographical Information Science* **12**(1): 47-62.
- Florinsky, I. V. (1998). Derivation of Topographic Variables from a Digital Elevation Model Given by a Spheroidal Trapezoidal Grid. *International Journal of Geographical Information Science* **12**(8): 829-852.

- Frank, A. U. (1992). Spatial Concepts, Geometric Data Models, and Geometric Data Structures. *Computers & Geosciences*, 18(4):409–417.
- Gesch, D., M. Oimoen, Z. Zhang, D. Meyer and J. Danielson (2012). Validation of the Aster Global Digital Elevation Model Version 2 over the Conterminous United States. *The International Archives of the Photogrammetry, Remote Sensing and Spatial Information Sciences*: 281-286.
- Gesch, D. B. (2007). Chapter 4 – the National Elevation Dataset. in Maune, D., ed., Digital elevationl model technologies and applications: The DEM Users Manual, (2nd ed.): Bethesda, Maryland, American Society for Photogrammetry and Remote Sensing: 99–118.
- Gesch, D. B., M. J. Oimoen and G. A. Evans (2014). Accuracy Assessment of the US Geological Survey National Elevation Dataset, and Comparison with Other Large-Area Elevation Datasets: Srtm and Aster, *US Geological Survey Open-File Report 2014–1008, 10 p.*
- Ghandehari, M., B. P. Buttenfield and C. J. Q. Farmer (2018). Slope-Adjusted Surface Area Computations in Digital Terrain, *Proceedings of Geomorphometry 2018 conference, the 5th International Conference of the ISG*, Boulder, Colorado:13-17
- Ghandehari, M., B. P. Buttenfield and C. J. Q. Farmer (2017). Cross-Scale Analysis of Sub-Pixel Variations in Digital Elevation Models, In: Peterson, M. P. (Ed.). *Advances in Cartography and GIScience. ICACI 2017. Lecture Notes in Geoinformation and Cartography*. Berlin: Springer: 359-373
- Gneiting, T. (2013). Strictly and Non-Strictly Positive Definite Functions on Spheres. *Bernoulli* **19**(4): 1327–1349.
- Gold, C. (2016). Tessellations in GIS: Part I—Putting It All Together. *Geo-spatial Information Science* **19**(1): 9-25.
- Gold, C. (2016). Tessellations in GIS: Part II—Making Changes. *Geo-spatial Information Science* **19**(2): 157-167.
- Goodchild, M. and S. Openshaw (1980). Algorithm 9: Simulation of Autocorrelation for Aggregate Data. *Environment and Planning* **12**(9): 1073-1081.
- Goodchild, M. F. (1992). Geographical Data Modeling. *Computers & Geosciences* **18**(4): 401-408.

- Goodchild, M. F. (2010). Twenty Years of Progress: GIScience in 2010. *Journal of Spatial Information Science* **1**(1): 3-20.
- Goodchild, M. F. and R. P. Haining (2004). GIS and Spatial Data Analysis: Converging Perspectives. *Papers in Regional Science* **83**(1): 363-385.
- Greenberg, J. A., C. Rueda, E. L. Hestir, M. J. Santos and S. L. Ustin (2011). Least Cost Distance Analysis for Spatial Interpolation. *Computers & Geosciences* **37**(2): 272-276.
- Griffin, J., H. Latief, W. Kongko, S. Harig, N. Horspool, R. Hanung, A. Rojali, N. Maher, A. Fuchs and J. Hossen (2015). An Evaluation of Onshore Digital Elevation Models for Modeling Tsunami Inundation Zones. *Frontiers in Earth Science* **3**(32): 1-16.
- Grohmann, C. H. (2004). Morphometric Analysis in Geographic Information Systems: Applications of Free Software Grass and R. *Computers & Geosciences* **30**(9-10): 1055-1067.
- Grohmann, C. H. (2015). Effects of Spatial Resolution on Slope and Aspect Derivation for Regional-Scale Analysis. *Computers & Geosciences* **77**: 111-117.
- Guth, P. (1992). Spatial Analysis of DEM Error. Proceedings of ASPRS/ACSM Annual Meeting. American Society of Photogrammetry and Remote Sensing, Washington DC: 187-196.
- Haralick, R. M. (1984). Digital Step Edges from Zero Crossing of Second Directional Derivatives. *IEEE Transactions on Pattern Analysis and Machine Intelligence*, **6**(1): 58-68.
- Hastings, B. (2012). *Comparison of Digital Terrain and Field-Based Channel Derivation Methods in a Subalpine Catchment, Front Range, Colorado*. Masters thesis. Department of Ecosystem Science and Sustainability, Colorado State University. Access on Aug 2018 from <https://mountainscholar.org/handle/10217/67880?show=full>
- He, Q., C. Zeng, P. Xie, Y. Liu and M. Zhang (2018). An Assessment of Forest Biomass Carbon Storage and Ecological Compensation Based on Surface Area: A Case Study of Hubei Province, China. *Ecological Indicators* **90**: 392-400.
- Hebeler, F. and R. S. Purves (2009). The Influence of Elevation Uncertainty on Derivation of Topographic Indices. *Geomorphology* **111**(1): 4-16.

- Hebeler, F. and R. S. Purves (2009). Modeling DEM Data Uncertainties for Monte Carlo Simulations of Ice Sheet Models. *The 5th International Symposium on Spatial Data Quality*, ITC, Enschede: 13-17. <https://www.zora.uzh.ch/id/eprint/3684/>
- Hagerstrand, T. (1968). Innovation Diffusion as a Spatial Process. *Geographical Analysis* **1**(3) 318-320.
- Heine, R. A., C. L. Lant and R. R. Sengupta (2004). Development and Comparison of Approaches for Automated Mapping of Stream Channel Networks. *Annals of the Association of American Geographers* **94**(3): 477-490.
- Hengl, T., S. Gruber and D. P. Shrestha (2004). Reduction of Errors in Digital Terrain Parameters Used in Soil-Landscape Modelling. *International Journal of Applied Earth Observation and Geoinformation* **5**(2): 97-112.
- Hengl, T. and H. I. Reuter (2008). *Geomorphometry: Concepts, Software, Applications*. Developments in Soil Science Series. Elsevier, **33**: 772 pp.
- Heuvelink, G. B. (1998). Error Propagation in Environmental Modelling with GIS. CRC Press, London.
- Hodgson, M. E. (1995). What Cell Size Does the Computed Slope/Aspect Angle Represent? *Photogrammetric Engineering and Remote Sensing* **61**(5): 513-517.
- Hodgson, M. E., J. Jensen, G. Raber, J. Tullis, B. A. Davis, G. Thompson and K. Schuckman (2005). An Evaluation of Lidar-Derived Elevation and Terrain Slope in Leaf-Off Conditions. *Photogrammetric Engineering & Remote Sensing* **71**(7): 817-823.
- Hoechstetter, S., N. X. Thinh and U. Walz (2006). 3d-Indices for the Analysis of Spatial Patterns of Landscape Structure. In: Kremers, H., Tikunov, V. (Eds.) *Proceedings of 12th International Conference on Geoinformation for Sustainable Development - InterCarto-InterGIS 12*, Berlin: 108-118.
- Hoechstetter, S., U. Walz, L. Dang and N. Thinh (2008). Effects of Topography and Surface Roughness in Analyses of Landscape Structure—a Proposal to Modify the Existing Set of Landscape Metrics. *Landscape Online* **3**: 1-14.

- Höhle, J. and M. Höhle (2009). Accuracy Assessment of Digital Elevation Models by Means of Robust Statistical Methods. *ISPRS Journal of Photogrammetry and Remote Sensing* **64**(4): 398-406.
- Holmes, K., O. Chadwick and P. C. Kyriakidis (2000). Error in a USGS 30-Meter Digital Elevation Model and Its Impact on Terrain Modeling. *Journal of Hydrology* **233**(1): 154-173.
- Homer, C., J. Dewitz, L. Yang, S. Jin, P. Danielson, G. Xian, J. Coulston, N. Herold, J. Wickham and K. Megown (2015). Completion of the 2011 National Land Cover Database for the Conterminous United States—Representing a Decade of Land Cover Change Information. *Photogrammetric Engineering & Remote Sensing* **81**(5): 345-354.
- Horn, B. K. (1981). Hill Shading and the Reflectance Map. *Proceedings of the IEEE* **69**(1): 14-47.
- Hu, P., X. Liu and H. Hu (2009). Isomorphism in Digital Elevation Models and its Implication to Interpolation Functions. *Photogrammetric Engineering & Remote Sensing* **75**(6): 713-721.
- Hunter, G. J. and M. F. Goodchild (1997). Modeling the Uncertainty of Slope and Aspect Estimates Derived from Spatial Databases. *Geographical Analysis* **29**(1): 35-49.
- Jaboyedoff, M., M. Choffet, M.-H. Derron, P. Horton, A. Loyer, C. Longchamp, B. Mazotti, C. Michoud and A. Pedrazzini (2012). Preliminary Slope Mass Movement Susceptibility Mapping Using DEM and Lidar DEM. In: Pradhan B., Buchroithner M. (eds) *Terrigenous Mass Movements*. Springer, Berlin, Heidelberg: 109-170.
- Jenness, J. S. (2004). Calculating Landscape Surface Area from Digital Elevation Models. *Wildlife Society Bulletin* **32**(3): 829-839.
- Jiang, B. (2015). The Fractal Nature of Maps and Mapping. *International Journal of Geographical Information Science* **29**(1): 159-174.
- Jjumba, A. and S. Dragićević (2016). Spatial Indices for Measuring Three-Dimensional Patterns in a Voxel-Based Space. *Journal of Geographical Systems* **18**(3): 183-204.
- Kidner, D., M. Dorey and D. Smith (1999). What's the Point? Interpolation and Extrapolation with a Regular Grid DEM. *Fourth International Conference on GeoComputation*,

Fredericksburg, VA, USA. Accessed 2018-08-24 from
www.geocomputation.org/1999/082/gc_082.htm

Kidner, D. B. (2003). Higher-Order Interpolation of Regular Grid Digital Elevation Models. *International Journal of Remote Sensing* **24**(14): 2981-2987.

Kienzle, S. (2004). The Effect of DEM Raster Resolution on First Order, Second Order and Compound Terrain Derivatives. *Transactions in GIS* **8**(1): 83-111.

Kienzle, S. W. (2011). Effects of Area under-Estimations of Sloped Mountain Terrain on Simulated Hydrological Behaviour: A Case Study Using the Acru Model. *Hydrological Processes* **25**(8): 1212-1227.

Kimerling, A. J., A. R. Buckley and P. C. Muehrcke (2012). *Map Use: Reading, Analysis, Interpretation*. ESRI Press Academic, Redlands, California.

Kraus, K. and N. Pfeifer (1998). Determination of Terrain Models in Wooded Areas with Airborne Laser Scanner Data. *ISPRS Journal of Photogrammetry and Remote Sensing* **53**(4): 193-203.

Krebs, P., M. Stocker, G. B. Pezzatti and M. Conedera (2015). An Alternative Approach to Transverse and Profile Terrain Curvature. *International Journal of Geographical Information Science* **29**(4) : 1-24.

Krivoruchko, K. and A. Gribov (2004). Geostatistical Interpolation and Simulation in the Presence of Barriers. In: Sanchez-Vila X., Carrera J., Gómez-Hernández J.J. (eds) *Geoenv IV—Geostatistics for Environmental Applications*, Springer, Dordrecht: 331-342.

Kundu, S. N. and B. Pradhan (2003). Surface Area Processing in GIS. *Proceedings of the Map Asia*: 1-6.

https://www.researchgate.net/publication/233390687_Surface_area_processing_in_GIS

Kyriakidis, P. C., A. M. Shortridge and M. F. Goodchild (1999). Geostatistics for Conflation and Accuracy Assessment of Digital Elevation Models. *International Journal of Geographical Information Science* **13**(7): 677-707.

Lam, N. S.-N. (1983). Spatial Interpolation Methods: A Review. *The American Cartographer* **10**(2): 129-150.

- Lee, J., P. Fisher and P. Snyder (1992). Modeling the Effect of Data Errors on Feature Extraction from Digital Elevation Models. *Photogrammetric Engineering and Remote Sensing* **58**: 1461-1461.
- Li, C., S. Zhao, Q. Wang and W. Shi (2018). Uncertainty Modeling and Analysis of Surface Area Calculation Based on a Regular Grid Digital Elevation Model (DEM). *International Journal of Geographical Information Science*: **32**(9) 1-23.
- Li, J., G. Taylor and D. B. Kidner (2005). Accuracy and Reliability of Map-Matched GPS Coordinates: The Dependence on Terrain Model Resolution and Interpolation Algorithm. *Computers & Geosciences* **31**(2): 241-251.
- Li, Z. (1993). Mathematical Models of the Accuracy of Digital Terrain Model Surfaces Linearly Constructed from Square Gridded Data. *The Photogrammetric Record* **14**(82): 661-674.
- Li, Z., C. Zhu and C. Gold (2004). *Digital Terrain Modeling: Principles and Methodology*. CRC press, Boca Raton, Florida.
- Little, L. S., D. Edwards and D. E. Porter (1997). Kriging in Estuaries: As the Crow Flies, or as the Fish Swims?. *Journal of Experimental Marine Biology and Ecology* **213**(1): 1-11.
- Liu, M., Y.-M. Hu and C.-L. Li (2017). Landscape Metrics for Three-Dimensional Urban Building Pattern Recognition. *Applied Geography* **87**: 66-72.
- Liu, X., H. Hu and P. Hu (2015). The “M” in Digital Elevation Models. *Cartography and Geographic Information Science* **42**(3): 235-243.
- Longley, P. A., M. F. Goodchild, D. J. Maguire and D. W. Rhind (2005). *Geographic Information Systems and Science*. John Wiley & Sons, West Sussex, England.
- Lu, B., M. Charlton, P. Harris and A. S. Fotheringham (2014). Geographically Weighted Regression with a Non-Euclidean Distance Metric: A Case Study Using Hedonic House Price Data. *International Journal of Geographical Information Science* **28**(4): 660-681.
- Maling, D. H. (1988). *Measurements from Maps: Principles and Methods of Cartometry*. Butterworth-Heinemann, Oxford, United Kingdom.
- Mandelbrot, B. B. (1967). How Long is the Coast of Britain. *Science* **156**(3775): 636-638.

- Márkus, B. (1986). Terrain Analysis in Consideration of Surface Curvature Conditions. *Periodica Polytechnica. Civil Engineering* **30**(1-2): 71.
- McMaster, K. J. (2002). Effects of Digital Elevation Model Resolution on Derived Stream Network Positions. *Water Resources Research* **38**(4): 13-11-13-18.
- Miller, H. J. and E. A. Wentz (2003). Representation and Spatial Analysis in Geographic Information Systems. *Annals of the Association of American Geographers* **93**(3): 574-594.
- Minár, J., M. Jenčo, I. S. Evans, J. Minár Jr, M. Kadlec, J. Krcho, J. Pacina, L. Burian and A. Benová (2013). Third-Order Geomorphometric Variables (Derivatives): Definition, Computation and Utilization of Changes of Curvatures. *International Journal of Geographical Information Science* **27**(7): 1381-1402.
- Mitasova, H., R. S. Harmon, K. J. Weaver, N. J. Lyons and M. F. Overton (2012). Scientific Visualization of Landscapes and Landforms. *Geomorphology* **137**(1): 122-137.
- Mitášová, H. and L. Mitáš (1993). Interpolation by Regularized Spline with Tension: I. Theory and Implementation. *Mathematical Geology* **25**(6): 641-655.
- Monckton, C. G. (1994). An Investigation into the Spatial Structure of Error in Digital Elevation Data. *Innovations in GIS* **1**: 201-211.
- Monterroso, P., N. Sillero, L. M. Rosalino, F. Loureiro and P. C. Alves (2013). Estimating Home-Range Size: When to Include a Third Dimension? *Ecology and evolution* **3**(7): 2285-2295.
- Montgomery, D. R. and E. Foufoula-Georgiou (1993). Channel Network Source Representation using Digital Elevation Models. *Water Resources Research* **29**(12): 3925-3934.
- Niedercorn, J. H. and B. V. Bechdolt Jr (1969). An Economic Derivation of the “Gravity Law” of Spatial Interaction. *Journal of Regional Science* **9**(2): 273-282.
- O'Callaghan, J. F. and D. M. Mark (1984). The Extraction of Drainage Networks from Digital Elevation Data. *Computer Vision, Graphics, and Image Processing* **28**(3): 323-344.
- O'Neil, G. and A. Shortridge (2013). Quantifying Local Flow Direction Uncertainty. *International Journal of Geographical Information Science* **27**(7): 1292-1311.

- Oksanen, J. (2006). *Digital Elevation Model Error in Terrain Analysis*. Ph.D. dissertation, University of Helsinki, Faculty of Science, Department of Geography.
<https://helda.helsinki.fi/handle/10138/21192>.
- Oksanen, J. (2013). Can Binning Be the Key to Understanding the Uncertainty of DEMs? *Proceedings of the GISRUK 2013*, April 3–5, 2013, University of Liverpool, UK.
- Oksanen, J. and T. Sarjakoski (2005). Error Propagation Analysis of DEM-Based Drainage Basin Delineation. *International Journal of Remote Sensing* **26**(14): 3085-3102.
- Oksanen, J. and T. Sarjakoski (2006). Uncovering the Statistical and Spatial Characteristics of Fine Toposcale DEM Error. *International Journal of Geographical Information Science* **20**(4): 345-369.
- Olaya, V. (2009). Basic Land-Surface Parameters. In: Hengl, T. and Reuter, H.I. (Eds), *Geomorphometry: Geomorphometry: Concepts, Software, Applications. Developments in Soil Science* **33**: 141-169.
- Passalacqua, P., P. Belmont, D. M. Staley, J. D. Simley, J. R. Arrowsmith, C. A. Bode, C. Crosby, S. B. DeLong, N. F. Glenn and S. A. Kelly (2015). Analyzing High Resolution Topography for Advancing the Understanding of Mass and Energy Transfer through Landscapes: A Review. *Earth-Science Reviews* **148**: 174-193.
- Pędzich, P. and M. Kuźma (2012). Application of Methods for Area Calculation of Geodesic Polygons on Polish Administrative Units. *Geodesy and Cartography* **61**(2): 105-115.
- Pelletier, J. D. (2013). A Robust, Two-Parameter Method for the Extraction of Drainage Networks from High-Resolution Digital Elevation Models (DEMs): Evaluation Using Synthetic and Real-World DEMs. *Water Resources Research* **49**(1): 75-89.
- Petras, V., D. J. Newcomb and H. Mitasova (2017). Generalized 3d Fragmentation Index Derived from Lidar Point Clouds. *Open Geospatial Data, Software and Standards* **2**(1): 2-9.
- Pike, R., I. Evans and T. Hengl (2009). Geomorphometry: A Brief Guide. *Developments in Soil Science* **33**: 3-30.
- Pike, R. J. (1988). The Geometric Signature: Quantifying Landslide-Terrain Types from Digital Elevation Models. *Mathematical Geology* **20**(5): 491-511.

Raablaub, L. D. (2002). The Effect of Error in Gridded Digital Elevation Models on Topographic Analysis and on the Distributed Hydrological Model TOPMODEL. Master Thesis, University of Calgary, Geomatics Engineering.

https://www.ucalgary.ca/engo_webdocs/MJC/02.20163.LDRaablaub.pdf

Raablaub, L. D. and M. J. Collins (2006). The Effect of Error in Gridded Digital Elevation Models on the Estimation of Topographic Parameters. *Environmental Modelling & Software* **21**(5): 710-732.

Rees, W. (2000). The Accuracy of Digital Elevation Models Interpolated to Higher Resolutions. *International Journal of Remote Sensing* **21**(1): 7-20.

Reuter, H., T. Hengl, P. Gessler and P. Soille (2009). Preparation of DEMs for Geomorphometric Analysis. In T. Hengl and H. Reuter (eds.) *Geomorphometry: Geomorphometry: Concepts, Software, Applications. Developments in Soil Science*. Oxford, UK, Elsevier. **33**: 87-120.

Richardson, L. F. (1961). The Problem of Contiguity. *General Systems Yearbook* **6**: 139-187.

Rogers, D., A. Cooper, P. McKenzie and T. McCann (2012). Assessing Regional Scale Habitat Area with a Three Dimensional Measure. *Ecological Informatics* **7**(1): 1-6.

Salleh, M. R. M., Z. Ismail and M. Z. A. Rahman (2015). Accuracy Assessment of Lidar-Derived Digital Terrain Model (DTM) with Different Slope and Canopy Cover in Tropical Forest Region. *ISPRS Annals of the Photogrammetry, Remote Sensing and Spatial Information Sciences* **2**(2): 183.

Samet, H. (1984). The Quadtree and Related Hierarchical Data Structures. *ACM Computing Surveys (CSUR)* **16**(2): 187-260.

Schilling, A., A. Schmidt and H.-G. Maas (2012). Tree Topology Representation from TLS Point Clouds Using Depth-First Search in Voxel Space. *Photogrammetric Engineering & Remote Sensing* **78**(4): 383-392.

Schmidt, J., I. S. Evans and J. Brinkmann (2003). Comparison of Polynomial Models for Land Surface Curvature Calculation. *International Journal of Geographical Information Science* **17**(8): 797-814.

- Schneider, B. (2001). On the Uncertainty of Local Shape of Lines and Surfaces. *Cartography and Geographic Information Science* **28**(4): 237-247.
- Shary, P. A. (1995). Land Surface in Gravity Points Classification by a Complete System of Curvatures. *Mathematical Geology* **27**(3): 373-390.
- Shary, P. A., L. S. Sharaya and A. V. Mitusov (2002). Fundamental Quantitative Methods of Land Surface Analysis. *Geoderma* **107**(1-2): 1-32.
- Shary, P. A., L. S. Sharaya and A. V. Mitusov (2005). The Problem of Scale-Specific and Scale-Free Approaches in Geomorphometry. *Geografia Fisica e Dinamica Quaternaria* **28**(1): 81-101.
- Shi, W. and Y. Tian (2006). A Hybrid Interpolation Method for the Refinement of a Regular Grid Digital Elevation Model. *International Journal of Geographical Information Science* **20**(1): 53-67.
- Shi, W., B. Wang and Y. Tian (2014). Accuracy Analysis of Digital Elevation Model Relating to Spatial Resolution and Terrain Slope by Bilinear Interpolation. *Mathematical Geosciences* **46**(4): 445-481.
- Shortridge, A. (2001). Characterizing Uncertainty in Digital Elevation Models. In: Hunsaker C.T., Goodchild M.F., Friedl M.A., Case T.J. (eds) *Spatial Uncertainty in Ecology*, Springer, New York: 238-257.
- Shortridge, A. and J. Messina (2011). Spatial Structure and Landscape Associations of SRTM Error. *Remote sensing of Environment* **115**(6): 1576-1587.
- Shortridge, A. M., J. V. Fayne and M. T. Rice (2017). Modeling Uncertainty in Digital Elevation Models. In: Douglas Richardson (ed.) *International Encyclopedia of Geography: People, the Earth, Environment and Technology: People, the Earth, Environment and Technology*: 1-10.
- Simpson, J. E., T. E. Smith and M. J. Wooster (2017). Assessment of Errors Caused by Forest Vegetation Structure in Airborne Lidar-Derived DTMs. *Remote Sensing* **9**(11): 1101.
- Sjöberg, L. E. (2006). Determination of Areas on the Plane, Sphere and Ellipsoid. *Survey Review* **38**(301): 583-593.

- Skidmore, A. K. (1989). A Comparison of Techniques for Calculating Gradient and Aspect from a Gridded Digital Elevation Model. *International Journal of Geographical Information System* **3**(4): 323-334.
- Skidmore, A. K. (2006). Evolution of Methods for Estimating Slope Gradient and Aspect from Digital Elevation Models. In: Fisher P (ed.) *Classics from IJGIS: Twenty Years of the International Journal of Geographical Information Science and Systems*, CRC Press, Boca Raton: 111-116.
- Sofia, G., F. Pirotti and P. Tarolli (2013). Variations in Multiscale Curvature Distribution and Signatures of Lidar DTM Errors. *Earth Surface Processes and Landforms* **38**(10): 1116-1134.
- Song, G., Y. Chen and Y. Zhou (2013). Algorithm for Estimating Mountainous Surface Area Based on Gps Data. In: Yang Y., Ma M. (eds) *Proceedings of the 2nd International Conference on Green Communications and Networks 2012 (GCN 2012)*, Lecture Notes in Electrical Engineering, Springer, Berlin, Heidelberg **224**: 679-687.
- Stanislawski, L. V., J. Falgout and B. P. Buttenfield (2015). Automated Extraction of Natural Drainage Density Patterns for the Conterminous United States through High-Performance Computing. *The Cartographic Journal* **52**(2): 185-192.
- Steinhaus, H. (1954). Length, Shape and Area. *Colloquium Mathematicae*, Institute of Mathematics Polish Academy of Sciences **3**(1): 1-13.
- Steinhaus, H. (1999). *Mathematical Snapshots*. Courier Corporation, Dover Publication, Mineola, New York.
- Stoker, J. M., (2018). The US Geological Survey Physical Scientist the Chief Elevation Scientist for the National Geospatial Program, personal communication (jstoker@usgs.gov).
- Stupariu, M., I. Pătru-Stupariu and R. Cuculici (2010). Geometric Approaches to Computing 3d-Landscape Metrics. *Landscape Online* **24**: 1-12.
- Tarboton, D. G. (2005). Terrain Analysis Using Digital Elevation Models (TauDEM). *Utah State University, Logan*. <http://hydrology.usu.edu/taudem/taudem3.0/>
- Tarboton, D. G., R. L. Bras and I. Rodriguez-Iturbe (1991). On the Extraction of Channel Networks from Digital Elevation Data. *Hydrological processes* **5**(1): 81-100.

- Tarolli, P. (2014). High-Resolution Topography for Understanding Earth Surface Processes: Opportunities and Challenges. *Geomorphology* **216**: 295-312.
- Tarolli, P., G. Dalla Fontana, G. Moretti and S. Orlandini (2009). Cell Size Dependence of Threshold Conditions for the Delineation of Drainage Networks from Gridded Elevation Data. *Proceedings of Geomorphometry* **31**: 208-217.
- Theobald, D. M. (1989). Accuracy and Bias Issues in Surface Representation. In: Goodchild, M.F. and Gopal, S. (eds.): *Accuracy of spatial databases*, New York, Taylor and Francis: 99-106.
- Tobler, W. R. (1963). Geographic Area and Map Projections. *Geographical review* **53**(1): 59-78.
- Tobler, W. R. (1993). Three Presentations on Geographical Analysis and Modeling: Non-Isotropic Geographic Modeling, Speculations on the Geometry of Geography and, Global Spatial Analysis. National Center for Geographic Information and Analysis, Technical Report 93-1. Santa Barbara, University of California-Santa Barbara.
- <https://escholarship.org/uc/item/05r820mz> (accessed on Aug 2018)
- Tomlin, D. C. (1990). *Geographic Information Systems and Cartographic Modeling*. Englewood Cliffs, NJ, Prentice-Hall.
- Usery, E. L., M. P. Finn, J. D. Cox, T. Beard, S. Ruhl and M. Bearden (2003). Projecting Global Datasets to Achieve Equal Areas. *Cartography and Geographic Information Science* **30**(1): 69-79.
- Van Laarhoven, P. J. and E. H. Aarts (1987). *Simulated Annealing: Theory and Applications*, Springer, Dordrecht, Reidel.
- Vaze, J., J. Teng and G. Spencer (2010). Impact of DEM Accuracy and Resolution on Topographic Indices. *Environmental Modelling & Software* **25**(10): 1086-1098.
- Venzin, C. (2013). *Analyzing the Impact of High Resolution DEM Uncertainty on Hydrological Models Using a Parallel Computing Approach*. Master Thesis, Geographisches Institut der Universität Zürich, https://www.geo.uzh.ch/dam/jcr:dcc07b13-fdc4-40e8-89dd-d05365924fcf/MSc_Thesis_Venzin.pdf

- Veregin, H. (1997). The Effects of Vertical Error in Digital Elevation Models on the Determination of Flow-Path Direction. *Cartography and Geographic Information Systems* **24**(2): 67-79.
- Ver Hoef, J.M. (2018). *Kriging Models for Linear Networks and non-Euclidean Distances: Cautions and Solutions*. Seattle Washington: NOAA fisheries Science Center Technical Report, Marine Mammal Laboratory, 42 pp.
- Ver Hoef, J. M. and E. Peterson, 2010. A Moving Average Approach for Spatial Statistical Models of Stream Networks (with discussion). *Journal of the American Statistical Association* **105**: 6–18.
- Von Thünen, J. H. (1875). Der Isolirte Staat in Beziehung Auf Landwirtschaft Und Nationalökonomie. Wiegant, Hempel & Parey.
- Walz, U., S. Hoechstetter, L. Drăguț and T. Blaschke (2016). Integrating Time and the Third Spatial Dimension in Landscape Structure Analysis. *Landscape Research* **41**(3): 279-293.
- Wang, H. and M. G. Ranalli, 2007. Low-rank Smoothing Splines on Complicated Domains. *Biometrics* **63**: 209–217.
- Weber, A. (1909). *Ueber Den Standort Der Industrien*. Рипол Классик, Robarts, University of Toronto.
- Wechsler, S. (2007). Uncertainties Associated with Digital Elevation Models for Hydrologic Applications: A Review. *Hydrology and Earth System Sciences* **11**(4): 1481-1500.
- Wechsler, S. P. (1999). Digital Elevation Model (DEM) Uncertainty: Evaluation and Effect on Topographic Parameters. *ESRI User Conference*: 1081-1090.
<https://pdfs.semanticscholar.org/e3d1/7c1bb3e67c5b4157fa3cdb46b48d35f28c40.pdf>
- Wechsler, S. P. and C. N. Kroll (2006). Quantifying DEM Uncertainty and its Effect on Topographic Parameters. *Photogrammetric Engineering & Remote Sensing* **72**(9): 1081-1090.

- Weibel, R. and M. Brändli (1995). Adaptive Methods for the Refinement of Digital Terrain Models for Geomorphometric Applications. *Zeitschrift fur Geomorphologie Supplementband 101*: 13-30.
- Weibel, R. and M. Heller (1993). Digital Terrain Modelling. In: Maguire, D.J., Goodchild, M.F. And Rhind, D.W. (Eds.). *Geographical Information Systems: Principles and Applications*. London, Longman: 269-297.
- Weng, Q. (2002). Quantifying Uncertainty of Digital Elevation Models Derived from Topographic Maps. In: Richardson D.E., van Oosterom P. (Eds.) *Advances in Spatial Data Handling*, Springer, Berlin, Heidelberg: 403-418.
- Wilson, J. P. (2012). Digital Terrain Modeling. *Geomorphology* 137(1): 107-121.
- Wilson, J. P. (2018). Environmental Applications of Digital Terrain Modeling. Wiley, Oxford, UK.
- Wilson, J. P. and J. C. Gallant (2000). *Terrain Analysis: Principles and Applications*. Wiley, New York.
- Wise, S. (2000). Assessing the Quality for Hydrological Applications of Digital Elevation Models Derived from Contours. *Hydrological Processes* 14(11-12): 1909-1929.
- Wolf, G. W. (2016). Scale Independent Surface Characterisation: Geography Meets Precision Surface Metrology. *Precision Engineering*, 49 (2017): 456-480.
- Wood, J. (1994). Visualizing Contour Interpolation Accuracy in Digital Elevation Models. *Visualisation in Geographical Information Systems*: 168-180.
- Wood, J. (1996). *The Geomorphological Characterisation of Digital Elevation Models*. Ph.D. dissertation, Deptment of Geography, University of Leicester.
- Wood, J. (1998). Modelling the Continuity of Surface Form Using Digital Elevation Models. *Proceedings of the 8th International Symposium on Spatial Data Handling*, IGU Commission of GIS, July 11-15th, Vancouver, Canada: 725-736.
- Wood, J. (1999). Visualization of Scale Dependencies in the Surface Models. *Proceedings of the 19th International Cartographic Association Annual Conference*, 14 – 21 August, Ottawa,

Canada.

<http://citeseerx.ist.psu.edu/viewdoc/download?doi=10.1.1.506.6527&rep=rep1&type=pdf>

Wood, J. (2009). Geomorphometry in Landserf. *Developments in Soil Science* **33**: 333-349.

Wood, J. D. and P. F. Fisher (1993). Assessing Interpolation Accuracy in Elevation Models.

IEEE Computer Graphics and Applications **13**(2): 48-56.

Wood, J. D. and P. F. Fisher (1993). Assessing Interpolation Accuracy in Elevation Models.

IEEE Computer Graphics and Applications (2): 48-56.

Wu, Q., F. Guo, H. Li and J. Kang (2017). Measuring Landscape Pattern in Three Dimensional Space. *Landscape and Urban Planning* **167**: 49-59.

Xie, P., Y. Liu, Q. He, X. Zhao and J. Yang (2017). An Efficient Vector-Raster Overlay Algorithm for High-Accuracy and High-Efficiency Surface Area Calculations of Irregularly Shaped Land Use Patches. *ISPRS International Journal of Geo-Information* **6**(6): 156.

Xue, S., Y. Dang, J. Liu, J. Mi, C. Dong, Y. Cheng, X. Wang and J. Wan (2016). Bias Estimation and Correction for Triangle-Based Surface Area Calculations. *International Journal of Geographical Information Science* **30**(11): 2155-2170.

Xue, S., Y. Dang, J. Liu, J. Mi, C. Dong, Y. Cheng, X. Wang and J. Wan (2018). Surface Area Calculation for DEM-Based Terrain Model. *Survey review* **50**(358): 8-15.

Xuejun, L. and B. Lu (2008). *Accuracy Assessment of DME Slope Algorithms Related to Spatial Autocorrelation of DEM Errors*. In: Zhou Q., Lees B., Tang G. (eds) *Advances in Digital Terrain, Analysis* Springer, Berlin, Heidelberg: 307-322.

Tarolli, P., D. P. Ames, A. Fonseca, D. Anderson, R. Shrestha, N. F. Glenn and Y. Cao (2014). What Is the Effect of Lidar-Derived DEM Resolution on Large-Scale Watershed Model Results? *Environmental Modelling & Software* **58**: 48-57.

Yao, J. and A. T. Murray (2013). Continuous Surface Representation and Approximation: Spatial Analytical Implications. *International Journal of Geographical Information Science* **27**(5): 883-897.

- Ying, L.-X., Z.-H. Shen, S.-L. Piao, Y. Liu and G. P. Malanson (2014). Terrestrial Surface-Area Increment: The Effects of Topography, DEM Resolution, and Algorithm. *Physical Geography* **35**(4): 297-312.
- Zandbergen, P. A. (2006). The Effect of Cell Resolution on Depressions in Digital Elevation Models. *Applied GIS* **2**(1): 04.01-04.35.
- Zandbergen, P. A. (2011). Characterizing the Error Distribution of Lidar Elevation Data for North Carolina. *International Journal of Remote Sensing* **32**(2): 409-430.
- Zevenbergen, L. W. and C. R. Thorne (1987). Quantitative Analysis of Land Surface Topography. *Earth Surface Processes and Landforms* **12**(1): 47-56.
- Zhang, J. and M. F. Goodchild (2002). *Uncertainty in Geographical Information*. CRC press, New York.
- Zhang, Y., L.-n. Zhang, W.-d. Bao and X.-x. Yuan (2011). Surface Area Processing in GIS for Different Mountain Regions. *Forestry Studies in China* **13**(4): 311-314.
- Zhang, Z., J. A. Zinda, Z. Yang, M. Yin, X. Ou, Q. Xu and Q. Yu (2018). Effects of Topographic Attributes on Landscape Pattern Metrics Based on Redundancy Ordination Gradient Analysis. *Landscape and Ecological Engineering* **14**(1): 67-77.
- Zhao, J., Q. Wang and X. Wang (2005). Real-Time 3d Road Animation Based on Digital Terrain Model. *Computer Engineering* **12**(31): 196-197.
- Zhilin, L. (2008). Multi-Scale Digital Terrain Modelling and Analysis. In: Zhou Q., Lees B., Tang G. (eds) *Advances in Digital Terrain Analysis*, Lecture Notes in Geoinformation and Cartography, Springer, Berlin, Heidelberg: 59-83.
- Zhiming, Z., F. Van Coillie, R. De Wulf, E. M. De Clercq and O. Xiaokun (2012). Comparison of Surface and Planimetric Landscape Metrics for Mountainous Land Cover Pattern Quantification in Lancang Watershed, China. *Mountain Research and Development* **32**(2): 213-225.
- Zhou, Q. (2017). Digital Elevation Model and Digital Surface Model. In: Richardson, D. (ed) *The international encyclopedia of geography: People, the earth, environment, and technology*, Wiley-Blackwell, Malden, MA and Oxford **13**:1-17

Zhou, Q., B. Lees and G.-a. Tang (2008). *Advances in Digital Terrain Analysis*. Lecture Notes in Geoinformation and Cartography, Springer Science & Business Media, Springer-Verlag Berlin Heidelberg.

Zhou, Q. and X. Liu (2004). Analysis of Errors of Derived Slope and Aspect Related to DEM Data Properties. *Computers & Geosciences* **30**(4): 369-378.

Zhou, Q., X. Liu and Y. Sun (2006). Terrain Complexity and Uncertainties in Grid-Based Digital Terrain Analysis. *International Journal of Geographical Information Science* **20**(10): 1137-1147.

Zou, H., Y. Yue, Q. Li and A. G. Yeh (2012). An Improved Distance Metric for the Interpolation of Link-Based Traffic Data Using Kriging: A Case Study of a Large-Scale Urban Road Network. *International Journal of Geographical Information Science* **26**(4): 667-689.